CENTER *for* MUSCULOSKELETAL RESEARCH

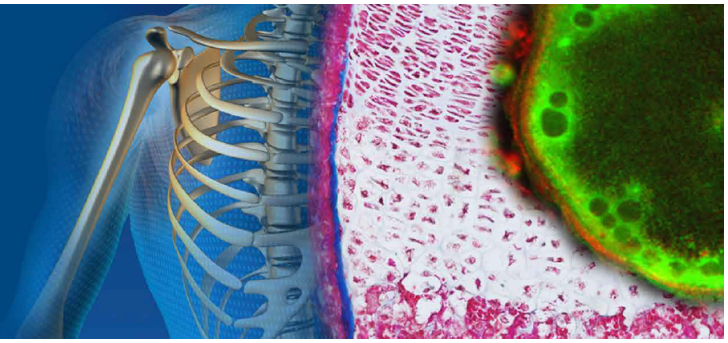

12th Annual CMSR Symposium

Wednesday, October 19, 2022

Sponsored By

Department of Orthopaedics and Rehabilitation
University of Rochester Medical Center
&
National Institute of Arthritis and Musculoskeletal and Skin Diseases (NIAMS) Grant T32 AR076950

MEDICINE *of* THE HIGHEST ORDER

UR MEDICINE

ROCMSK Training Program

The Annual CMSR symposium is the center piece of the NIH/NIAMS funded T32 program entitled "Rochester Musculoskeletal (ROCMSK) Training Program" at the University of Rochester Medical Center. This program is designed to provide interdisciplinary didactic and research training in musculoskeletal science.

The overarching goal of ROCMSK Training Program is to develop future generations of interdisciplinary musculoskeletal scientists and leaders of innovations. The program is administered in The Center for Musculoskeletal Research (CMSR) at the University of Rochester and integrates 21 highly-collaborative faculty with primary appointments in 7 academic and clinical departments. The CMSR and associated training faculty represent a highly integrated group of Mentors that provide research training opportunities in Bone Biology and Disease, Cartilage Mechanobiology, Arthritis, and Regenerative Therapies, Tendon Development, Repair and Regenerative Engineering, Muscle Biology and Disease, Drug Delivery, Fracture Repair and Bone Tissue Engineering, Musculoskeletal Infection, Stem Cells and Musculoskeletal Development and Regenerative Biology, and Skeletal Cancer Biology and Therapeutics, as can be seen from the abstracts featured in this symposium.

The education program ensures a comprehensive understanding of musculoskeletal science that is seamlessly accessible to all CMSR trainees at every academic level. ROCMSK training emphasizes basic and translational science education. The training experience aims to build competency in areas ranging from the most basic molecular and genetic studies to the design and execution of human clinical trials. This year, ROCMSK awarded 2 pre-doctoral and 2 post-doctoral training seats.

This symposium is a celebration of the Trainees' accomplishments.

Center for MusculoSkeletal Research

12th Annual CMSR Symposium
Wednesday, October 19, 2022

Zoom Link

https://urmc.zoom.us/j/94711958901?pwd=M2NoQ1Nyc3FvNWl5MVMxSDFiZ3RhUT09

Clinical Hour Presentations — Class of '62 Auditorium

7:00 am	*Welcome & Introduction*	***Paul Rubery, MD***
7:05 am	*Association of Total Knee Replacement Removal from the Inpatient-Only List with Outcomes in Medicare Patients*	***Derek Schloemann, MD*** *Caroline Thirukumaran, PhD*
7:20 am	*Ultrasound Shear Wave Metric for Assessing Flexor Tendon Healing: A Preliminary Cadaver Study*	***Gilbert Smolyak*** *Constantinos Ketonis, MD, PhD*
7:30 am	*Trends in total hip, knee, and shoulder arthroplasty procedures being performed in Ambulatory Surgery Centers in New York State*	***Thomas Sajda, MD*** *Benjamin Ricciardi, MD*
7:40 am	*Intraoperative blood loss with use of High or Low Dose Tranexamic Acid in metastatic spine tumor surgery, a matched case-control study*	***Mark Lawlor, MD*** *Addisu Mesfin, MD*
7:50 am	*Do Patient Reported Outcomes Collected in Clinic Predict the Need for Follow-up Visits After Surgery?*	***Jefferson Hunter*** *Judy Baumhauer, MD, MPH*

Rosier Award Trainee Presentations — Class of '62 Auditorium

	9:00 am	*Welcome & Introduction*	***Hani Awad, PhD*** ***Paul Rubery, MD***
	9:05 am	*The Importance of Musculoskeletal Research from the Patient Perspective*	***Karen Tucker*** ***(UR Alum 1973)***
Post-Doctoral Fellows	9:15 am	*Human NGFR$^+$/VCAM-1$^+$/MCAM$^+$ Bone Marrow-derived Stromal Cells (NVML) Provide Enhanced Support for Normal Hematopoiesis and Are Disrupted in Myelodysplastic Syndrome*	***Yuko Kawano, MD, PhD*** *Calvi Lab*
	9:30 am	*Single cell RNA sequencing reveals age-dependent decline of fibroblast population in murine knee synovium*	***Xi Lin, PhD*** *Xing Lab*
	9:45 am	*Efficacy of Bisphosphonate-Conjugated Sitafloxacin in a Murine 1-Stage Revision Model of S. aureus Osteomyelitis*	***Youliang Ren, PhD*** *Xie/Schwarz Lab*
Pre-Doctoral Trainees	10:00 am	*Elucidating Androgen Effects on Focal Erosions in TNF-Induced Inflammatory Arthritis*	***Kiana Chen*** *Rahimi Lab*
	10:15 am	*CXCR2$^+$TGFbeta1$^+$ callus senescent cells represent a specific detrimental subset that inhibits fracture healing and growth of mesenchymal progenitors*	***Jiatong Liu*** *Xing Lab*
	10:30 am	*Coffee Break*	
	10:45 am	*Detecting osteoporosis and predicting distal radius fracture strength using Raman spectroscopy in human fingers - A cadaveric study*	***Christine Massie*** *Berger/Awad Lab*
	11:00 am	*Insulin-Like Growth Factor 1 in the Bone Marrow Microenvironment Inhibits Mesenchymal Stromal Cell Efferocytosis*	***Noah Salama*** *Calvi Lab*
	11:15 am	*Effects of Elevated Lactate in the Bone Marrow Microenvironment during Acute Myeloid Leukemia*	***Celia Soto*** *Frisch Lab*
	11:30 am	*Detecting alterations in tendon microstructure in the presence of diabetes using high-frequency quantitative ultrasound*	***Sarah Wayson*** *Hocking/Dalecki Lab*
	11:45 am	*Three-Minute Teasers (3MT) – Finalists for Best Poster Presentations*	

12:15 – 2:15 pm ***Lunch & Poster Session*** — **Sarah Flaum Atrium**
2:15 pm ***Annual CMSR Photo*** — **Sarah Flaum Atrium**

Plenary Session — Class of '62 Auditorium

CMSR Faculty Spotlight

2:30 pm **Shu-Chi (Allison) Yeh, PhD**
Live-animal multiphoton imaging of the blood stem cell niche

3:00 pm **Gowrishankar Muthukrishnan, PhD**
IL-27 and Staphylococcus aureus bone infections

3:30 pm **Danielle Benoit, PhD**
Therapeutic biomaterials for musculoskeletal regeneration

Keynote Presentation

4:00 pm **Tamara Alliston, PhD**
Osteocytic Mechanisms of Bone Fragility and Joint Disease

5:30 pm ***Dinner and Rosier Awards Presentation*** — **Evarts Lounge- Helen Wood Hall**

MEDICINE of THE HIGHEST ORDER

UR MEDICINE

Keynote Speaker: Tamara Alliston, PhD

Professor of Orthopaedic Surgery
University of California San Francisco

Tamara N. Alliston, Ph.D., is a Professor in the University of California San Francisco Department of Orthopaedic Surgery. She pursued her undergraduate education in Biology at Trinity University in San Antonio, Texas. Dr. Alliston earned her doctoral degree in Cell Biology from Baylor College of Medicine in Houston, Texas in 1998, working under the guidance of Dr. JoAnne Richards. After receiving her doctorate, Dr. Alliston was named an Arthritis Foundation Fellow, working as a post-doctoral scientist in the lab of Dr. Rik Derynck at UCSF. In 2002, she was appointed an Assistant Adjunct Professor in the Department of Cell and Tissue Biology at UCSF.

Dr. Alliston is Founder and Director of the University of California, San Francisco, Musculoskeletal (MSK) center, which she organized in 2020. The goal of the center is to advance discovery and clinical impact, by nucleating and integrating musculoskeletal research and facilitating collaboration among basic, translational, computational, and clinical investigators, within and beyond musculoskeletal research. Since musculoskeletal conditions are the 2nd leading burden of disease worldwide, this program will benefit human health broadly.

Nationally and internationally renowned for her work in MSK research, Dr. Tamara Alliston is the recipient of the 2020 Adele L. Boskey Award from the American Society for Bone and Mineral Research in recognition of her research on bone quality. She also won the 2019 Women's Leadership Award from the Orthopaedic Research Society for outstanding scientific contributions. Her research helped change the paradigm of how bone cells support joint health, opening the door to the development of new therapies targeting bone to prevent or reverse cartilage degeneration or improve the success of cartilage repair. Other notable honors include a Hulda Irene Duggan Arthritis Investigator Award, the ASBMR Harold M. Frost Young Investigator Award, and the AIMM-ASBMR John Haddad Young Investigator Award.

Dr. Alliston's other service and leadership efforts focus on the development of the next generation of scientists and leaders. She serves the Orthopaedic Research Society as a member of the Board of Directors in her role as the Professional Development and Mentoring Council Chair. She currently serves as the Chair of the UC Berkeley/UCSF Graduate Program in Bioengineering Executive Committee and has played leadership roles in several other graduate programs.

Dr. Alliston's collaborative approach to pushing investigation beyond the structural function of these connective tissues led to additional key discoveries, including the role of bone as an intricate mechano-sensor that coordinates metabolism and endocrine function

Symposium Papers

Clinical Hour Abstracts

1	Derek Schloemann	Association of Total Knee Replacement Removal from the Inpatient-Only List with Outpatient Surgery Utilization and Outcomes in Medicare Patients
2	Gilbert Smolyak	Ultrasound Shear Wave Metric for Assessing Flexor Tendon Healing: A Preliminary Cadaver Study
3	Thomas Sajda	Trends in total hip, knee, and shoulder arthroplasty procedures being performed in Ambulatory Surgery Centers in New York State
4	Mark Lawlor	Intraoperative blood loss with use of High or Low Dose Tranexamic Acid in metastatic spine tumor surgery, a matched case control study
5	Jefferson Hunter	Do Patient Reported Outcomes Collected in Clinic Predict the Need for Follow-up Visits After Surgery?

Rosier Awards Post-Doctoral Trainee Presentations

6	Yuko Kawano	Human $NGFR^+/VCAM\text{-}1^+/MCAM^+$ Bone Marrow-derived Stromal Cells (NVML) Provide Enhanced Support for Normal Hematopoiesis and Are Disrupted in Myelodysplastic Syndrome
7	Xi Lin	Single cell RNA sequencing reveals age-dependent decline of fibroblast population in murine knee synovium
8	Youliang Ren	Efficacy of Bisphosphonate-Conjugated Sitafloxacin in a Murine 1-Stage Revision Model of S. aureus Osteomyelitis

Rosier Awards Pre-Doctoral Trainee Presentations

9	Kiana Chen	Elucidating Androgen Effects on Focal Erosions in TNF-Induced Inflammatory Arthritis
10	Jiatong Liu	CXCR2+TGFbeta1+ callus senescent cells represent a specific detrimental subset that inhibits fracture healing and growth of mesenchymal progenitors
11	Christine Massie	Detecting osteoporosis and predicting distal radius fracture strength using Raman spectroscopy in human fingers - A cadaveric study
12	Noah Salama	Insulin-Like Growth Factor 1 in the Bone Marrow Microenvironment Inhibits Mesenchymal Stromal Cell Efferocytosis
13	Celia Soto	Effects of Elevated Lactate in the Bone Marrow Microenvironment during Acute Myeloid Leukemia
14	Sarah Wayson	Detecting alterations in tendon microstructure in the presence of diabetes using high-frequency quantitative ultrasound

Rosier Award Best Poster Finalists

15	Raquel Ajalik	Human Tendon-on-a-Chip (hToC) platform for modeling fibrotic disease and screening therapeutic candidates
16	Rahul Alenchery	PAI-1 mediates TGF-β1 induced myofibroblast activation and senescence in tenocytes via mTOR signaling
17	Eloise Fadial	Spatiotemporal analysis reveals functional role of PRDM16 in chondrogenesis and limb development
18	H. Mark Kenney	Spatial and Single-Cell Transcriptomics Identify IgG2b Class-Switching with ALCAM-CD6 Co-Stimulation in Joint-Draining Lymph Nodes During Advanced TNF-Tg Arthritis
19	Gulzada Kulzhanova	Integrated scRNA-seq and spatial transcriptomics analysis uncovers distinct cellular populations and transcriptomes in human hip synovium between patients with femoroacetabular impingement and osteoarthritis
20	Alyson March	In vitro screening of proangiogenic engineered extracellular matrices to promote tissue engineerd periosteum-mediated allograft healing
21	Clyde Overby	Zwitterionic Peptide Sequence Dictates Anti-Fouling Behavior and Protein Adsorption Profile on Nanoparticle Surfaces
22	Yue Peng	Protective Role for Mast Cells in TNF-induced Inflammatory-Erosive Arthritis and Its Associated Lymphatic Dysfunction in Mice
23	Azmeer Sharipol	Bone Marrow Microenvironment on a Chip (BMME-Chip) for Investigating the BMME during Hemostasis and Acute Myeloid Leukemia
24	Brian Wise	Phenotypic characterization of a novel mouse hind limb explant model of Achilles tendon impingement

Posters

25	Brittany Abraham	Investigating peptide sequence effects on competing thiol-ene functionalization and crosslinking reactions in poly(ethylene glycol) hydrogels
26	Emmanuella Adjei-Sowah	Investigating the bio-distribution functionalized nanoparticles for tendon healing
27	Janitri Venkatachala Babu	Targeting TRPC6 for Chronic Discogenic Back Pain
28	Sayantani Basu	Transcriptome Analysis of Autograft Mediated Bone Healing to Efficiently Design Engineered Periosteum
29	Mina Botros	Percutaneous Versus Open Pedicle Screw Fixation in Spinal Tumor Resection and Reconstruction: A Matched-Cohort Study
30	Mina Botros	Racial Disparities in Surgical Outcomes after Pediatric Scoliosis Corrective Surgery
31	Katherine Broun	Chondrocyte mechano-sensitivity following a massive rotator cuff tear
32	Petra Cazzanelli	TLR-2 Activation Dysregulates miR-100-5p and miR-155-5p Leading to the Downregulation of c-Fos
33	Indika Chandrasiri	Reproducible and Controlled Peptide Functionalization of Polymeric Nanoparticles for Bone Targeted Drug Delivery

34	Chunmo Chen	Osteoblasts efferocytosis induces osteoblasts' senescence and apoptosis
35	Zhongxuan Chen	Overexpression of Cezanne Causes Early-Onset Osteoporosis in Mice
36	Michael Christof	Osteoclast Formation Dependent on Sex and Location of Derivation in Inflammatory Arthritis
37	Jordan Cruse	Analyzing the Characteristics of Geographic Regions with High Racial and Ethnic Disparities in Total Joint Replacement Use
38	Adwin Denasty	Surgical Management of Spinal Epidural Abscess: Risk Factors and Outcomes
39	David DiStefano	A comparison of intraoperative details and postoperative outcomes in stemmed and stemless humeral components in anatomic total shoulder arthroplasty
40	Chrysilla Emanuelle	Differential roles of Piezo1 and TRPV4 in Injury-induced Chondrocyte Death in situ
41	Katherine Escalera-Rivera	Elucidating the role of NR4A1 in cartilage homeostasis and osteoarthritis progression
42	Samuel Florentino	Identifying Knowledge Gaps in Medical Student Education of Patient Reported Outcomes
43	Vijay Singh Gondil	Targeting penicillin binding protein-4 as a novel target for treatment of Staphylococcus aureus induced osteomyelitis
44	Paul Guirguis	The Extent that Morbid Obesity is a Modifiable Risk Factor Among Morbidly Obese Patients with Joint Osteoarthritis without Participating in a Formal Perioperative Optimization Program
45	Victoria Hansen	Integration of single cell RNA sequencing and spatial transcriptomics reveal molecular components of cell-cell communication in chondrogenesis over time during embryonic limb development
46	Cih-Li Hong	Intravital tracking of bone remodeling and the hematopoietic stem cell niche.
47	Nick James	DNA damage-induced proinflammatory signaling and DNA repair in chondrocytes
48	Chen Jiang	In vivo Engineered Extracellular Matrix as Scaffolding Materials for Tissue-Engineered Periosteum
49	Alanna Klose	StaphAIR microarray detecting antibody responses to Staphylococcus aureus virulence factors in human serum
50	Haiyin Li	A Clinical Association of a Voltage-gated Calcium Channel Cav1.2 with Tendinopathy
51	Xi Lin	Combined Osteoprotegerin and VEGF-C treatment synergistically reduces age-related cartilage loss and synovial lymphatic dysfunction by preventing RANKL-mediated VEGFR3 degradation
52	Kevin Ling	Development of Tissue-Specific, Perfusable Vasculature in Microphysiological Systems
53	Serena Liu	adiographic outcomes and complications following cervical laminoplasty
54	Melissa, Kevin MacLiesh, Lee	Intravital microscopy for mapping the stem cell niches that support survival and clonal expansion of myeloid leukemia
55	Iker Martinez Zalbidea	Treatment of intervertebral disc cells with CRISPR modified MSC derived EVs

56	Nida Meednu	SLAMF7 expression on T-bet B cells is induced by RA synovial proinflammatory signals
57	Tianfeng Miao	Tracing the Fate of the Subtypes of Endothelial Cells during Auto and Allograft Bone Healing
58	Hayley Miller	A stretchable tendon-on-a-chip platform for investigating the role of mechanical forces in PAI-1-mediated tendon fibrosis
59	Ankit Punreddy	Can 4-AP be used for treatment and/or prevention of CIPN
60	Emily Quarato	Inhibition of Axl and Tyro3 blocks mesenchymal stromal cells efferocytosis and increases bone density in aged mice.
61	Gabriel Ramirez	Minimal Clinically Important Difference using the Patient-Reported Outcomes Measurement Information System in Orthopadic Outpatient Procedures of Cohort Size N=1
62	Youliang Ren	Intravital Multiphoton Laser Scanning Microscopy Quantification of the "Race for the Surface" Between Host Cells and Bacteria in a Murine Model of Staphylococcus aureus Implant-Associated Bone Infection
63	Tiffany Robinson	Regeneration Informed Design of a Tenogenic Biomaterial
64	Benjamin Rodems	The Role of TauT in Bone Formation and Maintenance
65	Motoo Saito	Identification of T cell exhaustion as a biomarker of S. aureus chronic osteomyelitis in humanized mice
66	Kyra Sandercock	Examining the role of CCL20/CCR6 chemokine signaling in Staphylococcus aureus osteomyelitis
67	Derek Schloemann	Racial and Ethnic Disparities in Treatment of Congenital Hand Differences in New York State
68	Churou Tang	Expression of TRAF3 by mature osteoblasts protects mice from age- and menopausal-related osteoporosis
69	Nicholas Wagner	Cellular Characterization of Human Peritendinous Fibrotic Scar Tissue by scRNA-seq
70	Baixue Xiao	Impacts of Nanoparticle Protein Corona on Macrophage Polarization
71	Ming Yan	3D Printable Carboxymethyl Chitosan-Amorphous Calcium Phosphate Nanoparticles Inhibit Osteoclast Maturation and Activity
72	Chen Yu	Crosstalk Between the Mitochondrial Permeability Transition Pore and Adipogenesis in BMSCs
73	Jane Zhang	Mesenchymal Stromal Cell Efferocytosis is Blocked in vitro by Inhibition of Tyro3, Axl and MerTK Receptors
74	Victor Zhang	Altering collagen type I:III ratio affects immune cell motility in in vitro hydrogel tissue models
75	Lindsay Schnur	B^2MTI Cores: Micro CT Imaging
76	Lindsay Schnur & Kyle Jerreld	B^2MTI Cores: IVIS Multipsectral Imaging
77	Kyle Jerreld	B^2MTI Cores: Biomechanics
78	Jeff Fox	HBMI Core: Histology and Immunohistochemistry

Clinical Hour Abstracts

Disclaimer

Title: **Association of Total Knee Replacement Removal from the Inpatient-Only List with Outpatient Surgery Utilization and Outcomes in Medicare Patients**

Presenting Author: Derek T. Schloemann, MD, MPHS

Co-Authors: Thomas Sajda, MD, PhD, Benjamin F. Ricciardi, MD, Caroline P. Thirukumaran, MBBS, MHA, PhD

Lab PI / Mentor: Caroline P. Thirukumaran, MBBS, MHA, PhD, OrthoPOD Lab

Abstract (3500 characters or 500 words Limit)

INTRODUCTION: Little is known about the impact of total knee replacement (TKR) removal from the Medicare inpatient-only (IPO) list in 2018 on outcomes in Medicare patients. Our objectives were to evaluate (1) patient factors associated with outpatient TKR use, (2) outcomes after outpatient versus inpatient TKR, and (3) whether the IPO policy was associated with changes in post-operative outcomes for patients undergoing TKR.

METHODS: We used 2016-2019 administrative claims data from the New York Statewide Planning and Research Cooperative System to examine outpatient TKR utilization and outcomes after TKR and THR. The key independent variables were procedure (TKR vs. THR) and time (before or after policy implementation). We estimated multivariable generalized linear mixed models to identify patient factors associated with outpatient TKR use, and with a difference-in-differences (DiD) strategy to examine association of the IPO policy with post-TKR outcomes relative to post-total hip replacement (THR) outcomes in Medicare patients. The study was approved by the Unversity of Rochester Institutional Review Board.

RESULTS SECTION: There were 37,588 TKR procedures performed from 2016-2019, with 1,684 outpatient TKR procedures from 2018-2019. Older, Black, and female patients; and patients treated in safety-net hospitals were less likely to undergo outpatient TKR. After IPO policy implementation in the TKR cohort, there were lower adjusted 30-day readmissions (adjusted difference [AD]: -2.11%, 95% confidence interval [CI]: -2.73 to -1.48, P<0.001), 90-day readmissions (AD: -3.23%, 95%CI: -4.04 to -2.42, P<0.001), 30-day ED visits (AD: -2.45%, 95%CI -3.17 to -1.72, P<0.001), 90-day ED visits (AD: -4.01%, 95%CI -4.91 to -3.11, P<0.001) and higher cost per encounter (AD: $2,988, 95%CI: 415 to 5,561, P=0.03). However, these changes did not differ from changes in the THR cohort except for increased TKR cost of $770 per encounter (AD: $770, 95%CI: 83 to 1,457, P=0.03) relative to THR.

DISCUSSION: Although patients undergoing outpatient TKRs have superior outcomes compared to those undergoing inpatient TKRs, older, Black, and female patients, and patients in safety-net hospitals may have lesser access to outpatient TKRs highlighting concerns of disparities. IPO policy was not associated with changes in overall healthcare use or outcomes after TKR, except for an increase of $770 per TKR encounter.

SIGNIFICANCE/CLINICAL RELEVANCE: This work demonstrates the impact of a change in Medicare policy on important outcome measures for patients undergoing lower extremity total joint replacements. This work also shows promising outcomes of outpatient total knee replacements in Medicare patients but also demonstrates evidence of disparities in access to these outpatient surgeries.

Title: **Ultrasound Shear Wave Metric for Assessing Flexor Tendon Healing: A Preliminary Cadaver Study**

Presenting Author: Gilbert Smolyak

Co-Authors: Michael Schrader, Alayna E. Loiselle, Michael S. Richards

Lab PI / Mentor: Constantinos Ketonis

Abstract (3500 characters or 500 words Limit)

Introduction: Flexor tendon (FT) injuries of the hand are common and functional restoration after surgical repair represents a challenge. Currently, there are no longitudinal non-invasive metrics of tendon healing. B-mode ultrasound (US) has been proposed as a metric to quantify scar-tissue volume (STV) during tendon healing, however STV is not a functional metric. We propose using shear wave elastography to measure the in vivo force in the tendon with a direct measure of the external force at the tip of the injured digit as functional metric of the mechanical efficiency of the tendon.

Methods: A custom rig was designed to hold cadaver hands in a fixed position. A force sensor was attached to the distal phalanx of the tested finger to maintain an isometric state during testing. The flexor digitorum profundus (FDP) tendon was attached to an Instron machine. A GE 9-LD linear array transducer was used to image the tendon in the palm, just distal to the transverse carpal ligament. A Verasonics Vantage 256 system was used to generate acoustic radiation pushes in the tendon and the shear wave speed (SWS) was measured at the push depth. Tendon force, SWS estimated force and fingertip force were acquired for 1 mm increments of tendon extension from rest up to a max SWS estimate of 25 m/s. SWS force measurement was compared to the Instron Force measurement using a linear regression. The baseline measurement of tendon force efficiency (EFFINS) was found by a linear regression of the Instron force versus fingertip force. The SWS estimated efficiency (EFFSWS) was similarly calculated for comparison.

Results: Linear regression of the US measured SWS estimated force versus Intron measured force resulted in slopes of 0.86 (R2=.91), 1.02 (R2=.83) and 1.28 (R2=.93). The calculated EFFSWS for these tendons were 0.09, 0.17 and 0.14 verses the EFFINS measurements of 0.08, 0.18 and 0.18 respectively.

Conclusions: Our preliminary data suggests the feasibility measuring the EFFSWS metric utilizing noninvasive SWS speed estimates to quantify the force in a FT while simultaneously measuring finger-tip force. In combination with a STV measurement for quantifying of scar tissue size, these clinical metrics have the potential to improve the longitudinal assessment of tendon healing following injury and guide patient specific therapy protocols.
Acknowledgements: This study was supported by a pilot award from the University of Rochester Medical Center's UNYTE Translational Research Network in the Clinical & Translational Science Institute.

References: [1] Deng, Yufeng, et al. "Ultrasonic shear wave elasticity imaging sequencing and data processing using a verasonics research scanner." IEEE transactions on ultrasonics, ferroelectrics, and frequency control 64.1 (2016): 164-176. [2] Martin, Jack A., et al. "Gauging force by tapping tendons." Nature communications 9.1 (2018): 1-9.

Title: **Trends in total hip, knee, and shoulder arthroplasty procedures being performed in Ambulatory Surgery Centers in New York State**

Presenting Author: Thomas Sajda MD PhD

Co-Authors: Derek T. Schloemann, MD, MPHS, Caroline P. Thirukumaran, MBBS, MHA, PhD, Benjamin Ricciardi MD

Lab PI / Mentor: Benjamin Ricciardi MD

Abstract (3500 characters or 500 words Limit)

Introduction:
The removal of total knee replacement (TKR) from the Medicare inpatient-only (IPO) list in 2018 spurred the expansion of outpatient TKAs, potentially allowing for significant decreases in healthcare costs while offering more efficient care to a larger number of patients. However, the full extent of these changes for patients, surgeons, and administrators continues to be evaluated. The recent addition of TKA to the Ambulatory Surgery Center (ASC) covered surgical procedures list in 2020 will likely potentiate this evolution not only for outpatient TKR, but for total hip and shoulder replacement (THR and TSR, respectively) as well, further underscoring the importance to evaluate and understand the impact of these decisions. Our objectives were to evaluate the trends in the proportion of total knee, hip and shoulder cases performed in ASC over time and identify patient characteristics associated with an increased likelihood of undergoing these procedures at an ASC.
Methods:
We used 2011-2020 administrative claims data from New York Statewide Planning and Research Cooperative System to examine ASC utilization for TKR, THR, and TSR. We presented unadjusted rates of ASC utilization and estimated multivariable logistic regression models to evaluate factors associated with higher or lower likelihood of surgery being performed in ASCs.
Results:
There were 651,230 total joint replacement (TJR, includes TKR, THR, and TSR) procedures performed during the study period, with 3,673 performed at ASCs. Since 2014, the percentage of THR, TKR, and TSR performed at ASCs increased each year throughout the remainder of the study period. In 2014, only 15 of the 60,390 (0.02%) procedures performed was completed at an ASC, while in 2020, 1,655 of 65,746 (2.52%) procedures performed were performed at an ASC
Multivariable analysis identified multiple characteristics associated with increased likelihood of undergoing TJA at an ASC. The odds of undergoing TJR at ASC were highest for Non-Hispanic Whites and other race and ethnicity (OR 4.14, 95%CI 3.21-5.32, P<0,001 and OR 5.28, 95%CR 4.04 - 6.91, P<0.001, respectively). Patients with a comorbidity score of 1, or 2 or more were significantly less likely to have a TJR performed at an ASC (OR 0.04, 95%CI 0.03 - 0.05, P<0,001 and OR 0.01, 95%CR 0.01 - 0.01, P<0.001, respectively). Patients with private insurance were also significantly more likely to undergo TJR procedures at an ASC, compared to those with Medicare, Medicaid, and Workers Compensation (OR 0.17, 95%CI 0.15 - 0.19, P<0,001, OR 0.03, 95%CI 0.02 - 0.05, P<0,001, and OR 0.32, 95%CI 0.27 - 0.37, P<0,001, respectively)
Conclusion:
Our study demonstrates increasing utilization of ASCs for TJR, describes the characteristics of patients undergoing TJR at ASCs, and identifies specific patient characteristics associated with a higher likelihood of undergoing TJR at an ASC. This study is clinically relevant because it examines the recent trends in TJR performed at ASCs and shows increasing rates of THR and TSR as well as TKR being performed at ASCs. Additionally, this study describes characteristics of patients who are more likely to undergo TJR at ASCs.

Title: **Intraoperative blood loss with use of High or Low Dose Tranexamic Acid in metastatic spine tumor surgery, a matched case control study**

Presenting Author: Mark C. Lawlor, MD

Co-Authors: Gabriel A. Ramirez, MS, Addisu Mesfin, MD

Lab PI / Mentor: Addisu Mesfin, MD

Abstract (3500 characters or 500 words Limit)

INTRODUCTION: Surgery for metastatic spine disease is increasing in prevalence due to increased life expectancy following cancer diagnosis. Antifibrinolytic agents such as Tranexamic Acid (TXA) have been used to reduce intraoperative blood loss. However, there is no universally accepted dosing protocol for its use during spinal tumor surgery. Use of TXA has been theorized to increase the risk of thromboembolic and cerebrovascular accident (CVA) related complications. The objectives of our study were (i) to compare estimated blood loss (EBL) with use of high dose TXA versus low dose TXA versus no TXA during metastatic spinal tumor surgery (ii) to determine the rates of thromboembolic and CVA events.

METHODS: Patients undergoing spine tumor surgery for metastatic spine disease with one surgeon from 1/2015 to 4/2022 and receiving either high dose TXA (30mg/kg loading and 5 or 10 mg/kg/hr maintenance), low dose TXA (10mg/kg loading and 1mg/kg/hr or 5mg/kg/hr) or no TXA were enrolled. Patient demographics, EBL, histology, level of surgery and thromboembolic/CVA complications were evaluated. Patients were matched according to age, gender, histology type and level of surgery (either cervical, thoracic or lumbar). A multivariable regression analysis was then performed.

RESULTS: A total of 87 adult patients met the inclusion criteria. 26 patients (29.9%) received High Dose TXA, 36 patients (41.4%) received low dose TXA, and 25 patients (28.7%) received no TXA. The mean age was 64.29 (SD12.87). 34 (39.08%) were female and 53 (60.92%) were male. 77 (88.51%) were White and 10 (11.49%) were non-white. 23 patients (26.44%) had cervical or cervicothoracic procedures, 40 patients (45.98%) had thoracic or thoracolumbar procedures and 24 patients (27.59%) had lumbar, lumbosacral or sacral procedures. 12 patients (13.79%) had metastatic breast cancer, 18 patients (20.69%) had metastatic lung cancer, 11 patients (12.64%) had multiple myeloma, 12 patients (13.79%) had metastatic prostate cancer, 8 patients (9.20%) had metastatic renal cell carcinoma, and 26 patients (29.89%) fell into the other cancer category including adenoid cystic, colon, endometrial, esophageal, hepatic, lymphoma, melanoma, ovarian, pancreatic, thyroid, rectal and urothelial carcinoma. There was no significant difference between EBL in the high dose TXA 535.58ml (SD:554.08), low dose TXA 608.33ml (SD:483.92) and no TXA 624.40ml (SD:604.63) (P=0.389). There were no cases of DVT, PE or CVA in the no TXA group (0%). There were 5 cases (8.06%) of DVT, PE or CVA in the High or Low Dose TXA group though this was not found to have significance (P=0.144). No significant associations were found when controlling for covariates.

DISCUSSION: Intraoperative use of High Dose TXA and Low Dose TXA compared to no TXA use did not show a significant decrease in EBL with use in metastatic spine tumor surgery. There was not a statistically significant higher incidence of clotting events with use of TXA compared to no TXA use in metastatic spine tumor surgery. Our sample size was underpowered and thus large prospective randomized studies are needed to evaluate the efficacy of TXA dosage in decreasing blood loss during spine tumor surgery.

Title: **Do Patient Reported Outcomes Collected in Clinic Predict the Need for Additional Follow-up Visits After Surgery?**

Presenting Author: Jefferson Hunter, MD/MBA (MD 2024 Candidate)

Co-Authors:

Gabriel Ramirez, MS

Caroline Thirukumaran, MBBS, MHA, PhD

Judith Baumhauer MD, MPH

Lab PI / Mentor: Judith Baumhauer MD, MPH

Abstract (3500 characters or 500 words Limit)

ABSTRACT

Background: The Patient-Reported Outcome Measurement Information System (PROMIS) is a group of validated Patient Reported Outcomes (PROs) that are used to quantify patients' symptoms and assess progress quickly and accurately. The purpose of this study is to determine patients' recovery pattern of improvement based on preoperative PROMIS Pain Interference (PI) scores and use this information to determine if a subsequent follow-up appointment is needed. The cost-savings obtained by using PROs to allow well progressing patients to follow-up on an as needed basis will be calculated.

Methods: Retrospective PROMIS PI data were obtained for common elective foot (n=832) and ankle (n=851) surgical procedures. Patients were divided into quartiles according to their preoperative PI score (quartile one being 25% of patients with the lowest PI scores). A cox proportional hazards model stratified by preoperative PI score quartile was used to predict patient recovery. Well-progressing patients were defined as having two consecutive minimal clinically important change scores (MCID) using distribution method.

Results: Two consecutive decreases in MCID measured by PI PROMIS t-scores were achieved 90 days post-operatively by 16%, 16%, 17%, and 23% of post-operative ankle patients in quartiles 1-4 respectively; post-operative foot patients achieved 18%, 11%, 20%, and 26% in quartiles 1-4 respectively. Days 30-60 recorded the greatest rate of improvement across quartiles with Q4 showing the greatest improvement. The least improvement occurred between days 90-120 across all quartiles. Patients receiving elective foot surgery averaged 1.80 visits while elective ankle surgery patients averaged 2.81 follow-up visits after achieving two consecutive MCID improvement. Costs of these visits average $160 and $238 in additional charges per foot and ankle patient respectively.

Conclusion: Patients who are progressing well may unnecessarily continue to visit the office. Asking patients to complete the PROMIS PI prior to a follow-up visit can inform the physician and patient of their progress and may reduce follow-up visits and associated direct and indirect costs.

Rosier Award Finalists Post-Doc Abstracts

Title: **Human NGFR+/VCAM-1+/MCAM+ Bone Marrow-derived Stromal Cells (NVML) Provide Enhanced Support for Normal Hematopoiesis and Are Disrupted in Myelodysplastic Syndrome**

Presenting Author: Yuko Kawano

Co-Authors: Yuko Kawano, Hiroki Kawano, Dalia Ghoneim, Thomas J. Fountaine, Daniel K. Byun, Mark W. LaMere, John M. Ashton, Mitra Azadniv, Jane L. Liesveld, Youmna Kfoury, David T. Scadden, Michael W. Becker, Laura M. Calvi

Lab PI / Mentor: Laura Calvi

Abstract (3500 characters or 500 words Limit)

The bone marrow microenvironment (BMME) is indispensable for support of normal and malignant hematopoiesis. Mesenchymal stem/stromal cells (MSCs) give rise to multiple non-hematopoietic components that play a pivotal role in myelodysplastic syndromes (MDS). However, therapeutic targeting of MSCs has been challenging, in part due to the limited definition of the heterogeneity of MSC populations from human bone marrow (BM). Using BM from normal healthy controls (NBM) obtained through aspirates, we successfully identified two novel distinctive subsets of human MSCs by combining three MSC cell surface markers: CD271/ Nerve Growth Factor Receptor (NGFR), CD106/ Vascular Cell Adhesion Molecule-1 (VCAM-1) and CD146/ Melanoma Cell Adhesion Molecule (MCAM). We first isolated three BM-derived non-endothelial lineage(CD45/CD235ab/CD34/CD31-) cell populations from NBM: CD271+/CD146- (NGFR+/Lineage- cells: NLCs), CD271+/CD146+/CD106+ NGFR+/VCAM1+/MCAM+/Lineage- NVML cells), and CD271+/CD146+/CD106- (NGFR+/MCAM+/Lineage-; NML cells). Transcriptional profiling by RNA-seq revealed that NLCs and NVML cells represent distinct populations, whereas NML cells are a transitional population. Transcriptional analysis suggested that NVML cells, compared to NLCs, have stem cell characteristics, including quiescence and multipotentiality, and express higher levels of key genes critical for the support of hematopoietic stem and progenitor cells (HSPCs), including CXCL12 (SDF1A), Kit ligand (KITLG) and Angiopoietin-1 (ANGPT1). This signature was compatible with BM-derived Leptin receptor+ MSCs with high capacity of supporting HSPCs based on previously reported single cell RNA-seq analysis in mice. Consistent with their transcriptome, functional analysis showed that NVML cells had higher colony forming units (CFU-F) and tri-lineage differentiation capacity compared to NLCs. Normal NLCs or NVML cells were also co-cultured with NBM or human MDS cell line (MDS-L) to evaluate the supporting ability of these MSC populations for HSPCs. NVML cells provided increased support for normal hematopoietic progenitors compared to baseline and NLCs, whereas NLCs showed increased ability of supporting MDS-L. We next profiled the transcriptome of NLCs and NVML cells from 17 patients with MDS in comparison with age-matched healthy controls. Despite the mutational heterogeneity in this MDS patient cohort, volcano plot of expression patterns of transcriptomes showed a distinctive shift of MDS-derived NVML cells compared to controls. Upregulated pathways and gene ontology analysis of differentially expressed transcripts in NVML cells from MDS compared to controls identified signals related to DNA/RNA processing, while most of the down-regulated transcripts identified cytokines/chemokines critical for HSPCs. Moreover, critical genes for HSPC support highly expressed in normal NVML cells (e.g. SDF1A, ANGPT1) were significantly down-regulated with MDS-derived NVML cells compared to control. Together these data suggest that, despite the mutational heterogeneity in the hematopoietic clone, MDS may differentially impact these novel human marrow MSC subsets, decreasing normal HSPC support by disrupting NVML cells. Therefore, our novel strategy to enrich critical human BM MSC subsets that differentially support normal and malignant hematopoiesis represents a new paradigm to accelerate therapeutic targeting of the BMME in MDS and other hematologic malignancies.

Title: **Single cell RNA sequencing reveals age-dependent decline of fibroblast population in murine knee synovium**

Presenting Author: Xi Lin

Co-Authors: Hengwei Zhang, Andrew McDavid, Brendan F. Boyce, Lianping Xing

Lab PI / Mentor: Lianping Xing

Abstract (3500 characters or 500 words Limit)

Aging is an important risk factor for (OA). Pathology in the synovium has been reported to play an important pathogenetic role in OA. Although many studies have utilized transcriptomic techniques to study synovial tissues from elderly OA patients, these samples are typically from advanced stage OA and thus do not allow exploration of temporal changes in affected joint synovium during aging, in particular detection of transcriptomic changes during early OA. Transcriptomic studies on post-traumatic (PT) OA synovial samples in mouse models, revealed significant involvement of synovial fibroblasts in maintaining joint homeostasis by producing growth factors, collagens, and lubricants for the joint, as well as detrimental molecules. However, unlike age-related OA, PTOA has a defined time-point for the onset of OA. Thus, it is critical to explore the transcriptional profile of OA synovium, especially of samples taken before a prominent OA phenotype develops. To examine synovial cell populations in a natural aging mouse model of OA, we performed single-cell RNA sequencing (scRNA-seq) on 6108, 6210, and 9151 TER119-DAPI- cells that were directly isolated from 4-m (young), 15-m (middle-aged), and 27-m (aged) mouse knee synovium, respectively. Synovial cells were annotated by combining unsupervised clustering and putative markers, identifying a total of 21 clusters. Myeloid lineage cells included monocytes (Itgam+, cluster 0, 1, 4, 10), macrophages (Cd68+, cluster 5, 6, 8, 14, 17), neutrophils (Elane+, cluster 9), B cells (Cd79a+, cluster 9, 11, 15), T cells (Cd3e+, cluster 7), granulocytes (Gzma+, cluster 13), and mast cells (Cpa3+, cluster 16). The major non-myeloid lineage cells were mainly fibroblasts (Col6a1+, cluster 2), and smaller populations, including skeletal stem progenitor cells (Acta2+, cluster 18), smooth muscle cells (Acta1+, cluster 19), and endothelial cells (Emcn+, cluster 20). To explore whether there is a shift in populations in the synovium during aging, we compared population percentage longitudinally. Consistent with reports that inflammation increases during aging, we found that most myeloid lineage populations increased during aging, except for one sub-population of macrophages, characterized by MHCII-related genes. Interestingly, non-myeloid lineage cells, most prominently the fibroblast population, markedly decreased during aging. Whether the decrease of synovial fibroblasts is due to decreased proliferation, increased apoptosis, or transition into other cell types requires future investigation. Of note, we did not find clear changes in genes related to proliferation or apoptosis in our dataset. Finally, to characterize the fibroblast population in the synovium, we inquired levels of Prg4 and Thy1 expression in our dataset, which are markers for lining and sublining fibroblasts, respectively. Consistent with literature reports, synovial fibroblasts can be divided roughly into lining and sublining cells. Unsupervised clustering within the fibroblast population revealed 8 subclusters. Despite the overall decrease of the fibroblast cell number, the percentage of subcluster 2 Thy1+MMP3+ of sublining fibroblasts increased during aging, suggesting a slower decline of this population, which may be a distinct feature for aged-related OA. In summary, we confirmed that there is heterogeneity in synovial cell populations and discovered an age-dependent decline in the synovial lining fibroblast population.

Title: **Efficacy of Bisphosphonate-Conjugated Sitafloxacin in a Murine 1-Stage Revision Model of S. aureus Osteomyelitis**

Presenting Author: Youliang Ren

Co-Authors: Jason Weeks, Thomas Xue, Joshua Rainbolt, Karen L. de Mesy Bentley, Ye Shu, Chad A. Galloway, Yuting Liu, Philip Cherian, Jeffrey Neighbors, Frank H. Ebetino, T. Fintan Moriarty, Shuting Sun, Edward M. Schwarz, Chao Xie.

Lab PI / Mentor: Chao Xie

Abstract (3500 characters or 500 words Limit)

INTRODUCTION: Methicillin-resistant S. aureus (MRSA) infection of bone is considered difficult to be cured due to its ability to colonize the osteocyte-lacuno canalicular network (OLCN) and S. aureus community (SAC) formation. However, standard of care (SOC) antibiotics delivered systemically and locally have no effect on SAC and OLCN in bone. To address this issue, we developed hydroxybisphosphonate or bisphosphonate conjugated sitafloxacin (HBCS or BCS) that bind to metabolically active bone surfaces after systemic administration completing the “target-and-release” drug delivery. Here we tested the hypothesis that the combination of a SOC antibiotic vancomycin with HBCS can prevent osteolysis by killing S. aureus within the OLCN and SAC in a one-stage-revision murine model of S. aureus chronic osteomyelitis.

METHODS: All experiments with C57 BL/6 female mice (n=5 or 10) were performed on IACUC-approved protocols. We utilized a murine 1-stage exchange model of fluorescent strain MRSA (USA300LAC::lux) contaminated femoral implants. Following an infection surgery, the original plate and two screws were removed on day 7, and exchanged with sterile implants. Mice were randomized to seven groups for day 7-21 treatment: 1) Baseline (Harvested at day 7, no treatment); 2) HPBP (vehicle control for BCS) + vancomycin; 3) HPHBP (vehicle control for HBCS) + vancomycin; 4) Vancomycin; 5) Sitafloxacin; 6) BCS+vancomycin; and 7) HBCS+vancomycin. The initial infection status was assessed via colony forming units (CFU) on explanted hardware. Bioluminescent imaging (BLI) was performed on days 0, 1, 3, 5, 7, 8, 10, 12, and 14. Mice were euthanized on day 21 for micro-CT, Brown & Brenn and TRAP stained histology and TEM as previously described. Data are presented as means + SD for each group, and statistical $p<0.05$ was considered significant.

RESULTS: 1) Longitudinal BLI demonstrated that BCS and HBCS have stronger antimicrobial efficacy than free vancomycin and sitafloxacin. This is consistent with our previous findings in acute infection. 2) BCS + Vancomycin and HBCS + Vancomycin significantly reduced the occurrence of fracture in infected bone. X-rays and Micro-CT at day 21 revealed catastrophic femur fractures in all experimental groups except BCS + Vancomycin and HBCS + Vancomycin treated groups (n=3). The Micro-CT volumetric quantification of screw holes showed significantly low osteolytic bone loss compared with the other groups (*$p<0.05$). These results were confirmed by the TRAP-stained histology of osteoclasts, which were significantly decreased in BCS and HBSC treatment groups. 3) TEM evidence of BCS and HBCS killing of MRSA in SACs within the bone marrow space. Representative TEM images of the bacteria within SACs or canaliculi of the infected bone are shown to illustrate the morphology of the bacteria within SACs or canaliculi on day 14 post one-stage revision. TEM of the infected bone demonstrated strong evidence of HBCS and BCS induced cytotoxicity from drug inhibited DNA gyrase and topoisomerase IV as our previous described.

DISCUSSION: We demonstrate the 1st proof of concept that BCS and HBSC can kill bacteria within SACs and OLCN in a chronic infection model, which also decrease osteolysis and fractures. The excellent benefits of vancomycin and HBCS administered together could provide novel insights into the treatment of MRSA bone infection.

Rosier Award Finalists Pre-Doc Abstracts

Title: **Elucidating Androgen Effects on Focal Erosions in TNF-Induced Inflammatory Arthritis**

Presenting Author: Kiana L. Chen

Co-Authors: Kiana L. Chen, H. Mark Kenney, Edward M. Schwarz, and Homaira Rahimi

Lab PI / Mentor: Homaira Rahimi

Abstract (3500 characters or 500 words Limit)

Rheumatoid arthritis (RA) is a chronic inflammatory joint disease and is female predominant. In the TNF-transgenic (TNF-Tg) mouse model of RA, females develop more aggressive inflammatory-erosive arthritis than males of the same age and die significantly earlier (1). However, the mechanisms responsible for this sexual dimorphism remain unknown. Studies suggest sex hormone variations as a possible explanation, with androgens providing a protective effect against joint disease and TNF-mediated bone erosion (2,3). Thus, we tested the hypothesis that androgens' anti-inflammatory effects mediate erosive arthritis progression.

Orchiectomies and sham surgeries were performed on 4-week-old male TNF-Tg and wildtype (WT) mice (n=3-8 mice/group). Micro-computed tomography (μCT) scans of hindpaws were taken at 3-months of age for each group and compared with scans of same age TNF-Tg females (n=5). Total bone volumes were determined utilizing a validated semi-automated segmentation method (4). Cuboid bone volume (mm3) was compared between groups, along with the bone volumes of the distal ends of the fourth and fifth (most lateral) metatarsals to quantify periarticular erosions seen in hindpaws. Statistics include one-way ANOVA with Tukey's post-test for cuboid and metatarsal volume comparison, and an unpaired t-test for comparison with TNF-Tg female cuboid volumes. Values are reported as mean ± standard deviation.

Orchiectomized TNF-Tg mice had significantly reduced cuboid bone volume than sham TNF-Tg and WT cohorts (0.37 ± 0.03 Orchiectomized TNF-Tg; 0.42 ± 0.06 Sham TNF-Tg; 0.45 ± 0.05 Orchiectomized WT; 0.43 ± 0.04 Sham WT). There was similar cuboid bone volume between orchiectomized TNF-Tg and female TNF-Tg mice (0.37 ± 0.03 Orchiectomized TNF-Tg vs 0.36 ± 0.05 TNF-Tg Female). Orchiectomized TNF-Tg mice had significantly less bone volume than other cohorts in the fourth (0.2607 ± 0.03421 Orchiectomized TNF-Tg; 0.3580 ± 0.07852 Sham TNF-Tg; 0.3553 ± 0.02025 Orchiectomized WT; 0.3691 ± 0.04991 Sham WT) and fifth metatarsal (0.2117 ± 0.04045 Orchiectomized TNF-Tg; 0.3328 ± 0.07521 Sham TNF-Tg; 0.2843 ± 0.01852 Orchiectomized WT; 0.3107 ± 0.04619 Sham WT). There were also similar metatarsal volumes between orchiectomized TNF-Tg and female TNF-Tg mice in the fourth (0.2607 ± 0.03421 Orchiectomized TNF-Tg vs. 0.2525 ± 0.03397 TNF-Tg Female) and fifth metatarsal (0.2117 ± 0.04045 Orchiectomized TNF-Tg vs 0.2292 ± 0.03282 TNF-Tg Female).

Orchiectomized TNF-Tg mice have significantly less bone volume than other male cohorts and bone volume loss similar to TNF-Tg females, which suggests that bone loss in orchiectomized males may be equivalent to accelerated erosive disease in females. Erosions in the orchiectomized TNF-Tg distal metatarsal periarticular region are reminiscent of focal erosions seen in RA patients and exhibit increased inflammatory-erosive disease. These results suggest that androgens delay bone resorptive activity from osteoclasts and osteoclastogenesis accelerated by inflammation. Further studies using in vivo androgen treatment and in vitro examination of androgen's effects on osteoclasts are necessary to delineate androgen mediated inhibition of bone erosion.

1) Bell R.D. et al. Arthritis Rheumatol 71(9): 1512-1523. 2019.
2) Traish A et al. J Clin Med 7(12): 549. 2018.
3) Lashkari M et al. Electron Physician 10(3): 6500-6505. 2018.
4) Kenney H.M. et al. Bone Rep 16:101167. 2022.

Title: **CXCR2+TGFbeta1+ callus senescent cells represent a specific detrimental subset that inhibits fracture healing and growth of mesenchymal progenitors**

Presenting Author: Jiatong Liu

Co-Authors: Xi Lin; Andrew McDavid; Hengwei Zhang; Brendan F. Boyce; Lianping Xing

Lab PI / Mentor: Lianping Xing

Abstract (3500 characters or 500 words Limit)

Cellular senescence plays important roles in many age-related diseases. Senescent cells (SCs) can have both detrimental and beneficial effects on adjacent and distant cells, depending upon the conditions. Thus, it is important to be able to distinguish SC subsets so that detrimental SCs can be targeted. Recently, we reported that SCs are markedly increased in fracture callus of aged mice and that senolytic drugs promoted fracture healing in aged, but not in young mice, indicating heterogeneity in the effects of callus SCs. We also found that 70% of callus SCs are CD45- stromal cells, and SC numbers peaked at day 10 post-fracture (dpf). We applied single cell RNA sequencing (scRNA-seq) to callus CD45- stromal cells collected at 10 dpf from young and aged mice and found that aged stromal cells have an increased inflammatory phenotype.

Here, we reanalyzed our scRNA-seq data set to investigate phenotypic and functional heterogeneity of callus SCs and SCs were defined as cells expressing the senescent genes, Cdkn1a, Cdkn2a or Cdkn2c. Unsupervised clustering of SCs revealed 3 subsets, which showed distinct gene expression profile. Combining unsupervised clustering and putative markers of senescence-associated secretory phenotypes (SASP) and top differentially-expressed genes, SCs were sub-clustered into 3 populations, which corresponded to the expression status of CXCR2 and TGFb1. In vivo, flow analysis of callus SCs confirmed the presence of 3 subsets: cluster1 (CXCR2+TGFb1+); cluster2 (CXCR2-TGFb1+) and cluster3 (CXCR2-TGFb1-). All 3 SC subsets were increased in the callus of aged mice compared to young mice, but increased SCs resided mostly in the CXCR2+ TGFb1+ subset (9-fold increase) vs. in the CXCR2-TGFb1+ and CXCR2-TGFb1- subsets (2 and 4-fold increase, respectively). Conditioned media (CM) from these 3 SC populations had different effects on growth of callus-derived mesenchymal progenitor cells (CaMPCs). CM from sorted CXCR2+TGFb1+ SCs, but not CXCR2-TGFb1+ and CXCR2-TGFb1- SCs, significantly inhibited the growth of CaMPCs. Intra-callus injection of CXCR2+TGFb1+ SCs, but not CXCR2-TGFb1+ SCs, significantly reduced bone strength of fractured bones of young mice. No systemic effects of injected SC subsets were observed on bone strength of the contralateral legs.

In conclusion, we have identified 3 subsets of callus SCs: CXCR2+TGFb1+; CXCR2-TGFb1+; and CXCR2-TGFb1-. Among them, CXCR2+TGFb1+ SCs are the major increased SC subset in aged mice and they inhibited the growth of CaMPCs and fracture healing in young mice. CXCR2+TGFb1+ SCs represent a specific detrimental SC subset in bone callus of aged mice. In the future, we will examine the SASP expression profile of different SC subsets and study SC subsets in middle-aged mice to investigate if the detrimental role of SCs in fracture healing occurs before aging begins.

Title: **Detecting osteoporosis and predicting distal radius fracture strength using Raman spectroscopy in human fingers – A cadaveric study**

Presenting Author: Christine Massie

Co-Authors: Emma Knapp, Keren Chen, Andrew J. Berger, Hani A. Awad

Lab PI / Mentor: Hani Awad

Abstract (3500 characters or 500 words Limit)

Osteoporosis is diagnosed by measuring bone mineral density (BMD) using dual energy X-ray absorptiometry (DXA). Even though DXA T-scores are the gold standard for osteoporosis diagnosis, DXA screening rates are alarmingly low. There is a critical need for pre-screening to detect osteoporosis at earlier stages. Raman spectroscopy can serve as a non-invasive transcutaneous pre-screen for bone quality assessment, which could indicate a subsequent DXA scan for definitive diagnosis. Here we explored the potential of using Raman spectra from proximal phalanges for assessing bone quality.

Twelve fresh-frozen cadaver arm samples were obtained from the Anatomy Gifts Registry (AGR) (Hanover, MD). For each of the specimens, DXA scans were performed by AGR to measure the distal radius BMD and respective osteoporotic diagnostic T-score. Mechanical testing was performed on intact forearms to simulate a fall and induce a reproducible distal radius fracture, using methods adapted from Lochmuller et al. (2002). Raman measurements were subsequently performed both transcutaneously on the hand and on the excised proximal phalanges using an 830 nm, 120 mW laser.

Raman spectra collected from the excised phalanges showed the mean healthy spectrum (n = 3) had a relatively higher phosphate signal and lower matrix signal when compared to osteopenia (n = 4) and osteoporosis (n = 5). Principal component analysis revealed that the first principal component, mainly attributed to phosphate and matrix signals, indicated the 95.4% of the variance in the spectral dataset was due to osteoporotic related bone changes. Phosphate mineralization to matrix ratios significantly decreased with osteoporosis, while carbonate mineralization to matrix ratio and carbonate substitution significantly increased with osteoporosis. Osteoporotic samples showed a 35% reduction in maximum distal radius fracture load when compared to healthy samples, albeit these differences did not reach statistical significance. We further investigated how a non-destructive model could predict this property. By accounting for BMI, age, and distal radius BMD in a partial least squares regression, we achieved a significant prediction of maximum fracture load with a RMSECV of 245 N and a correlation coefficient (r) of 0.86 ($p < 0.05$). We investigated if Raman performed on a remote, easily assessable site yielded a comparable model. By replacing BMD with Raman ratios phosphate mineral to matrix, carbonate mineral to matrix, and carbonate to phosphate ratios measured at the diaphysis region of the phalanges, we achieved a comparable prediction model (RMSECV=309 N and r=0.79 ($p < 0.05$)). Through preliminary analysis from the transcutaneous data, we found that a direct transcutaneous measurement on the phalanges were able to predict the T-score (r = 0.71). By using a spectral unmixing algorithm, we were able to accurately extract the bone spectrum, indicated by phosphate mineralization to matrix ratio (r = 0.70). We showed our algorithm recapitulated the excised bone findings, by estimating the healthy subjects having a higher phosphate mineralization to matrix ratio when compared to osteoporosis ($p < 0.05$).

Our findings demonstrate the feasibility of using Raman spectroscopy in the peripheral bones of the proximal phalanges as a pre-screening tool to assess bone health and fracture risk in clinically relevant sites such as the distal radius.

Title: **Insulin-Like Growth Factor 1 in the Bone Marrow Microenvironment Inhibits Mesenchymal Stromal Cell Efferocytosis**

Presenting Author: Noah Salama

Co-Authors: Emily R. Quarato, Chunmo Chen, Yuko Kawano, Daniel K. Byun, Allison Li, Roman A. Eliseev, Jane L. Liesveld, Michael W. Becker

Lab PI / Mentor: Laura M. Calvi

Abstract (3500 characters or 500 words Limit)

The bone marrow is a major site of cellular clearance, removing ~10^11 apoptotic cells daily. Professional phagocytes in the bone marrow microenvironment (BMME) such as bone marrow macrophages (bMΦs) clear apoptotic cells through efferocytosis, a non-inflammatory form of phagocytosis. Imbalanced efferocytosis is seen in a variety of inflammatory conditions, and we demonstrated that defects in efferocytosis induces accumulation of apoptotic cells and hematopoietic dysfunction. Non-professional phagocytic cells can assist with clearance and recruit professionals. Our lab identified mesenchymal stromal cells (MSCs) as an important non-professional phagocyte which assists bMΦs in clearing apoptotic cells from the BMME at homeostasis. However, our preliminary data show that MSCs performing efferocytosis have increased cellular senescence aand apoptosis in a dose-dependent fashion. Therefore, signals that regulate and coordinate the efferocytic responses in the BMME could be manipulated to decrease MSC efferocytosis thereby reducing their senescence. Since studies on non-professional phagocytes in other systems have shown that Insulin Like Growth Factor 1 (IGF1) produced by MΦs restrains efferocytic activity by non-professionals, we hypothesized that the IGF1 axis could regulate MSC efferocytosis in the BMME. In support of this hypothesis, IGF1 transcripts were significantly decreased in bMΦs from aged (20–24-month-old) versus young (3–4-month-old) mice (Log2FC -2.24, adjustedP=2.02x10^-9).
Primary cell cultures from aged mice had a > 20-fold decrease in bioavailable IGF1 (ratio of IGF1:IGFBP3) compared to young mice, consistent with the reduced IGF1 reported by other labs as a functional indicator of aged bone marrow. We next tested whether addition of IGF1 in vitro decreases MSCs efferocytosis in cell lines and primary cells and found that IGF1 treatment significantly decreased the rate and efficiency of MSC efferocytosis at 3- and 24-hours. These data suggest that reduced bioavailable IGF-1 observed in aged cultures could tip the system toward excessive efferocytosis by MSC, leading to increased senescence and apoptosis. By better understanding the relationship between bMΦs and MSCs in the BMME, we may identify novel therapeutic targets that balance the clearance of ACs while mitigating the detrimental impact on stromal progenitor cells. This strategy may be helpful in scenarios where ACs can accumulate such as aging, or in pathologic states such as fracture.

Title: **Effects of Elevated Lactate in the Bone Marrow Microenvironment during Acute Myeloid Leukemia**

Presenting Author: Celia A. Soto, MS

Co-Authors: Maggie Lesch and Joshua C. Munger, PhD

Lab PI / Mentor: Benjamin J. Frisch, PhD

Abstract (3500 characters or 500 words Limit)

Acute myeloid leukemia (AML) continues to have one of the lowest cancer survival rates (~29% at five years) due to dysfunction of the bone marrow microenvironment (BMME) and loss of hematopoiesis. To define metabolomic changes in the bone marrow during disease, we assayed global extracellular metabolite levels using liquid chromatography coupled with mass spectrometry (LC/MS). This unbiased analysis demonstrated that lactate levels are elevated in the bone marrow of AML patients at diagnosis compared to healthy controls (mmol/L = 3.62 vs 1.31, $p < 0.05$, $n = 5$). We hypothesized that lactate secreted to the BMME by AML cells contributes to bone marrow dysfunction and leukemia progression including loss of normal hematopoiesis. To test this, we used both: (i) a murine model of blast crisis chronic myelogenous leukemia (bcCML), which recapitulates the metabolomic analysis of the human AML BMME, and (ii) C57BL/6J wild type or transgenic mice with a global knockout of the G-protein-coupled lactate receptor GPR81 that do not display hematopoietic defects. Bone marrow support for hematopoiesis was assayed by utilizing cocultures of murine hematopoietic stem and progenitor cells (HSPCs) maintained by a stromal monolayer of mesenchymal stem cells (MSCs) and macrophages. Exposure to physiologically-relevant elevated lactate levels reduced the ability of HSPCs to form colonies in methylcellulose-containing media (CFU-C =12.17 vs 1.167, $p < 0.05$, $n = 3$). Next, we wanted to establish which of these critical HSPC-supportive cells in the BMME are altered by excess lactate. Increasing lactate reduced MSC colony-forming ability in vitro (area in pixels = 330146 at 0 mmol/L vs 146325-18502 at 10-15 mmol/L, $p < 0.05$, $n = 3$). Also, in bcCML, leukemia-associated macrophages (LAMs) were found to overexpress a M2-like marker, mannose receptor CD206, and GPR81 signaling contributed to this phenotype in vivo (CD206 MFI = 5784 vs 2633, $p < 0.05$, $n = 3$). To determine if LAMs adversely affect hematopoiesis, coculture assays were repeated without lactate treatment, where the addition of LAMs reduced HSPC colony-forming ability compared to addition of an equal number of normal macrophages (mean fold-change CFU-C normalized to non-leukemic control = 1.00 vs 0.63, $p < 0.0001$, $n = 4$). This effect is reduced when LAMs from bcCML in GPR81-/- mice are added, compared to LAMs from bcCML in wt mice (mean fold-change CFU-C normalized to non-leukemic control = 0.69 vs 0.78, $p < 0.05$, $n = 2$), suggesting that GPR81 signaling produces LAMs that have reduced support for hematopoiesis. Finally, leukemic progression was substantially lessened by mid-stage disease when bcCML was initiated using GPR81-/- leukemia cells (% leukemia in bone = 45.54 vs 11.75, $p < 0.05$, $n = 5$). This research investigates the role of lactate as a critical driver of AML-induced BMME dysfunction and leukemic progression, thus identifying GPR81 as an exciting and novel therapeutic target for the treatment of this devastating disease. Furthermore, as lactate production is a hallmark of cancer, this mechanism is potentially applicable to multiple malignancies with bone marrow involvement including additional types of leukemia as well as bone marrow metastases of solid tumors.

Title: **Detecting alterations in tendon microstructure in the presence of diabetes using high-frequency quantitative ultrasound**

Presenting Author: Sarah E. Wayson

Co-Authors: María Helguera, Todd Jackson, Jim Chwalek

Lab PI / Mentor: Denise C. Hocking and Diane Dalecki

Abstract (3500 characters or 500 words Limit)

Parallel collagen fiber alignment is a structural feature of healthy tendon that provides tensile strength and can be disrupted in the presence of disease or injury. One challenge facing physical therapists is developing protocols for tendon mobilization without exacerbating degeneration or re-rupturing surgical repair sites. This challenge is complicated further in patients with diabetes, which impairs collagen fiber alignment, mechanical properties, and tendon healing. The objective of this work was to develop a high-frequency, quantitative ultrasound technique to characterize collagen microstructure in wildtype and diabetic murine tendon non- invasively and non-destructively. The goal of quantitative ultrasound is to advance beyond conventional B-mode imaging by extracting parameters from backscattered echoes that characterize features of the underlying tissue microstructure and are independent of the image acquisition system.

Backscattered echoes were acquired from intact murine tail tendon and skin, and excised liver at multiple insonification angles. The integrated backscatter coefficient (IBC) is a quantitative ultrasound parameter that estimates scattering strength in tissue. IBC parametric images and the average IBC in a region of interest were computed at each insonification angle. The IBC exhibited angular-dependence in tendon and angular- independence in skin and liver. The IBC was anisotropic at the intratendon and intrafascicular levels. Three metrics were investigated: (1) maximum IBC, (2) ΔIBC within ten degrees of the maximum, and (3) slope of the tangent of the IBC as a function of angle. All three metrics were significantly lower in diabetic compared to wildtype tendon. These data suggest that the IBC can be used to characterize differences in collagen microstructure between wildtype and diabetic murine tendon. This work advances quantitative ultrasound tendon characterization to study pre-clinical healing to guide rehabilitation.

Rosier Award Finalists 3MT Posters

Title: **Human Tendon-on-a-Chip (hToC) platform for modeling fibrotic disease and screening therapeutic candidates**

Presenting Author: Raquel Ajlaik

Co-Authors: Rahul Alenchery

Lab PI / Mentor: James L. McGrath & Hani Awad

Abstract (3500 characters or 500 words Limit)

Evidence indicates proliferation of myofibroblasts from quiescent tenocytes upon injury is influenced by the secretome of infiltrating immune cells and more specifically TGF-β1, leading to chronic inflammation and fibrosis. This is consistent with the hemorrhage due to vascular injury when the tendon is ruptured, yet the crosstalk between the tendon fibroblasts (TC), endothelial cells (ECs) and inflammatory cells has thus far been understudied. We hypothesized that direct and paracrine interactions between injured tendon's resident macrophages (tMϕ) and TCs mediate transvascular infiltration of circulating monocytes and their subsequent activation to secrete inflammatory cytokines and factors, including TGF-β1. This ultimately leads to activation of myofibroblasts, senescent fibroblasts and the release of senescence-associated secreted proteins (SASP), which perpetuate feedback signaling leading to chronic inflammation and a fibrovascular scar. To model this, we designed a 3D multicompartmental human tendon-on-a-chip (hToC) to investigate these interactions between TCs, ECs, circulating monocytes (cMϕ) and tMϕ's in the healing tendon's fibrovascular scar. Upon validation of the fibrotic phenotype in the hToC, we studied its use as a drug screening platform by introducing Rapamycin or Ibuprofen and monitoring the secretory and phenotypic changes of the tissues.
We observed that treatment with TGF-β1 accelerated tissue contraction, increased myofibroblast activation evident through increased expression of α-SMA, activated senescent phenotypes through upregulation of γH2A.X foci, P16, and P21 in myofibroblast indicative of an increase in DNA damage. hToC cultures showed elevated CCL3, IL-6, IL-1β, and TNF-α, indicative of a pro-inflammatory SASP profile. This was concomitant with expression of pro-inflammatory tMϕ/cMϕ markers for CD86, CD274, HLA-DR, and iNOS in the culture. Additionally, the tendon construct was processed for histology at 72-hrs of culture and immunofluorescence for TGF-β1, PTEN, and phosphorylated mTOR proteins Raptor, AKT, 4EBP1 and P70S6K colocalized with α-SMA as a control stain for myofibroblast activation in culture. Lastly, to test its use as a screening platform, Rapamycin and Ibuprofen were assessed for their immunosuppressant and anti-inflammatory effects, which could mitigate the fibrotic condition in the hToC, as both mTOR inhibitors, and NSAIDs are clinically used as antifibrosis treatments. Both therapeutic doses were selected to be in range of human serum levels during standard pharmacotherapy, yet neither treatment decreased inflammatory SASP levels compared to control, which could be an indication of the healing inefficiency seen in patients treated with common NSAIDs and mTOR inhibitors.

Human tissue-on-chip devices provide powerful tools for disease modeling and serve as platforms for evaluating the safety and efficacy during the early stages of drug development for informing clinical trial planning and executions. The activation of the mTOR pathway and upregulation of key SASPs in the hToC allows for targeted therapeutic screening of biological therapies, which aim to diminish fibrotic effects and ultimately resolve fibrovascular adhesions, which addresses unmet clinical needs in hand surgery and other tendon pathologies.

Title: **PAI-1 mediates TGF-β1 induced myofibroblast activation and senescence in tenocytes via mTOR signaling**

Presenting Author: Rahul Alenchery

Co-Authors: Raquel Ajalik, Kyle Jerreld

Lab PI / Mentor: Hani Awad

Abstract (3500 characters or 500 words Limit)

We have shown that transforming growth factor-beta (TGF-β1), the prominent driver of fibrosis, is causatively associated with tendon matrix turnover, cell proliferation, α-SMA activation and importantly, the upregulation of the putative senescence marker, PAI-1. Interestingly, recent RNA-Seq data contrasting injured and uninjured models of C57BL/6J (WT) and PAI-1 knockout (KO) mice found PTEN pathways to be significantly enriched in KO mice. PTEN is a master regulator of mTOR signaling and has been associated with the regulation of cellular proliferation and senescence as precipitating factors in fibrosis. Therefore, we hypothesized that TGF-β1/PAI-1 mediated inhibition of PTEN in tenocytes induces fibrotic tendon pathobiology through the PI3K/AKT/mTOR pathway. To test this hypothesis, tenocytes were isolated healthy KO and WT littermates and then treated with TGF-β1 (10 ng/ml) for 24 hours. Treated samples were analyzed using ICC, Western blot and Flow cytometry.

Previously, we reported the loss of PAI-1 to blunt the activation of myofibroblasts independent of TGF-β1. In this experiment, we explored mTOR signaling as an intermediary mechanism of TGF-β1/PAI-1 mediated fibrosis. We observed phosphorylated PTEN to be significantly decreased upon TGF-β1 treatment in WT tenocytes. Interestingly, in PAI-1 KO cells, TGF-β1-induced inhibition of phosphorylated PTEN is significantly attenuated when compared to WT. The results indicate that in primary tenocytes, PAI-1 plays a pivotal role in regulating PTEN expression. Contrary to our hypothesis, semi-quantitative Western blot analysis suggested that loss of PAI-1 did not influence downstream mTORC1 signaling (phosphorylated SMAD3, AKT, 4E-BP1 and S6) despite significantly perturbing phosphorylated PTEN levels. We reasoned that TGF-β1 activation of αSMA+ cells likely represents a heterogenous population. Therefore, we employed flow cytometry analysis with gating for pAKT and p4E-BP1 to measure αSMA activation, Ki67 proliferation, and γ-H2AX senescence in populations of cells with high mTOR activity (pAKT high/p4E-BP1 high) and populations of cells with low mTOR activity (pAKT low/p4E-BP1 low). Our results indicated TGF-β1 to increase overall levels of α-SMA expression in both WT and PAI-1 KO conditions. Interestingly, we observe a dramatic increase in α-SMA expression as a result of mTOR activation along the AKT-4E-BP1 axis (pAKT high/p4E-BP1 high; higher Q). Furthermore, we observe this α-SMA activation to be completely mitigated in response to the loss of PAI-1 regardless of TGF-β1 induction. Furthermore, while increased mTOR signaling was associated with increased Ki67 in both WT and KO cells, TGF-β1 treatment dramatically decreased the number of Ki67+ KO cells. Our results also show γ-H2AX, a sensitive marker of DNA damage, to be increased in response to TGF-β1, and this increased DNA damage is concomitant with increased mTOR signaling in WT cells. To the contrary, the increase in DNA damage with TGF-β1 treatment was attenuated in KO cells with high mTOR signaling activity. This flow cytometry analysis strategy has allowed us to make novel discoveries that support a critical role for PAI-1 in regulating mTOR signaling to confer the fibrogenic effects of TGF-β1 in tenocytes. To our knowledge, this is the first evidence that PAI-1 regulates mTOR signaling as an intermediate node in the context of fibrosis. As so, these experiments provide a novel therapeutic target for future in vivo studies.

Title: **Spatiotemporal analysis reveals functional role of PRDM16 in chondrogenesis and limb development**

Presenting Author: Eloise Fadial

Co-Authors: Victoria Hansen, Guulzada Kulzhanova, Gourango Pradhan, Helen Shammas, John Reuter, Eliya Tashbib, Jennifer Jonason

Lab PI / Mentor: Chia-Lung Wu

Abstract (3500 characters or 500 words Limit)

INTRODUCTION: Cartilage development is a complex process regulated by tightly-coordinated transcription factor networks modulated by epigenetics. Previous studies have reported that global knockout of epigenetic regulator Prdm16 in mice results in abnormal osteogenic differentiation. Microdeletion of a chromosome 1 locus including PRDM16 is associated with limb defects in humans. However, the detailed molecular mechanisms by which PRDM16 regulates chondrogenesis and limb development remain largely unknown. Here, we hypothesize that PRDM16 is a key regulator in chondrocyte specification, limb development, and cartilage homeostasis. We aim to elucidate the regulatory mechanisms of PRDM16 by using human induced pluripotent stem cells (hiPSCs) and cartilage-specific, conditional knockout (KO) mouse models.
METHODS: hiPSCs (n=3) were differentiated into chondrocytes using our established protocol. Cells were harvested at various stages of differentiation and submitted for bulk RNA-seq. Mouse hindlimbs were harvested from cartilage-specific Prdm16 KO mice (Col2a1-Cre; Prdm16flox/flox; (KO)) at E15.5 and E18.5 according to IACUC approved protocol. Cre-negative littermates were used as controls (WT). Prdm16 KO was confirmed by western blot at E15.5. Hindlimbs from 4-week-old mice (sex investigated independently) were submitted for microCT analysis and stained by Safranin O/Fast green. Results were analyzed with either Student's t-test or one-way ANOVA accordingly.
RESULTS & DISCUSSION: RNA-seq of hiPSC chondrogenesis revealed co-upregulation of PRDM16 with COL2A1, RUNX1, ACAN, and SOX6 at the chondrogenic progenitor (Cp) and day 7 (d7) of chondrogenic pellet stages, suggesting that PRDM16 may be involved in chondrocyte fate specification. Western blot of PRDM16 from 2 unique hiPSC lines further confirmed increased PRDM16 expression at protein levels at the Cp stage compared to hiPSCs. To validate our Prdm16 KO model, we harvested cells from costal bones and cartilage from E15.5 embryos. Western blotting confirmed that the reduction of PRDM16 was only detected in cartilage, but not in the bone of KO mice. Through histological analysis, we observed that Prdm16 KO mice exhibited decreased hypertrophic and columnar proliferative chondrocytes, but increased proliferative chondrocytes compared to WT at E18.5. No significant difference in zonal length between WT and Prdm16 KO was detected in earlier development. This loss of PRDM16 early in development appears to impair endochondral ossification. Specifically, Prdm16 KO mice aged 4 weeks, exhibited significantly altered skeletal development including reduced bone volume/total volume (BV/TV) and bone mineral density in the medial meniscus and patella (only in male mice), as well as a trend toward decreased BV/TV of tibia tuberosity and entire knee joints as compared to WT mice.
CONCLUSIONS: Our hiPSC and mouse models have identified a regulatory role of PRDM16 in knee chondrogenesis. Analysis of embryonic limbs revealed altered chondrogenesis beginning at E18.5, leading to delayed bone development. We believe that this may result from the reduced chondrocyte hypertrophy in KO mice at E18.5. Currently, we are performing single-cell RNA and CUT&RUN -seq on our established PRDM16 knockdown and overexpression hiPSC lines. The findings from this study will elucidate the functional role of PRDM16 in embryonic chondrogenesis and may be used to enhance cartilage tissue engineering for clinical applications.

Title: **Spatial and Single-Cell Transcriptomics Identify IgG2b Class-Switching with ALCAM-CD6 Co-Stimulation in Joint-Draining Lymph Nodes During Advanced TNF-Tg Arthritis**

Presenting Author: H. Mark Kenney

Co-Authors: H. Mark Kenney, Javier Rangel-Moreno, Yue Peng, Kiana L. Chen, Jennifer Bruno, Abdul Embong, Elizabeth Pritchett, Jeffrey I. Fox, Sally Quataert, Gowrishankar Muthukrishnan, Ronald W. Wood, Benjamin D. Korman, Jennifer H. Anolik, Lianping Xing, Christopher T. Ritchlin, Edward M. Schwarz, Chia-Lung Wu

Lab PI / Mentor: Edward Schwarz & Chia-Lung Wu

Abstract (3500 characters or 500 words Limit)

Severe inflammatory-erosive arthritis in tumor necrosis factor transgenic (TNF-Tg) mice is associated with B-cell translocation into sinuses of joint-draining popliteal lymph nodes (PLNs) via unknown mechanisms (1). Here, we comprehensively analyzed the transcriptional changes in PLNs of TNF-Tg mice at Early vs. Advanced stages of arthritis and unveiled the potential mechanisms orchestrating B-cell translocation by integrating spatial and single-cell transcriptomics findings.

PLNs from TNF-Tg male mice with Early (5-7-months, n=6 PLNs) and Advanced (Adv, >8-months, n=12 PLNs) arthritis were processed for spatial transcriptomics. In addition, 8,000-9,000 cells from pooled PLNs of Early and Adv TNF-Tg groups were subjected to droplet-based single-cell RNA-sequencing (scRNAseq, n=6 PLNs/group) and immune profiling scRNAseq (n=2 PLNs/group, 2 replicates). Data were analyzed with Seurat, NicheNet (cell interaction), and scRepertoire (clonality) R packages. PLN immunofluorescence (IF), flow cytometry, and ELISPOT were utilized to validate protein expression from transcriptomic analysis. Micro-CT was performed on mouse ankles to assess bone loss.

Spatial transcriptomics revealed a significant and selective increase in *Ighg2b*/*Ighm* expression ratio (1.4 ± 0.5 vs 0.5 ± 0.1 counts/counts; $p<0.001$) and considerable accumulation of IgG2b$^+$ cells in Marco$^+$ peri-follicular medullary PLN sinuses of Adv vs Early conditions. *Ighg2b* expression significantly correlated with increased bone erosions and reduced talus bone volumes in the afferent ankle joint (R^2=0.54, $p<0.001$). IF confirmed the accumulation of IgG2b$^+$/B220$^-$ plasma cells within Marco$^+$ sinuses, as shown by transcriptional analysis. Flow cytometry further demonstrated increased IgG2b$^+$/CD138$^+$ cells in PLNs of Adv vs Early TNF-Tg mice, along with increased numbers of IgG2b antibody-secreting cells by ELISPOT. PLN scRNAseq resolved 18 distinct cell populations with a notable increase in the numbers of *Slamf7*$^+$*Cd93*$^+$*Irf4*$^+$*Cxcr4*$^+$ plasma cells (2.0% Adv vs 0.08% Early of total B-cells) and an unexpected increase in T-cells (15.8% vs 2.0%) and macrophages (7.4% vs 3.6% of total cells) for Adv vs Early PLNs. NicheNet analysis indicated a high probability interaction between ALCAM$^+$ macrophages and CD6$^+$ T-cells. IF further confirmed the close proximity of ALCAM$^+$ and CD6$^+$ cells only in the Adv condition. Assessment of B-cell clonality revealed 15 polyclonal clusters and a single oligoclonal population (>20 cells of same clonotype). Differential gene expression analysis of the oligoclonal population showed increased *Ighg2b* expression along with unique variable light chain expression (*Igkv17-21*) in the Adv condition, which has been previously associated with specificity for sphingosine-1-phosphate (S1P) (2).

B-cell translocation into PLN sinuses is associated with the generation of IgG2b$^+$ plasma cells in Adv but not Early arthritis. These B-cell changes are concomitant with T-cell accumulation and potentially linked to activation via ALCAM$^+$/CD6$^+$ interaction. Bioinformatic analysis and previous studies (2) suggest the presence of clonal S1P-specific plasma cells that may compromise S1P-dependent cell egress in PLNs and alter lymphatic function in inflammatory arthritis. Future studies will assess the generation of S1P-specific plasma cells and evaluate the therapeutic potential of CD6 blockade in TNF-Tg arthritis (3).

References

1. Bouta et al. *Nat Rev Rheumatol*. 14(2):94-106. 2018.
2. Farokhi et al. *Antibodies (Basel)*. 9(2):10. 2020.
3. Rodriguez et al., *Clin Exp Immunology*. 191(2):229-39. 2018.

Title: **Integrated scRNA-seq and spatial transcriptomics analysis uncovers distinct cellular populations and transcriptomes in human hip synovium between patients with femoroacetabular impingement and osteoarthritis**

Presenting Author: Gulzada Kulzhanova

Co-Authors: John Reuter, Eloise Fadial, Benjamin Ricciardi, Brian Giordano

Lab PI / Mentor: Chia-Lung Wu

Abstract (3500 characters or 500 words Limit)

Cartilage degradation during osteoarthritis (OA) was significantly associated with inflammation and pathological changes in the knee synovium. Nevertheless, hip and knee OA have been established as immunologically distinct types of joint diseases due to unique cytokine profiles of their synovial fluid. Previous studies suggested that hip OA may result from Cam-type femoroacetabular impingement (FAI) that may be accompanied with labral tears and cartilage delamination, gradually leading to onset and progression of hip OA. Here, we propose that FAI and hip OA patients have distinct transcriptomic profiles and signaling pathways in their synovial tissues. We aim to identify the unique genetic markers, underlying signaling pathways and cellular interactions that may be involved in disease progression by using scRNA-seq, Spatial-seq, and bioinformatic analyses.

Cam FAI and OA (secondary to FAI) de-identified human hip synovial tissues were harvested according to approved IRB protocols at UR. Tissue samples were submitted to UR Genomics Research Center for scRNA-seq and Spatial-seq (10X Genomics). Bioinformatics packages including Seurat, Monocle, RcisTarget, and CellChat were used to determine distinct cell populations based on expression of differentially expressed genes (DEGs), construct differentiation trajectories, and determine cell-cell interactions.

Four conserved groups (NK cells, endothelial cells, myeloid cells, and non-hematopoietic cells) were identified in both FAI and OA hip synovium. Sub-clustering of integrated FAI and OA non-hematopoietic cells further yielded 5 distinct cell types including lining, sublining and transitional fibroblast-like synoviocytes (FLS) as well as endothelial cells (ECs) and pericytes. In comparison to FAI synovium, OA synovium exhibited a significant increase in the number of pericytes and endothelial cells, which is supported by the previous evidence showing increased synovial vascularity in OA. To further investigate the origin of these populations, we performed pseudotime analysis and it revealed that pericytes may differentiate from C34+/C3+ perivascular sublining FLS. Using DNA-binding motif analysis, KLF4, SOX5 and CREB3L2 are identified as putative critical transcription factors regulating this differentiation process. For instance, the highest expression levels of KLF4 were observed in perivascular sublining FLS, whose inactivation was previously reported to enhance the expression of pericyte markers. Importantly, by integrating scRNA-seq and Spatial-seq datasets, we were able to map spatial location of identified cell clusters and observed that pericytes are in close proximity to SPP1+/KDR+ capillary ECs and identified that VISFATIN-(ITGA5+ITGB1) and SPP1-CD44 are critical signaling pathways between these two cell populations in OA synovium. This observation aligns with previous studies that highlight a significant contribution of endothelial cells-pericytes interactions to OA pathogenesis.

By integrating scRNA-seq and Spatial-seq datasets of human hip FAI and OA synovial samples, we identified increased number of endothelial cells and pericytes as well as their unique signaling pathways in OA synovium. Our next step is to investigate changes in cell-cell crosstalk between myeloid cells and fibroblasts during disease progression. Indeed, we have observed elevated accumulation of “hybrid” macrophages expressing both pro- and anti-inflammatory markers (IL10+/IL1α+/IL1β +) in the hip OA.

Title: **In vitro screening of proangiogenic engineered extracellular matrices to promote tissue engineerd periosteum-mediated allograft healing**

Presenting Author: Alyson March

Co-Authors: Yiming Li, YoungJoo Lee, Regine Choe, and Danielle S. W. Benoit

Lab PI / Mentor: Danielle S. W. Benoit

Abstract (3500 characters or 500 words Limit)

Although allografts remain the gold standard for treatment of critical size bone defects, approximately 60% fail within ten years. Allograft failure is directly linked to the absence of periosteum, a highly vascularized tissue that promotes bone healing and host tissue recruitment through periosteal paracrine signaling. We have developed a tissue engineered periosteum (TEP) to improve allograft healing. The TEP is comprised of matrix metalloproteinase (MMP) degradable poly(ethylene glycol) (PEG) hydrogels encapsulating mouse mesenchymal stem cells (mMSCs) and osteoprogenitor cells (mOPs) to mimic periosteal cell types and subsequent paracrine signaling. However, evaluation of TEP efficacy requires in vivo studies, which are low throughput, costly, and time and resource-consuming. In preliminary data, a positive correlation was observed between encapsulated endothelial cell angiogenesis within hydrogel in vitro and TEP-mediated allograft vascularization and healing in vivo. Therefore, in this work, in vitro surrogates for vascularization were investigated by leveraging a 3D endothelial cell spheroid sprouting assay to predict hydrogel-mediated vascularization in vivo. Spheroids were composed of human umbilical vein endothelial cells (HUVECs) and human mesenchymal stem cells (hMSCs), pericyte-like cells. Hydrogels entrapping spheroids were formed via MMP-degradable (DL) or non-degradable (NDL) linkers and functionalized with the cell adhesive peptide RGD or a scrambled control RGE. Spheroid sprouting was evaluated using brightfield and fluorescent microscopy and quantified using the ImageJ 'Sprout Morphology' plug-in. Data indicate that spheroid sprouting is promoted in DL RGD hydrogels, as DL RGD hydrogels have significantly greater network formation than all groups at all time points. In contrast, NDL RGD hydrogels have little to no sprouts or network formation over time. Interestingly, DL RGE hydrogels support sprouting from the spheroid at later time points, as indicated by sprout quantification. However they do not support robust network formation, suggesting hydrogel degradation is necessary for angiogenesis, but RGD is required for sustained network growth in vitro. A mouse femur graft model was used to correlate in vitro results with in vivo healing. Longitudinal changes in graft vascularization and healing were analyzed using spatial frequency domain imaging (SFDI), microcomputed tomography (μCT), and histology at 1- and 3-weeks post-implantation. μCT shows that DL RGD TEP-modified allografts exhibited a ~100-fold increase in graft localized vascular volume over unmodified allografts at 3-weeks post-operation. Verification of vessel structure within hydrogels in vitro using immunostaining and tissue-specific angiocrine signal analyses, in vivo studies using SFDI, and evaluation of other hydrogel groups are on-going. Preliminary findings indicate that the TEP improves allograft vascularization and healing and that the 3D endothelial cell spheroid assay trends correlate to in vivo healing. These data suggest that the 3D endothelial cell spheroid assay with analysis of sprout length, vascular structure, and angiocrine signatures may be well suited for evaluating various complex hydrogel compositions for TEP hydrogel optimization and other tissue engineering approaches.

Title: **Zwitterionic Peptide Sequence Dictates Anti-Fouling Behavior and Protein Adsorption Profile on Nanoparticle Surfaces**

Presenting Author: Clyde Overby

Co-Authors: Baixue (Dorothy) Xiao, Tiana Salomon

Lab PI / Mentor: Danielle S.W. Benoit

Abstract (3500 characters or 500 words Limit)

Nanoparticles (NPs) are a clinically proven RNA delivery platform. However, recent data indicate that NPs exhibit poor systemic delivery characteristics due to protein adsorption, which accelerates NP clearance via opsonization and macrophage uptake [1]. Anti-fouling NP modifications such as poly(ethylene glycol) (PEG) and zwitterionic (ZI) polymers are efficacious but are susceptible to immunological reactions due to consumer product exposure and repetitive structures [1] and have limited control over the identity of adsorbed proteins, reducing control over biodistribution [2]. As an alternative, we computationally designed diverse ZI peptides (ZIPs) to modify NPs. We hypothesize that ZIPs will control protein adsorption as modeled by ZIP-protein interactions, and that the many possible identities of ZIPs will allow for many immunologically unique surfaces. To investigate these hypotheses, the design, synthesis, and characterization of ZIP-NPs in vitro and in vivo was explored.
Materials and Methods: 15-mer ZIPs were generated in silico and scored using an algorithm derived from a peptide interaction model (PASTA) [3] for interaction potential with the top 50 most abundant serum proteins. ZIPs were synthesized via solid phase peptide synthesis and confirmed through mass spectrometry. NPs were assembled from diblock copolymers of a poly(dimethylaminoethyl methacrylate) (DMAEMA) first block and 25% DMAEMA, 50% butyl methacrylate, and 25% propylacrylic acid second block synthesized via reversible addition fragmentation chain transfer (RAFT) polymerization [4]. Conjugation of ZIP or 2 kDa PEG to NP via carbodiimides was confirmed via fluoraldehyde assay and NMR. NP aggregation in serum was evaluated via dynamic light scattering; adsorbed protein was analyzed using the bicinchoninic acid assay, SDS-PAGE, and proteomics. NP-mediated siRNA knockdown of GAPDH in mouse mesenchymal stem cells (MSCs) was assessed via RT-PCR. Macrophage and MSC uptake of NP was evaluated by flow cytometry and in vivo pharmacokinetics were characterized via intravital fluorescent microscopy of Cy7 labeled NPs.
Results and Discussion: Adsorbed protein identity correlated with sequences but not with composition of ZIPs, and the ZIPs with the lowest energy (LE-ZIPs) and highest energy (HE-ZIPs) protein adsorption potentials were used for further experiments. LE-ZIP-NP serum protein adsorption is reduced by 65% and 35% compared to unfunctionalized NP and PEG-NPs. LE-ZIP-NP uptake by macrophages is reduced by 30% and MSC uptake increased by 55% compared to NPs, similar to PEG-NPs. siRNA GAPDH knockdown in MSCs by LE-ZIP-NP is equivalent to or greater than NP in all conditions tested, correlating with reduced aggregation [5]. LE-ZIP-NP circulation time increased 5-fold over NPs, exhibiting a half-life of 32 minutes.
Conclusions: Data suggest that LE-ZIP functionalization reduces protein adsorption of NPs, alters adsorbed protein composition, and enhances systemic circulation time without affecting siRNA delivery to MSCs. Future work will focus on evaluating in vivo biodistribution, correlation of protein corona with biological interactions, and adaptive immune response of ZIP-NPs.
Refs: 1. Verhoef, J.F., et al. Drug Discov. Today 19.12 (2014). 2. Aggarwal, P et. al. Adv. Drug Deliv. Rev. 61 (2009). 3. Trovato, A., et al. PEDS 20.10 (2007). 4. Convertine, A.J. & Benoit, D.S.W., et al. J. Control. Release 133.3 (2009). 5. Malcolm, D.W., et al. Bioeng transl med 1.2 (2016)

Title: **Protective Role for Mast Cells in TNF-induced Inflammatory-Erosive Arthritis and Its Associated Lymphatic Dysfunction in Mice**

Presenting Author: Yue Peng

Co-Authors: H. Mark Kenney, Karen L. de Mesy Bentley, Lianping Xing, Christopher T. Ritchlin, Edward M. Schwarz

Lab PI / Mentor: Edward M. Schwarz

Abstract (3500 characters or 500 words Limit)

Background: Inflammatory-erosive arthritis is exacerbated by lymphatic dysfunction in ankle joint-draining popliteal lymphatic vessels (PLVs). Mast cells (MCs) regulate lymphatic vessels by releasing inflammatory and vasoactive mediators (e.g. histamine) through degranulation. Previous publications emphasized the pro-inflammatory role of MCs in rheumatoid arthritis, while recent papers identified anti-inflammatory effects of MCs in tissues. Here we aimed to elucidate the effects of MCs on lymphatic function and inflammatory-erosive arthritis in tumor necrosis factor transgenic (TNF-Tg) mice with genetic deficiency of MCs or pharmacologic inhibition of MC degranulation.

Methods: Whole mount immunofluorescent microscopy (WMIFM) and toluidine blue (TB) stained histochemistry were performed to quantify peri-PLV MCs, and degranulating MCs were identified by numerous extracellular granules. Scanning electron microscopy (SEM) was used to visualize peri-PLV MCs (n=2 wild-type (WT) mice). Ankle bone volumes were assessed by μCT as a biomarker of erosive arthritis in WT, TNF-Tg, and KitW-sh/W-sh (cKit-/-) mice that have a selective hematopoietic MC deficiency. Near-infrared imaging of indocyanine green (NIR-ICG) was used to quantify ICG clearance, an outcome measure of PLV draining function. 4-month-old female TNF-Tg mice received cromolyn sodium, a clinically used MC stabilizer (3.15mg/g/day/i.p., n=6), or saline (n=5) for 3 weeks. ICG clearance and μCT were performed at baseline and after 3-weeks of treatment , followed by ex vivo WMIFM and TB histology.

Results: SEM showed that numorous MCs localized to the peri-PLV area. WMIFM and TB histochemistry demonstrated a significant increase in the number of peri-PLV MCs in TNF-Tg mice vs. WT littermates, while the percentage of degranulating MCs was inversely correlated with ICG clearance. TB histochemistry also identified a population of MCs embedded within the PLV wall, enveloped between lymphatic muscle and endothelial cell layers, with unknown function. Treatment of TNF-Tg mice with cromolyn sodium significantly exacerbated ankle bone erosions and decreased ICG clearance. Increased bone erosions and decreased ICG clearance were similarly observed in cKit-/- x TNF-Tg vs. TNF-Tg mice, and these effects were unrelated to PLV αSMA coverage between groups.

Conclusion: TNF-Tg mice exhibit increased numbers of peri-PLV MCs with increased proportions of activated/degranulated MCs, which are inversely correlated with lymphatic function. Along with peri-PLV MCs, we also discovered intra-PLV MCs embedded within the PLV structural architecture, demonstrating potential heterogeneity in the lymphatic-associated MC population. Although increased peri-PLV MC activity enhances arthritic severity, both genetic ablation of MCs and pharmacological inhibition of MC degranulation also exacerbate TNF-induced inflammatory-erosive arthritis with decreased lymphatic clearance. Together, these findings support a dual inflammatory role of activated/degranulated peri-PLV MCs during arthritic progression and homeostatic role of intra-PLV MCs with protective function that sustains lymphatic clearance. Non-specific ablation or inhibition of MCs leads to a loss of protective MCs that supersedes the effect of reducing inflammatory MC activity, and ultimately leads to worse disease. Thus, future studies are warranted to characterize distinct peri-PLV MC sub-populations and develop strategies to target MCs for regulation of

Title: **Bone Marrow Microenvironment on a Chip (BMME-Chip) for Investigating the BMME during Hemostasis and Acute Myeloid Leukemia**

Presenting Author: Azmeer Sharipol

Co-Authors: Maggie L. Lesch, Celia A. Soto, Danielle S.W. Benoit, Benjamin J. Frisch

Lab PI / Mentor: Benjamin J. Frisch, Co-PI : Danielle S.W. Benoit

Abstract (3500 characters or 500 words Limit)

Acute myeloid leukemia (AML) is the most common acute leukemia in adults characterized by the disruption of hematopoiesis. Standard therapies result in an abysmal 5-year survival rate of less than 30%. Thus there is an urgent need to investigate new therapeutic strategies to improve patient prognosis. A major challenge in the field is the inability to study the role of the bone marrow (BM) microenvironment (BMME) in AML progression due to the lack of reliable in vitro models. Our group and others have shown that the loss of normal hematopoiesis due to the BMME dysfunction drives much of the morbidity and mortality associated with AML. To study the specific interactions of leukemic cells with the BMME, we are developing a tissue-engineered BMME on a chip (BMME-chip) consisting of key components crucial for regulating hematopoiesis. We hypothesized that this approach will overcome the limitations of conventional models by providing a conducive environment for the maintenance of hematopoietic stem and progenitor cells (HSPC) and a reliable recapitulation of phenotypic BMME changes due to AML in vitro. We first generated a murine BMME-chip model with hematopoietic and vascular compartments using a dual-channel microfluidics system, Emulate Chip S1. The hematopoietic compartment (top channel) is made up of a fibrin hydrogel containing bone marrow stromal cells (BMSC) and hematopoietic stem and progenitor cells (HSPC) and an osteoblastic layer differentiated from BMSC on the top wall surface. The vascular compartment (bottom channel) contained an endothelial monolayer on the porous membrane surface with continuous media flowing throughout the culturing period. After 2 weeks of culture, flow cytometry data showed that HSPC (Lin- Sca+ cKit+) frequency was maintained at 0.29 ± 0.13% of total cells, within a 2-fold difference relative to freshly isolated BM at 0.15 ± 0.04%. HSPCs were further able to successfully engraft in a murine competitive stem cell transplant model and gave rise to ~60% of total peripheral blood mononuclear cells (PMBC) with myeloid and lymphoid cells at similar frequencies compared to fresh BM transplant controls (~18% and ~82% respectively at 28-week post-transplant). Further engraftment of isolated cells into secondary recipients showed maintenance of long-term HSPC function. At 8 weeks post-transplant, 20-30% of total cells, monocytes, and B-lymphocytes in PMBC were derived from chip HSPC. In the AML BMME-chip model which contained leukemic cells, a similar osteoblastic function loss as previously reported in vivo was observed by the reduction of calcium nodules via Von Kossa staining and significant decrease of Osteocalcin I (39.72 ± 0.13%) gene expression compared to control BMME-chip. These findings validate the ability of the BMME-chip to provide a supportive microenvironment for HSPC and recapitulate the BMME phenotypic changes during AML.

Title: **Phenotypic characterization of a novel mouse hind limb explant model of Achilles tendon impingement**

Presenting Author: Brian Wise

Co-Authors:

Lab PI / Mentor: Mark Buckley, Whasil Lee

Abstract (3500 characters or 500 words Limit)

Tendon impingement generates a disparate mechanical strain environment distinguished by elevated compressive strains oriented transverse to the longitudinal axis, which elicits a localized fibrocartilage phenotype rich with glycosaminoglycans (GAGs). Although fibrocartilage is a normal feature in impinged regions of healthy tendon, excessive GAG content is a hallmark of tendinopathy, which frequently develops in regions of impingement. As such, tendon impingement is clinically recognized as an extrinsic factor in tendinopathy pathogenesis. Despite these observations, the underlying mechanisms by which cells regulate this fibrocartilaginous phenotype in adaptation to mechanical impingement are understudied, which obscures our understanding of tendinopathy pathogenesis and results in inadequate treatment. Indian hedgehog (Ihh) signaling is known to mediate patterning of mineralization gradients and fibrocartilage formation at the tendon-bone enthesis in response to mechanical load during embryonic and early postnatal development, and while recent evidence implicates Ihh signaling in the development of tendinopathy secondary to subacromial impingement, the exact role of Ihh signaling in regulating fibrocartilage homeostasis in adaptation to mechanical impingement beyond postnatal development has yet to be fully described. Our lab has previously developed a novel murine hind limb explant system that recreates impingement of the calcaneus upon the Achilles tendon through passive dorsiflexion of the ankle. Because this model is highly controllable, maintains tendon viability over at least 7 days, and can be interfaced with ultrasound or multiphoton imaging to visualize the mechanical strain environment in impinged tendon regions, it provides a unique opportunity to interrogate the mechanobiology of Achilles tendon impingement. Explants were loaded into this platform to maintain the Achilles tendon insertion under static impingement for 7 days, while contralateral limbs were cultured unloaded. Serial tissue sections were stained with Toluidine blue to visualize GAG-rich fibrocartilage, and custom color image analysis indicated statistically significant changes in Toluidine blue staining at the insertion after 7 days of static impingement compared to contralateral unloaded limbs, suggesting enhanced fibrocartilage formation in response to impingement. Additional tissue sections were immunofluorescently labeled using antibodies for Ihh, Patched1, and Gli1. Fluorescent image analysis demonstrated statistically significant increases in Patched1+ and Gli1+ cells at the Achilles tendon insertion after 7 days of static impingement compared to contralateral unloaded limbs. These data demonstrate that static impingement of the Achilles tendon insertion elicits increased GAG deposition and fibrocartilage formation over 7 days in this novel mouse hind limb explant model, particularly in deep tissue regions where we have previously measured maximum transverse compressive strains. Additionally, immunofluorescent labeling indicates increased Patched1+ cells at the impinged insertion over 7 days, suggesting Ihh signaling may increase in response to static impingement in our model. In the future, we will evaluate whether perturbing the Ihh pathway alters the fibrocartilaginous phenotype generated by impingement in our model.

Posters

Title: **Investigating peptide sequence effects on competing thiol-ene functionalization and crosslinking reactions in poly(ethylene glycol) hydrogels**

Presenting Author: Brittany L. Abraham

Co-Authors: Sayantani Basu, Alyson March, Kevin C. Ling, Robert Brown, Arvind R. Srivatsava

Lab PI / Mentor: Danielle S.W. Benoit

Abstract (3500 characters or 500 words Limit)

Biomaterials are commonly designed to mimic the biochemical and biophysical cues from the native extracellular matrix (ECM) to coordinate cell functions requisite for tissue engineering. In particular, synthetic hydrogels, such as those composed of poly(ethylene glycol) (PEG), are highly-hydrated yet biologically inert ECM mimetics that can be crosslinked with enzymatically degradable peptides and also functionalized with cell-adhesive peptide ligands to facilitate cell remodeling and cell-material interactions, respectively. Thiol-ene click chemistry is a simple, bio-orthogonal method to form these hydrogels using PEG macromolecular monomers functionalized with norbornene, cysteine-containing crosslinker/ligand peptides, and a photoinitiator that is activated by long-wave, low-intensity UV light. However, differences in thiol reactivity between the crosslinker and ligand peptides may result in competition during conjugation that can affect the hydrogel material properties. Additionally, when a high percentage of available norbornenes are conjugated with peptides in a particular gel formulation, any effects caused by competition during peptide incorporation can be amplified. Therefore, this work investigates how peptide sequence choice and amount of norbornene loading can affect peptide incorporation efficiency and hydrogel material properties to ensure the engineered ECM mimetic gels are well-controlled and reproducible.

Peptides based on the adhesive peptide ligand RGD (specifically, GCGRGDSFG (GRGDF) and CGRGDSFG (RGDF)) were chosen to examine how designing ligands with terminal or non-terminal cysteines impact PEG hydrogel incorporation efficiency of crosslinkers and ligands. Gel formulations were tested in triplicate, and the modulus of each was determined. At the same time, the number of unreacted peptides present after polymerization was determined using Ellman's reagent and high-performance liquid chromatography (HPLC). In gel formulations where 60% of norbornene sites were consumed by crosslinker and peptide ligands occupied an additional 10%, the hydrogel modulus was constant across samples with or without ligand added, and >95% incorporation of crosslinkers and ligands was observed via Ellman's assay and HPLC. However, in gel formulations with enough peptide to react with 100% of available norbornenes, such as 80% crosslinker and 20% ligand, the gel mechanical properties were affected by apparent competition between ligands and crosslinkers. Gels formed with the RGDF or GRGDF ligand had a two-fold or four-fold lower modulus, respectively than those without ligand included, indicating that ligand peptides were outcompeting crosslinkers during the thiol-ene reaction, resulting in a gel with fewer crosslinks and a lower modulus. Ellman's assays supported incomplete crosslinking in these gels, which revealed up to 2.5 times more unreacted thiols within gels containing ligand than those without ligand. Notably, the magnitude of these differences was found to be more prominent when incorporating GRGDF compared to RGDF, demonstrating that the position of the cysteine residue can impact incorporation efficiency in thiol-ene conjugations and therefore should be considered when designing peptides for synthetic ECMs. In ongoing work, formulations with varied norbornene loading are being examined to determine the maximum loading that can be achieved while providing hydrogels with robust, reproducible material properties.

Title: **Investigating the Bio-Distribution of Peptide-Functionalized Nanoparticles to Promote Tendon Healing**

Presenting Author: Emmanuella Adjei-Sowah

Co-Authors: none

Lab PI / Mentor: Danielle Benoit, PhD; Alayna Loiselle, PhD

Abstract (3500 characters or 500 words Limit)

Satisfactory tendon healing following acute injury is marred by a fibrotic response that impairs complete functional recovery. Current approaches in treating tendon injuries involve surgical and physical therapy techniques, however, there is a need for biological augmentation of the healing process to promote regenerative healing. Specifically, the ability to target the tendon via systemic drug delivery would substantially enhance the translational feasibility of newly discovered disease modifying treatments. However, a major limitation is the poor targeting efficiency of the tendon with systemic drug treatments. To investigate efficient tendon targeting mechanisms for delivering pharmacotherapies, using spatial transcriptomics, we identified a spatio-molecular cluster associated with inflammation, which was defined by the expression of Acp5, the gene that encodes Tartrate resistant Acid Phosphatase (TRAP). We hypothesize that employing a TRAP binding peptide nanoparticle (TBP-NP) delivery system will result in high affinity targeting of TRAP+ cells in the healing tendon. More importantly, identifying an optimal time window for therapeutic delivery is critical, since the tendon progresses through different phases of healing after injury, with different mechanisms underlying each phase. In this study, we investigated the biodistribution of TBP-NPs delivered at three independent timepoints (Day 3, Day 7, Day 14 post-surgery) and assessed the accumulation and retention of TBP-NPs delivered at each of these timepoints to establish therapeutic windows of TBP-NP delivery for tendon regeneration.

Results from live imaging and analysis showed that although SCP-NPs demonstrated accumulation at the repair site, TBP-NPs showed a significantly greater accumulation (~ten-fold) and retention. Specifically, TBP-NPs preferentially accumulated at the tendon repair site after administration and were retained for 14 days compared to SCP-NPs which showed no preferential accumulation and were cleared within 7 days. Furthermore, we observed highest accumulation of TBP-NPs in the D7 treatment group which was highly retained for 14 days, implying that TBP-NP affinity for TRAP was the major mechanism driving NP homing during the proliferative phase. While the D3 treatment showed initial high accumulation, there was drastic loss in signal beginning at D8. This suggests that the main mechanism for homing during the inflammatory phase was the 'Enhanced Permeability & Retention' (EPR) effect. Moreover, when we delivered TBP-NPs at day 14, we observed very low accumulation, and the TBP-NPs were cleared within 12 days, implying that D14 was the least effective treatment time.

Future studies will assess the predominant cell population that uptakes TBP-NPs at the tendon repair site using flow cytometry and deliver therapeutics to target cells/mechanisms to promote healing. Collectively, these data will define the temporal, spatial, and cell-type specific targeting of TBP-NPs to the healing tendon and establish a novel therapeutic delivery system for tendon repair.

Title: **Targeting TRPC6 for Chronic Discogenic Back Pain**

Presenting Author: Janitri Venkatachala Babu

Co-Authors: Alexandra Sadowska, Addisu Mesfin, Karin Wuertz-Kozak

Lab PI / Mentor: Karin Wuertz-Kozak

Abstract (3500 characters or 500 words Limit)

INTRODUCTION:
Degenerative disc disease (DDD) is the cause of back pain in up to 42% of cases and results from nerve ingrowth, inflammation, and hypermobility. During degeneration, extracellular matrix (ECM) loss occurs, which affects the load-bearing capacity and flexibility, contributing to disease progression. The mechanotransduction in the disc is affected by varying mechanical loads, and TRP channels are established mechanosensitive ion channels. Many of these channels are expressed in chondrocytes and intervertebral disc (IVD) cells, the cells involved in degenerative joint diseases like osteoarthritis and DDD. Amongst the various transient receptor potential (TRP) channels, TRPC6 is of specific interest to DDD as its activation has been shown to promote catabolism, inflammation, and pain in other diseases, all of which are hallmarks of DDD. In numerous cell types, TRPC6 can be activated by mechanical loading as well as by 1,2-diacylglycerol (DAG), which is released as a by-product of Phospholipase C (PLC) activity. We hypothesize that degenerated IVDs produce DAG, which leads to activation of TRPC6 and induces inflammation. Consequently, we hypothesize that inhibition of TRPC6 activity could be a promising therapeutic target to treat the pathophysiological processes underlying DDD.
METHODS:
Human IVD samples of degenerated (n=22) and non-degenerated (n=12) discs were isolated for mRNA and analyzed using RT-qPCR for TRPC6 expression. To activate TRPC6, a channel-specific pharmacological agonist, Hyp9 (0.5 µM for 18 hours) and a physiological agonist, 1-Oleoyl-2-acetyl-sn-glycerol (OAG = DAG Analog) at 100 µM for 18 hours was used on human IVD cells (n=6) isolated from degenerated human IVDs. The IVD cells were treated with TRPC6 specific inhibitor, SAR7334 (10 nM for 18 hours) after 2 hours of pre-treatment with TNF-α (10 ng/mL) or HYP9 (0.5 µM). Following the treatment, mRNA was isolated, and qPCR analysis of proinflammatory cytokines was assessed. Untreated cells and vehicle controls were included in the study. All the statistical analyses were done using GraphPad Prism 9.0.2 for windows (GraphPad Software). The statistical tests performed include testing normality, t-Tests, and one-way ANOVA.
RESULTS:
Degenerated hIVDs show a higher expression of TRPC6 compared to non-degenerated IVDs. Human IVD cells treated with the TRPC6 activator, HYP9 showed a significant increase in the expression of pro-inflammatory cytokines. There was a significantly higher expression of IL6 ($p<0.05$), IL 8 ($p<0.01$), MMP3 ($p<0.01$), and MMP1 ($p<0.051$) in comparison to vehicle controls. The expression of genes was normalized to the vehicle controls. Similarly, the treatment with OAG (DAG analog) increased the expression of pro-inflammatory cytokines compared to the vehicle controls.
DISCUSSION:
Due to the increased expression of TRPC6 during degeneration, this mechanosensitive ion channel constitutes an attractive potential therapeutic target for DDD. Our results on TRPC6 activation underline the therapeutic potential of TRPC6 modulation as both the pharmacological activator (HYP9) and the physiological activator (OAG) induce an inflammatory response in vitro. Very preliminary results indicate that TRPC6 inhibition (SAR7334) reduces the inflammatory cytokine expression. Further experimentation in both in vitro and in vivo animal models will validate the role of TRPC6 in IVD degeneration and pathophysiology.

Title: **Transcriptome Analysis of Autograft Mediated Bone Healing to Efficiently Design Engineered Periosteum**

Presenting Author: Sayantani Basu

Co-Authors: Andrew McDavid and Danielle S.W. Benoit

Lab PI / Mentor: Danielle S.W. Benoit

Abstract (3500 characters or 500 words Limit)

Approximately two million bone graft surgeries are performed in the US annually, among which ~550,000 are massive bone allograft procedures. Despite being the gold standard bone graft, the widespread use of autografts is hindered by tissue harvesting complications and limited tissue volumes. Allografts, the alternative for massive bone defect repairs, are tissue harvested from cadaveric donors and denuded of all living cells and soft tissue. However, compared to autografts, allografts are associated with an increased risk of failure due to poor integration with the host tissue, resulting in a 60% failure rate at ten years post- implantation. Healing deficiencies observed with allografts stem from the absence of periosteum, the thin layer of vascularized and innervated tissue that surrounds all bone tissue and coordinates bone healing in autografts. This thin layer is a reservoir of multiple cell types, including stem cells and osteoprogenitors, that release myriad signaling molecules to orchestrate the fracture repair process. However, there are limited studies focusing on understanding the dynamic changes of the periosteal layer in terms of host cell recruitment, temporal changes in cell population and/or paracrine factors, average turnover time of periosteal cells. Therefore, our objective is to understand the underlying mechanism of periosteal mediated healing to better design tissue engineering approaches that can modulate the healing response of allografts comparable to autografts.

RNA sequencing was performed on graft-associated cells from 8-10 weeks-old female C57BL/6 mice following autograft surgeries to understand the underlying mechanism of periosteal-mediated healing. Grafts were harvested on days 1, 2, 5, 7, and 14 after surgery to capture dynamic changes at critical stages of healing, and the periosteal cells were isolated for sequencing analysis. Analyses showed that periosteal cell population from contralateral controls are grouped together in the principal component analysis (PCA) plot which clusters samples based on their similarities in gene expression profiles. In contrast, samples at different time points have different identities in terms of principal component 1 (PC1) and principal component 2 (PC2). The highest number of differentially expressed genes were observed on Day 1 with 2769 upregulated, and 2152 downregulated, whereas, with time, the transcriptional changes reach an equilibrium with the least number of DEGs on day 14 with 90 downregulated and 1259 upregulated ones. A KEGG pathway analysis was used to investigate a potential link between the transcriptomic profiles and possible pathways. Neurotrophin signaling and neuroactive ligand-receptor pathways were upregulated on day 1, whereas axon guidance pathways were upregulated through day 14. We observed elevated levels of Slit3 and Robo1 at early time points up to a week following autograft transplantation. Previous studies report the necessity of Slit3-Robo1 signaling for nerve regeneration following spinal cord injury.

Neurotrophic factors NGF and NPY exhibited a robust temporal variation in expression, with peak expression at day 7. In sum, these data emphasize the importance of nerve regeneration during the early phases of periosteum-mediated bone healing. Ongoing studies focus on single-cell sequencing analysis of the periosteal cells where the grafts are harvested from eCFP-positive mice to differentiate between host versus graft cellular responses.

Title: **Percutaneous Versus Open Pedicle Screw Fixation for the Management of Metastatic Spine Disease: A Matched-Cohort Study**

Presenting Author: Mina Botros, M.D.

Co-Authors: Clarke Cady-McCrea M.D., Mark Lawlor M.D., Takaki Shimizu M.D.

Lab PI / Mentor: Addisu Mesfin M.D.

Abstract (3500 characters or 500 words Limit)

INTRODUCTION: There has been increased interest in applying minimally invasive fixation techniques to stabilize the spine in this physiologically frail population. Our objective it to compare surgical outcomes and complications following Percutaneous pedicle screw fixation (PPSF) versus open pedicle screw fixation (OPSF) of metastatic spinal tumor (MST) reconstructions.

METHODS: This is a retrospective study of patients with MST undergoing surgical intervention at a level 1 tertiary academic medical center. 29 patients PPSF between 2015-2022 were matched based on vertebral tumor location (Cervical, Thoracic, & Lumbar), number of vertebral segments instrumented, and number of segments decompressed to 29 patients undergoing OPSF from 2005-2018. To compare PPSF therapeutic impact to OPSF, examination of perioperative variables: blood loss, operative time, complications, length of hospital stay, epidural spinal cord compression (ESCC) scale; and treatment outcomes: post-op survival time, post-op narcotic use, changes in patient reported outcomes as assessed via PROMIS: pain interference (PI), physical function (PF), and depression. Qualitative statistical data and a two-sample t-test were used to examine the therapeutic impact of PPSF compared to OPSF of MST patients. Statistical significance set at $p < 0.05$.

RESULTS: This is a matched cohort study that included 29 patients underwent PPSF (age: 66.55 ± 10.1) with 12 (40%) female matched to 29 patients underwent OPSF (age: 61.5 ± 15.6) with 11(37.9%) female. Patients undergoing PPSF were older than those undergoing OPSF ($p<0.001$). OPSF is associated with greater estimated blood loss (mean [SD]: 990.0[596.8]) compared to PPSF (390.5[372.2], $p<0.001$). Further, OPSF had a longer surgical time (457[106.8]) compared to PPSF (221[78.6], $p<0.001$). Peri-operative complications among PPSF included: wound infection requiring I&D (n=3), aspiration pneumonia (n=2), and death (n=2) due to significant tumor burden; compared to OPSF: Dural Tear (n=3), deep wound infection (n=3), DVT(n=2), and death (n=1). Post-operative survival for PPSF and OPSF were similar 405.9 days [338.7] versus 366.75day[332.0], $p=0.449$).

Patients undergoing PPSF and OPSF reported that they had a significant difference between average pre- and post-operative pain interference score ($p<0.01$). Also, post-operatively patient reported improvement in physical function score ($p=0.025$) and depression ($p=0.038$). There is no statistical difference between PPSF and OPSF in their improvement of patient PROMIS score (PI, PF, and depression).

There is no statistical difference between pre- and post- operative oral morphine equivalent (OME) between PPSF and OPSF($p=0.164$). Both palliative procedures were effective in reducing the OME used by the patient pre- and post-operatively at day 14 (OPSF: 57.7[20.6] versus 32.5[17.9], $p<0.001$; and PPSF: 48.3[18.6] versus 36[19.8], $p<0.001$).

CONCLUSION: This study identifies that PPSF is associated with less blood loss and shorter surgical time. Both palliative procedures are effective in improving physical function and reducing pain and depression. Further, both are effective palliative procedures in reducing the amount of OME prescribed.

Title: **Racial Disparities in Surgical Outcomes after Pediatric Scoliosis Corrective Surgery**

Presenting Author: Mina Botros, M.D.

Co-Authors: Phoebe Huang B.A.,

Lab PI / Mentor: Caroline Thirukumaran, MBBS, MHA, PhD

Abstract (3500 characters or 500 words Limit)

INTRODUCTION: Pediatric spine deformity surgery is a safe and effective procedure to address various types of scoliosis deformities. However, there is a paucity of literature evaluating racial and ethnic disparities in outcomes following pediatric spine deformity surgery. The objective of the study is to examine racial and ethnic disparities in the outcomes of scoliosis corrective surgery using a prospectively collected clinical data from a nation-wide database.

METHODS: We used the NSQIP-P data which is a large multicenter clinical registry of major pediatric surgical procedures conducted in the United States and includes clinical data abstracted by trained clinical reviewers. We used Current Procedural Terminology (CPT) codes to identify all patients undergoing spinal deformity surgery between 2016-2019. The key outcomes of interest included post-operative complications classified as major complications (return to the OR, pulmonary embolism, cardiac arrest, unplanned intubation, deep surgical site infection, wound disruption, sepsis, septic shock, cerebrovascular accident (CVA), acute renal failure, ventilation > 48hrs) and minor complications (superficial SSI, urinary tract infection, DVT, pneumonia, nerve injury, post-op C. diff); and readmissions. The key independent variable was the patient's race/ethnicity (non-Hispanic White [NHW], non-Hispanic Black [NHB], Hispanic, and Other). We used chi-square, Kruskal-Wallis tests, and multivariable logistic regressions to examine the association of the patient's race and ethnicity with the outcomes of interest. All multivariable models controlled for patient- and procedure-level confounders.

RESULTS: Among the 19624 cases (Age (mean[SD], 11.7[5.0], Female: 63.4%;) of scoliosis corrective surgery, 68.8% were Non-Hispanic White, 16.0% were Non-Hispanic Black, 10.7% were Hispanic, and 4.3% belonged to other racial groups. The 30-day overall, major, and minor complication rates were 11.7%, 8.2%, 3.5%, respectively. The most frequently occurring complications were related readmissions (4.5%) and unplanned re-operation (3.2%). With risk adjustment and compared to NHW patients, the odds of any complications were 24% higher for NHB patients (adjusted odds ratio [AOR], 1.220; 95% Confidence Interval [CI]: 1.067 to 1.394; p=0.004), . Additionally, NHB are much more likely to develop a major complication (AOR, 1.391; 95% CI: 1.117 to 1.737; p=0.003) compared to NHW (AOR, 0.811; 95% CI: 0.671 to 0.981; p=0.031). There is a low risk that NHB and NHW develop minor complications (AOR, 0.647; 95% CI: 0.5 to 0.837; p<0.001 versus AOR, 0.779; 95% CI: 0.646 to 0.940; p=0.009, respectively). The highest incidence of blood transfusion was highest among NHB (60.4%, p<0.001) compared to NHW (46.8%) and Hispanic (45.7%). Surgical duration was longest among NHB (mean[SD], 257.1(116.70)) compared to NHW and Hispanic patients (234.0 (126.7) and 227.2(127.6), p<0.001, respectively). There is no statistical difference between race group for related readmissions.

CONCLUSION: This study demonstrates that NHB are 28% more likely to develop postoperative complications compared to NHW patients. Additionally, NHB patients are 39% more likely to develop major postoperative complication, relative to other race groups. NHB patients tend to have a higher incidence of blood transfusion and operative time relative to other race groups.

Title: **Chondrocyte mechano-sensitivity following a massive rotator cuff tear**

Presenting Author: Katherine G. Broun

Co-Authors: Devon E. Anderson MD,PhD, Alexander Kotelsky PhD, Sandeep Mannava MD, PhD

Lab PI / Mentor: Whasil Lee PhD

Abstract (3500 characters or 500 words Limit)

The rotator cuff—a group of four tendons from corresponding scapular muscles—unites onto the humerus around the ball-and-socket glenohumeral joint and provides dynamic joint stabilization. Symptomatic rotator cuff disorders are common and arise from either acute traumatic injury or chronic degeneration with pathology ranging from isolated tendinopathy to full-thickness multi-tendon tears, termed a massive rotator cuff tear (RCT). Left untreated, a massive RCT leads to joint destabilization with superior humeral head migration and degenerative changes. The objective of this study was to elucidate the role of Piezo1-mediated chondrocyte mechanotransduction in the altered environment from a massive RCT to develop potential therapeutic strategies to attenuate cartilage degeneration following rotator cuff tear. We hypothesized that a massive RCT in a mouse model increases Piezo1 expression and Piezo1-dependent chondrocyte susceptibility against mechanical loading.
Methods: Ethical approval from UCAR was obtained. Humeri of wild-type 12–14-week-old C57Bl/6 male mice were harvested, incubated with Yoda1, a Piezo1-specific agonist, or vehicle control (DMSO 0.25%, n=6/group), and subjected to a 2mJ impact load via a custom apparatus quantifying chondrocyte vulnerability before and after impact with a Live/Dead assay. A surgical model was developed with a deltoid splitting approach of the right shoulder of 14-week-old C57Bl/6 male mice where a RCT model had surgical tear of the supraspinatus and infraspinatus tendons; a sham surgery discluded tendon tear. Animals were sacrificed at 4- or 14-weeks post-surgery to assess early and long-term outcomes, respectively, through mechano-sensitivity, histological analysis, and quantitative immunohistochemistry for Piezo1 expression (n=3/group). Student t-tests evaluated differences between treatment and control groups and ANOVA compared multiple groups, with statistical significance set to $p<0.05$.
Results: There was a significant increase in humeral head chondrocyte cell death after impact following Yoda1 loading when compared with controls indicating that Piezo1, in part, drives chondrocyte vulnerability to injurious loading ($p<0.01$). In early injury, there was a 15% decrease in cartilage thickness RCT shoulders relative to sham controls. A trend of increased chondrocyte vulnerability and cell death in response to impact loading for both RCT and sham surgery relative to uninjured contralateral control limbs was seen, but no difference in Piezo1 expression was seen. In long-term injury, chondrocytes were more vulnerable to subsequent impact injury with a trend toward increased cell death ($p=0.11$) and a corresponding significant increase in Piezo1 expression in RCT humeral chondrocytes relative to contralateral control ($p<0.05$) and sham surgery chondrocytes ($p<0.01$).
Discussion: Murine humeral head chondrocytes respond to injurious mechanical loading in part via mechanically gated calcium ion channel Piezo1 upregulation. When activated by Yoda1, chondrocytes have increased vulnerability and cell death following impact. A surgically induced RCT model alters the glenohumeral joint biomechanics causing chondrocytes to subsequently increase Piezo1 expression and subsequent vulnerability. These results demonstrate that chondrocytes are vulnerable to alterations in biomechanical loading after massive RCT. Future work includes the impact of GsMtx4 injection on cartilage rescue post massive RCT.

Title: **TLR-2 Activation Dysregulates miR-100-5p and miR-155-5p Leading to the Downregulation of c-Fos**

Presenting Author: Petra Cazzanelli

Co-Authors: Mikkael Lamoca, Oliver Nic Hausmann, Addisu Mesfin and Karin Wuertz-Kozak

Lab PI / Mentor: Karin Wuertz-Kozak

Abstract (3500 characters or 500 words Limit)

INTRODUCTION: Inflammation has been proven to be one of the key factors of intervertebral disc (IVD) degeneration. Dysregulated inflammation is characterized by the increased secretion of proinflammatory cytokines, which can lead to the infiltration of immune cells and nociceptive nerve fibers into the damaged IVD tissue. The accumulation of proinflammatory cytokines is also known to enhance the degradation of the extracellular matrix and contribute to cellular senescence and apoptosis. One of the known regulators of inflammation are toll-like receptors (TLRs), amongst which TLR-2 has been shown to be specifically relevant in IVD degeneration. This inflammatory signaling pathway can be activated by pathogen- or damage-associated molecular patterns and downstream signaling leads to the expression of pro-inflammatory cytokines through the activation of transcription factors NFκB and AP-1 (c-Fos and c-Jun heterodimer). MicroRNAs (miRNAs) play a crucial role in regulating gene expression and their dysregulation has been connected to multiple pathologies. However, the role of miRNAs in TLR signaling in IVD degeneration is still poorly understood and was hence investigated in this study.
METHODS: For the identification of TLR-2 associated miRNAs, human IVD cells (n=5) isolated from degenerated IVDs (Pfirrman grade: 3-4) were treated with the TLR-2/6 agonist PAM2CSK4 (100ng/mL for 6 hours) in order to activate the TLR-2 signaling pathway. TLR-2 knockdown (siRNA) cells were used as a control. Following TLR-2 activation, miRNAs were isolated for Illumina small RNA sequencing. A selection of 10 differentially expressed miRNAs identified by next-generation sequencing (NGS) were validated in human Nucleus pulposus (hNP) and Annulus fibrosus (hAF) cells (n=5) by RT-qPCR. The most significantly up- and downregulated miRNAs were further selected for target and pathway prediction with the miRabel prediction tool (http://bioinfo.univ-rouen.fr/mirabel/). Gene expression of predicted miRNA targets was analyzed by RT-qPCR. Statistical analysis was conducted by performing Kruskal-Wallis test, as well as Shapiro-Wilk test for normality and a two-tailed Student's t-test using GraphPad Prism version 9.0.2 for Windows.
RESULTS: The expression profile of miRNAs in human IVD cells showed significant changes after the activation the of TLR-2 signaling pathway. Specifically, 10 differentially expressed miRNAs were identified by NGS and validation of the selected miRNAs showed the most significant TLR-2 dependent changes in the expression of miR-100-5p and miR-155-5p. These effects were fully or partially reversed in TLR-2 knockdown cells, where the TLR-2 knockdown was confirmed by RT-qPCR (77.7 ± 3.5 %). Pathway prediction of miR-100-5p and miR-155-5p shows their involvement in inflammation and cell growth-related pathways such as mTOR, TNF, PI3K/Akt, and MAPK signaling pathways. Preliminary screening of miR-155-5p specific targets showed a significant decrease in c-FOS gene expression during TLR-2 activation and concomittant miR-155-5p upregulation.
DISCUSSION: The TLR-2 dependent dysregulation of the miRNAs miR-100-5p and miR-155-5p presents a possible link between inflammatory signaling pathways and pathways involved in the regulation of cell growth and autophagy. This was confirmed by miRNA target and pathway prediction as well as initial target screening. Ongoing experiments study the functional role of these miRNAs in IVD pathophysiology and inflammation.

Title: **Reproducible and Controlled Peptide Functionalization of Polymeric Nanoparticles for Bone Targeted Drug Delivery**

Presenting Author: Indika Chandrasiri

Co-Authors: Yuxuan Liu, Emmanuela Adjei-Sowah, Baixue Xiao, and Danielle S. W. Benoit

Lab PI / Mentor: Danielle S. W. Benoit

Abstract (3500 characters or 500 words Limit)

Polymeric nanoparticles containing multiple amines and carboxylates have been frequently used in drug delivery research. Reproducible and controlled conjugation among these multifunctional biomaterials is necessary to achieve efficient drug delivery platforms. However, multiple functional groups increase the risk of unintended intramolecular/intermolecular reactions during conjugation. Herein, conjugation approaches and possible undesired reactions between multi-amine functionalized peptides, multi-carboxylate functionalized polymers, and anhydride-containing polymers used in bone-targeted drug delivery were investigated under different conjugation strategies (carbodiimide chemistry and anhydride ring-opening via nucleophilic addition elimination). Coupling reactions between PSMA-b-PS [Poly(styrene-alt-maleic anhydride)-b-poly(styrene)] and tartrate-resistant acid phosphatase (TRAP) binding peptide (TBP, sequence: TPLSYLKGLVTVG) were selected as the model system for this study because of synthetic accessibility and application relevance. A series of polymer-peptide conjugation reactions were performed to investigate the effect of multiple primary amines within TBP on bioconjugation reactions. Carbodiimide chemistry and anhydride ring opening chemistry were used for conjugations. Conjugation behaviors of a series of peptides containing 1 to 3 primary amines were investigated. Multi-amine peptides led to extensive crosslinking between polymers regardless of the conjugation chemistry. Results also indicate that conventional peptide quantification methods (i.e., o-phthalaldehyde assay, bicinchoninic acid assay) are unreliable. Gel permeation chromatography (GPC) provided more accurate qualitative and quantitative evidence for intermolecular crosslinking. Crosslinking densities were correlated with higher feed ratios of multifunctional peptides and carbodiimide coupling reagents. Selectively protected peptides (Lys-Alloc) exhibited no crosslinking and yielded peptide-polymer conjugates with controlled dispersity and molecular weight. Furthermore, anhydride ring-opening (ARO) nucleophilic addition elimination was successfully introduced as a facile yet robust peptide conjugation approach for cyclic anhydride-containing polymers.

Title: **Osteoblasts efferocytosis induces osteoblasts' senescence and apoptosis**

Presenting Author: Chunmo Chen

Co-Authors: Emily Quarato, Yuko Kawano, Noah A Salama, Allison Li, Hiroki Kawano, Michael W. Becker

Lab PI / Mentor: Laura Calvi

Abstract (3500 characters or 500 words Limit)

Myelodysplastic syndromes (MDS) are a heterogeneous group of clonal stem cell disorders with an inherent tendency for leukemic transformation. More than 10,000 new cases occur in the US annually and the incidences increase with age. Limited therapies emphasize the need for more studies on the underlying pathology of MDS. Increased cellular apoptosis is commonly seen in MDS, but whether clearance of apoptotic cells by phagocytes plays a role in disease progression is not known. Our laboratory recently found that bone marrow (BM) macrophages are highly defective in MDS, with decreased efferocytic rates and increased inflammatory mediators. Mesenchymal stromal cells (MSCs) and osteoblasts (OBs) function as non-professional phagocytic cells capable of engulfing apoptotic cells, also known as efferocytosis. The increased apoptotic burden and defective macrophages would be expected to recruit non-professional phagocytes in the bone and bone marrow. Therefore, we hypothesize that OBs participate in the clearance of apoptotic cells in the bone marrow microenvironment (BMME), maintaining bone marrow homeostasis, but he increased osteoblastic efferocytic burden in MDS contributes to OBs' senescence and/or apoptosis as a mechanism of MDS progression

We utilized murine BM MSCs isolated from wildtype mice and NHD13 mice which will develop MDS-like symptoms in age of 4 months. Our in vivo data in NHD13 mice observed higher percentage of end- stage neutrophils.The increasing end-stage neutrophils need to be cleared out by phagocytes via efferocytosis (process of phagocytose apoptotic cells). Murine BM MSCs were differentiated into OBs using mineralization media and were incubated with end-stage neutrophils for 24 hours. Microscopic images and flow cytometry data show that nearly 70% of differentiated BM-derived MSCs are efferocytic. High levels of efferocytosis were associated with increased apoptosis in differentiated BM- derived MSCs. We also measured the baseline senescence and apoptosis of MSCs and OBs in NHD13 mice. In the MDS- like environment, the OBs' efferocytosis capacity was increased compared to that of OBs in the normal microenvironment. The increased efferocytic ability might explain the higher percentage of apoptotic OBs we observed in NHD13 mice. In conclusion, our data demonstrate that OBs can perform efferocytosis and will lead to different cellular fates depending on the BMME.

Our data may define novel mechanisms to explain the excessive senescence in MDS contributing to disease progression. Future experiments will involve modulating the efferocytosis rate by clinical drug targeting of efferocytic receptors, contributing to a novel therapeutic approach for MDS patients.

Title: **Overexpression of Cezanne Causes Early-Onset Osteoporosis in Mice**

Presenting Author: Zhongxuan (Kari) Chen

Co-Authors: Rong Duan, Xin Liu, Churou (Leah) Tang, Zhenqiang Yao

Lab PI / Mentor: Zhenqiang Yao

Abstract (3500 characters or 500 words Limit)

TNF receptor associated factor 3 (TRAF3) maintains osteoblasts differentiation directly by limiting GSK-3β-induced β-catenin degradation and inhibits osteoclast formation by negatively regulating non-canonical NF-kB activation. TRAF3 protein is degraded through Ubiquitin-Proteasome System (UPS) in the bone during age-related osteoporosis (AROP). Thus, stabilizing TRAF3 would be a new stragegy to treat AROP. However, we found that a small molecular coumpound that stabilizes TRAF3 by degrading inhibitor of apoptosis proteins (IAPs), a class E3 ubiquin ligase, was unable to treat AROP in mice (vertebral BV/TV 17.3+/-1.2 % vs. 18.8+/-1.3% of the vehicle) probably becasue the animals are inherently resistant or develop resistance to the IAP antagonist, like many proteasome inhibitors in human. One potential strategy is to target upstream components of the UPS such as deubiquitinases (DUBs), which remove ubiquitin to limit protein degradation. OTUD7b (Cezanne, Cez) is a DUB that was reported to inhibit TRAF3 ubiquitin degradation in B and T cells. The role of Cez in bone metabolism remains unknown. We found that DUB activity and Cez protein levels were markedly increased in the bone from aged mice vs. young mice. To investigate the role of Cez on the development of osteoporosis, we generated a Cez knock-in (CezKI) mouse at the locus of ROSA26 through CRISPR/Cas-mediated genome engineering. The CezKI mice were crossed with osteocalcin-cre (OCNcre) mice to generate CezKI-OCNcre mice, called osteoblast Cez conditional knock-in (Cez KI-OB) mice. We found that trabecular bone mass in Cez KI-OB mice was markedly and significantly reduced compared to that in WT control (CezKI) mice by 12-month-old (Vertebral BV/TV 19.0+/-3.7% vs 29.3+/-3.6%). Consistent with this, osteoblast surface was markedly reduced while osteoclast number and surface were not changed on the trabecular surface in the vertebrae from CezKI-OB mice compared to that from CezKI control mice. Furthermore, bone marrow stromal cells from CezKI-OB had reduced ALP+ osteoblast differentiation compared to that from CezKI control mice (ALP+ OB area 0.26+/-0.09 mm2 vs 1.81+/-0.2 mm2 of WT control mice) while RANKL-induced osteoclast formation from bone marrow cells did not show difference between CezKI-OB and CezKI control mice. In summary, over-expression of Cez in mature osteoblasts inhibits bone formation to cause early onset osteoporosis. We conclude that development of Cez inhibitor would be a novel strategy to treat osteoporosis.

Title: **Osteoclast Formation Dependent on Sex and Location of Derivation in Inflammatory Arthritis**

Presenting Author: Michael Christof

Co-Authors: Kiana L. Chen, Xi Lin, Edward M. Schwarz, and Homaira Rahimi

Lab PI / Mentor: Homaira Rahimi

Abstract (3500 characters or 500 words Limit)

Background: Rheumatoid arthritis (RA) is a chronic inflammatory autoimmune disorder characterized by synovial inflammation, cartilage destruction, and bone erosions. We study these erosions and inflammatory arthritis using the TNF transgenic (TNF-Tg) mouse model of RA, which displays a strong sexual dimorphism in which females have worse disease than males. To better understand this dimorphism, we aimed to determine whether bone marrow-derived osteoclasts yield similar numbers to peripheral blood mononuclear cell-derived osteoclasts in male versus female mice. We hypothesized that more osteoclasts will differentiate from bone marrow than peripheral blood mononuclear cells and from female than male TNF-Tg mice.

Methods: Peripheral blood mononuclear cells (PBMC) and bone marrow cells (BM) were harvested from 3-month-old male and female TNF-Tg mice (n=3 mice/group) and cultured in osteoclast differentiation media at a seeding density of 50,000 cells/well with 5 ng/mL of Macrophage Colony Stimulating Factor (M-CSF) for 2 days, followed by 30ng/mL M-CSF and 30 ng/mL Receptor Activator of Nuclear Factor Kappa-B Ligand (RANK-L) for 3 days. Afterwards, cells were fixed with 4% paraformaldehyde (PFA) and stained for tartrate-resistant acid phosphatase (TRAP). The total number of osteoclasts (≥3 nuclei, TRAP+ cells) were quantified in each well. From that total count, we identified the number of osteoclasts with >10 nuclei. BM and PBMC-derived cells were analyzed with unpaired t-tests and male and female values from BM and PBMC were analyzed with a two-way ANOVA with Tukey's post-test. Values are reported as mean +/- standard deviation.

Results: Cultures of BM-derived cells had a significantly greater number of differentiated osteoclasts than PBMC (392.6 +/- 83.65 vs 200.5 +/-87.28). However, PBMC had a significantly greater percentage of osteoclasts with >10 nuclei than BM-derived cells (35.85 +/-10.73% vs 22.5 +/- 7.83%). There was no significant sex difference within BM and PBMC-derived cells. However, there were more total male-derived and female-derived BM cells than female-derived PBMC cells (399.9 +/- 47.24 and 385.3 +/- 122.9 vs 147.2 +/- 49.39). There were also more male-derived PBMC cells than female-derived BM cells for the percentage of osteoclasts with >10 nuclei (42.17 +/- 11.24% vs 17.27 +/- 7.48%).

Conclusions: Here we show that BM produces more osteoclasts (OCs) than PBMC, yet PBMC-derived osteoclasts have more 10+ nuclei OCs (an indication of more active cells), suggesting that the origin of osteoclast precursors may affect osteoclast activity. Furthermore, there is variability of OC numbers based on origin of sex, suggesting a sexual dimorphism of osteoclast precursors. Further studies to examine osteoclast activity of PBMC and BM cells as well as sex origin will be needed to determine the nature of sexual dimorphism in murine inflammatory erosive disease.

Title: **Analyzing the Characteristics of Geographic Regions with High Racial and Ethnic Disparities in Total Joint Replacement Use**

Presenting Author: Jordan Cruse

Co-Authors:

Lab PI / Mentor: Caroline Thirukumaran, MBBS, MHA, PhD

Abstract (3500 characters or 500 words Limit)

Background: Total joint replacement surgeries (TJRs), which include total hip replacements (THRs) and total knee replacements (TKRs), are successful surgeries for the treatment of severe osteoarthritis in these joints. However, it has been well established that significant racial and ethnic disparities in TJR utilization exist. Notably, the use of TJRs is 38-40% lower for Black older adults compared to their White counterparts. Furthermore, there is significant geographic variation in the magnitude of these disparities across the country. Whether the variation in these disparities can be attributed to geographic and healthcare supply factors is unknown. This knowledge can potentially inform policy that seeks to improve the equity in TJR use by addressing these factors.

Methods: We used previously calculated age- and sex-standardized rates of inpatient THRs and TKRs per 1,000 beneficiaries (separate for White and Black patients) between 2013–2019 in each of the 306 Hospital Referral Regions (HRRs) utilizing Medicare enrollment and claims data. We quantified racial disparity in each procedure as the difference in rate between White and Black patients, and then categorized it into quintiles. A disparity greater than zero represents the extent to which Black patients undergo fewer surgeries than White patients. Potential explanatory variables were aggregated from the Agency for Healthcare Research and Quality (AHRQ)'s Social Determinants of Health (SDOH) database as well as the Dartmouth Atlas of Health. Data obtained at the zipcode-level were averaged to the HRR-level. For descriptive analyses, we used Kruskal-Wallis tests and chi-square tests for continuous and categorical variables, respectively, to compare the distribution of explanatory variables across disparity quintiles for the baseline year. We used multivariable mixed-effects linear regression analyses with HRR-level random effects to examine the HRR-level disparities separately for THRs and TKRs.

Results: Of the 237 HRRs in the study cohort, the mean HRR-level disparity was 1.45 surgeries/1,000 beneficiaries for THRs and 3.52 surgeries/1,000 beneficiaries for TKRs in 2013. HRRs within the Northeast region of the US have disproportionately high rates of THR disparity as 25.53% of HRRs in the 5th quintile are in this region, despite making up only 13.92% of the country. Racial disparities in TKRs are found predominantly in the Midwest as 44.68% of HRRs in the 5th quintile are in this region, despite making up only 24.05% of HRRs. The averaged median household income and the percent of HRR residents that are Black were positively associated with disparity in TJRs. For every $10,000 increase in income, disparity in THRs and TKRs increased by 0.19 (95% Confidence Interval [CI]: 0.04 to 0.34, p=0.01) and 0.36 (95% CI: 0.08 to 0.63, p=0.01), respectively. For every 1% increase in Black residents, disparity in THRs and TKRs increased by 0.02 (95% CI: 0.01 to 0.03, p=0.001) and 0.03 (95% CI: 0.01 to 0.05, p=0.001).

Conclusion: Our work identifies important geographic and healthcare predictors of racial disparities in the use of THRs and TKRs. Designing interventions that are targeted towards these markers of disparities will likely yield value in promoting the equity in joint replacement care.

Title: **Surgical Management of Spinal Epidural Abscess: Risk Factors and Outcomes**

Presenting Author: Adwin Denasty, MD

Co-Authors: Karim Elmobdy,Robert Molinari, Addisu Mesfin, Paul Rubery,Emmanuel Menga

Lab PI / Mentor: Addisu Mesfin, MD

Abstract (3500 characters or 500 words Limit)

Background: A spinal epidural abscess (SEA) is often a surgical emergency and delayed diagnosis can lead to permanent neurological deficits and mortality. The incidence of SEAs has more than doubled over the past three decades. The aim of this study was to analyze the demographics and clinical outcomes of patients undergoing surgery for SEA to decrease diagnostic delay and elucidate factors associated with prognosis.

Methods: We retrospectively reviewed electronic medical recordsf adult patients diagnosed with SEAs and surgically managed from September 2003 to December 2021 at a single center.

Results: Study patients (n=70, 43 men, 27 women) had an average follow-up of 7.5 +/- 16.0 months. SEA was most common in the thoracic (n=24, 33.8%) and lumbar (n=22, 31.0%) spine. Patient comorbidities included DM (n=21, 30.0%), IVDU (n=11, 15.7%), and co-existing infections (n=49, 69%). Surgical intervention consisted of: transpedicular decompressions (n=9, 12.7), corpectomies (n=17, 14.4%), laminectomy without fusion (n =43, 56/6%), and fusions (n=25, 32.9%).
Mean labs on presentation were WBC (12.4), ESR (40.7), and CRP (119.2). The most cultured organism was S. aureus (n=48, 63.2%). During latest-follow-up, ASIA score improvement was seen in 8/43 patients (17.8%); no change in 34/43 patients (79.1%); deterioration in 2 patients (4.7%).

Conclusions : Most SEAs occurred in the thoracic and lumbar spinal regions. Patients typically have a history of DM, IVDU, or co-existing infections. S. aureus is the most cultured organism. At the latest follow-up, most patients showed either no change or improvement in post-operative versus pre-operative ASIA scores.

Title: **A comparison of intraoperative details and postoperative outcomes in stemmed and stemless humeral components in anatomic total shoulder arthroplasty**

Presenting Author: David DiStefano, MD

Co-Authors: Dylan Greif, MD

Lab PI / Mentor: Raymond J Kenney, Sandeep Mannava, Ilya Voloshin, MD

Abstract (3500 characters or 500 words Limit)

Background:
The number of anatomic total shoulder arthroplasties (TSA) has risen dramatically in the past decade in the United States. With this rise in prevalence, there has been an evolution in component design. Stemless humeral components have been developed with numerous theoretical advantages including preservation of bone stock, reduced intraoperative time and risk of periprosthetic fracture. Disadvantages include risk of component loosening before adequate biologic fixation occurs. The goal of this study is to compare the intraoperative details, postoperative outcomes with PROMIS and ASES scores, postoperative range of motion, and implant-related complications between stemmed and stemless TSA. Our hypothesis is that stemless TSA would have a shorter intraoperative time, less surgical blood loss, with no difference in PROMIS scores, ASES scores, postoperative range of motion, or implant-related complications.

Methods:
We included patients who underwent TSA and completed preoperative and 1-year follow up of PROMIS Upper Extremity (UE), Physical Function (PF), Pain Interference (PI), and Depression scores (DEP), as well as ASES and ASES-P scores. Postoperative outcome measures were recorded 2 weeks, 7 weeks, 3 months, and 12 months postoperatively. Range of motion (ROM) was recorded as forward flexion (FF) and external rotation (ER) at the 7-week and 3-month marks. Patient demographics, intraoperative surgical time, intraoperative blood loss, postoperative range of motion, and postoperative complications were recorded by manual chart review. Intraoperative time was recorded as the time from starting incision to the start of wound closure. Statistical analysis was performed with a $p = 0.05$ to determine significance.

Results:
We included 56 patients (27 stemless TSA, 29 stemmed TSA) in this study. There were no significant differences in baseline characteristics between the groups. Intraoperative surgical time was significantly shorter in the stemless compared to the stemmed group (66.4 ± 11.9 mins vs 75 ± 12.2 mins, $p = 0.009$). Intraoperative blood loss was significantly lower in the stemless compared to the stemmed group (118.5 ± 63.8 mL vs 187.9 ± 159.5 mL, $p = 0.020$). ASES and ASES-P scores were significantly different between the stemmed and stemless groups preoperatively, and PROMIS UE scores were significantly different at the 2-week mark. There were no significant differences in PROMIS UE, PI, PF, DEP, ASES and ASES-P scores at any other timepoint. The stemless cohort had greater ER ROM at the 7-week mark (48.6 ± 14.0 degrees vs 35.7 ± 13.8 degrees, $p = 0.003$), however there were no differences in FF or ER ROM at 3 months. There were no humeral component-related complications in either group at 1 year postoperatively.

Conclusion:
Compared to conventional TSA with stemmed humeral components, stemless humeral TSA offers similar improvements in postoperative PROMIS scores, ASES scores, and range of motion, with a reduced intraoperative time and blood loss, with no significant difference in implant-related complications.

Title: **Differential roles of Piezo1 and TRPV4 in Injury-induced Chondrocyte Death in situ**

Presenting Author: Chrysilla Emanuelle

Co-Authors: Johann Kintzel

Lab PI / Mentor: Whasil Lee

Abstract (3500 characters or 500 words Limit)

Introduction: Degeneration of articular cartilage (AC) is an attribute of osteoarthritis (OA), a debilitating joint condition suffered by over 300 million people worldwide. Chondrocytes in the AC sense and transduce a wide range of mechanical loading. Increased chondrocyte death by mechanical trauma is observed in the onset and pathogenesis of OA. We and others have reported critical roles of Ca2+-permeating mechanosensitive ion channels – Piezo1, Piezo2, and TRPV4 – in extracellular matrix (ECM) remodeling and cartilage homeostasis, but knowledge gaps exist in the roles of these channels during chondrocyte death. Since promoting chondrocyte survival by tuning mechanosensitive channels may provide new therapeutic strategies for OA, the goal of this study is to quantify the effect of channel activation and inhibition on chondrocyte damage post-mechanical injury. We report here robust expressions of these channels by immunohistochemistry and the differential roles of each channel on injury-induced death of chondrocytes in situ at 3h post-injury by treating it with currently available chemical activators and inhibitors.

Methods: Cylindrical cartilage plugs were harvested from femoral condyles of mature pig joints using a 4 mm biopsy punch. Cartilage plugs were fixed, embedded in paraffin, sectioned with a thickness of 20 μM, and labeled with primary antibodies: anti-Piezo1, anti-Piezo2, and anti-TRPV4 (Proteintech, 1:200) and a secondary antibody (Invitrogen, Alexa Fluor 594). Samples were imaged by a fluorescent microscope (Keyence). Cartilage plugs loaded with calcein/PI (Invitrogen) were treated with or without GsMTx4 (pan-Piezo antagonists, 40 μM), Yoda1 (Piezo1-specific agonists, 20 μM), or GSK101 (TRPV4-specific agonist, 10 nM) for 20 mins and injured by a 1 mm biopsy punch using a custom-built injury system. Cartilage plugs were imaged on a confocal microscope (Olympus, 10x). ImageJ was used to analyze the wound thickness and cellular viability at 3 hrs post-injury. Student t-tests or One-way ANOVA was used to compare two or multiple groups, statistical significance set to $p<0.05$.

Results: Qualitative interpretation of immunofluorescence images confirmed the robust expression of Piezo1, Piezo2, and TRPV4 channels in the superficial zone of porcine cartilage. Differential effects of Yoda1, GSK101, and GsMTx4 treatments were observed in terms of chondrocyte viability post-biopsy injury. GsMTx4-pretreated cartilage plugs exhibit significantly reduced wound thickness compared to untreated controls (76.9 ± 6.8 μM vs. 58.1 ± 5.7 μM, unpaired t-Test, N=4~6), but not in Yoda1 (83.0 ± 7.7 μM) or GSK101-treated (65.1 ± 6.9 μM) groups. Cellular death percentiles over 1 mm x 1 mm x 40 μM of control, Yoda1-treated, GSK101- treated, and GsMTx4-treated groups are 39.2 ± 4.9 %, 52.9 ± 3.9 %, 44.1 ± 2.2 %, and 24.3 ± 3.5 %, respectively.

Discussion: Piezo1-, Piezo2-, and TRPV4-mediated mechanotransduction mechanisms of chondrocytes play major roles in cartilage degradation. We demonstrated that Piezo1 activation by Yoda 1 and TRPV4 activation by GSK101 increases wound thickness and cell death 3h post-injury. However, Piezo1 inhibition using GsMTx4 provided a chondroprotective effect by limiting cellular death. Since promoting chondrocyte survival post-injury may delay cartilage degradation, these results indicate that the inhibition of Piezo1 using GsMTx4 is a promising therapeutic target for the pathogenesis of OA.

Title: **Elucidating the role of NR4A1 in cartilage homeostasis and osteoarthritis progression**

Presenting Author: Katherine Escalera-Rivera

Co-Authors: Eduardo Peralta-Herrera

Lab PI / Mentor: Jennifer H. Anolik and Jennifer H. Jonason

Abstract (3500 characters or 500 words Limit)

Osteoarthritis (OA) is a degenerative joint disease that currently affects over 30 million United States adults, with aging and injury as two of its main risk factors. OA is characterized by irreversible damage to the articular cartilage, which is mainly composed of chondrocytes. These cells are responsible for maintaining the homeostasis of the cartilage extracellularmatrix (ECM) by regulating expression of both anabolic and catabolic ECM components. Matrix metalloproteinases (MMPs), for example, degrade collagen molecules and mediate catabolism of the ECM, ultimately leading to cartilage degradation. As OA progresses, chondrocytes increase secretion of MMPs and cytokines, which are released into the joint synovial fluid. These molecules are recognized by other cells in the joint, which start secreting inflammatory mediators, creating a continuous feedback loop between cartilage and other joint tissues that constitutes the initiation of chronic inflammation. NR4A1 is a transcription factor rapidly induced by inflammatory stimuli and a negative regulator of NF-kappaB signaling in multiple cell types, including macrophages, commonly found in the inflamed synovium. However, the role of NR4A1 in regulating cartilage homeostasis and chondrocyte response to injury is not well-defined. Using immunohistochemistry to measure NR4A1 protein levels in chondrocytes of the articular cartilage of mice, we find a significant decrease in NR4A1 in joints subjected to meniscal/ligamentous injury (MLI) when compared to sham joints. To elucidate the role of NR4A1 during post-traumatic OA (PTOA) onset and progression, we performed MLI in wild-type (WT) C57BL/6J and age-matched NR4A1 global knockout (KO) mice and harvested the knee joints 4 weeks later for histology. We found increased levels of MMP-13 in the sham joints of NR4A1 KO mice compared to WT mice. Effects on cartilage area, however, are variable at this timepoint with some animals experiencing accelerated cartilage loss. In vitro, overexpression of NR4A1 in a chondrogenic cell line treated with IL-1 beta led to decreased transcription of several MMPs. Our data lead us to propose that NR4A1 in chondrocytes normally prevents uncontrolled secretion of MMPs, a homeostatic role that is disrupted by decreased protein expression following joint injury, promoting enhanced cartilage matrix catabolism.

The Center for Musculoskeletal Research (CMSR)
12th Annual Symposium – October 19, 2022

Title: **Identifying Knowledge Gaps in Medical Student Education of Patient Reported Outcomes**

Presenting Author: Samuel Florentino

Co-Authors: Judy Baumhauer, MD MPH, Suzanne Karan, MD, Gabriel Ramirez

Lab PI / Mentor: Judy Baumhauer, MD MPH

Abstract (3500 characters or 500 words Limit)

Introduction: Patient Reported Outcomes (PROs) are health assessments directly answered and entered by the patient into the medical record without interpretation by healthcare professionals. Routinely collected PROs improve patient-provider communication, symptom reporting, patient satisfaction, and the quality of care in treatment and management. PRO use has expanded into quality and payment models, and is required by the American Board of Orthopaedic Surgery as part of board certification. Despite their importance, PRO education is not required in medical education. The purpose of this study was to examine medical students' knowledge of PROs. Secondarily, we assessed the impact formal education on PROs had on medical student knowledge.

Methods: A 20-question survey was developed using validated methodology (expert review, cognitive interviews, pilot study) and distributed to medical students at two US medical schools. To determine the effectiveness of formal education on medical students' knowledge of PROs, 4th-year medical students at the host institution were invited to complete a survey inquiring about their knowledge of PROs before and two weeks after an educational lecture.

Results: 137 medical students responded to the survey and the response rate was 15%. Medical students' knowledge levels of PROs were low. Only 54% correctly identified the definition of a PRO and <25% of respondents understood the need to incorporate PROs into patient care as identified by the CMS. Less than 8% received formal education on PROs. Responses did not significantly differ by year in school.

Respondents demonstrated positive attitudes towards PROs. 78% of responding medical students agreed PROs are important in delivering high-quality patient care. 84% were interested in learning about PROs. Only 16% of respondents felt prepared to utilize PROs in a patient care setting.

Among 121 responding 4th year medical students, 67% correctly answered the definition of PROs prior to formal education compared to 82% after. Additionally after education, 88% agreed PROs are an important component of providing high-quality care.

Conclusions: The results of this survey provide important insight into current medical students' gap in knowledge of PROs. Deficiencies in knowledge are supported by the low proportion of students who feel prepared to utilize PROs in a clinical setting. Routine collection, interpretation, and utilization of PROs highlight the voice of the patient by providing direct and relevant information about how the patient is feeling and functioning in the context of their health. The gaps in the knowledge and preparedness to use PROs are a barrier to the delivery of high-quality care. Medical students agreed they would like to receive education on PROs (>80%), and improvements in knowledge of PROs were identified with the implementation of formal education into medical education curriculum. With the proven benefits of PRO collection and integration into care, sufficient training and education for current and future clinicians is an important step linking clinician action and with measurable outcomes. Based on the current study, the implementation of formal education of PROs into medical education curriculum may help fill that gap.

Title: **Targeting penicillin binding protein-4 as a novel target for treatment of Staphylococcus aureus induced osteomyelitis**

Presenting Author: Vijay Singh Gondil

Co-Authors: Mikaeel Young, Danica J. Walsh, Hailey S. Butman, Elysia Masters, Emily Laskey, Hani Awad, James McGrath, Edward M. Schwarz, Christian Melander

Lab PI / Mentor: Paul M. Dunman

Abstract (3500 characters or 500 words Limit)

Staphylococcus aureus colonization of cortical bone osteocyte lacuno-canalicular networks (OLCNs) is thought to allow the organism to cause chronic is mediated, in part, by a set of penicillin binding proteins (PBPs), which catalyze peptidoglycan crosslinking and are the cellular targets of β-lactam antibiotics. S. aureus PBP4, has recently been identified as a critical factor in conferring a high level and broad-spectrum resistance towards entire class of b-lactam antibiotics. Moreover, S. aureus PBP4 has been shown to be essential for OLCN invasion. Consequently, small molecule inhibitors of S. aureus PBP4 may have therapeutic promise as alternative agents that may reverse antibiotic resistance, and/or reduce re- occurring osteomyelitis. We developed a high throughput screen and secondary assays to identify putative PBP4 inhibitors. A subset of compounds reduced S. aureus PBP4 mediated β-lactam resistance in several strain backgrounds but had no impact on human cell viability. Hits were further distinguished as agents that may reduce S. aureus PBP4 transcription or those that are likely to bind and inhibit the protein directly as evaluated by real-time expression and fluorescent b-lactam based assays, respectively. The frontrunner compound, 9314848, is a relatively strong PBP4 inhibitor (apparent IC50 13.4 μM), and reduced PBP4- mediated ceftobiprole resistance up to 16-fold. PBP4-mediated transmigration through in-vitro μSiM-CA channel pores engineered to mimic OLCNs, suggesting it is a promising scaffold for translational development. μSiM-CA based assay exhibited the dose dependent inhibition of transmigration ability of S. aureus upon treatment with 9314848 suggesting therapeutic potential of the inhibitor in impeding OCLN invasion and colonization (EC50 6.25 μM; 2.5 μg/ml). Computational modeling and follow-on chemical design have allowed a workable structure activity relationship and synthesis of analogs with improved PBP4 inhibitory activities that are now the subject of lead generation.

Title: **The Extent that Morbid Obesity is a Modifiable Risk Factor Among Morbidly Obese Patients with Joint Osteoarthritis without Participating in a Formal Perioperative Optimization Program**

Presenting Author: Paul Guirguis

Co-Authors: Dr. Mina Botros, Dr. Benjamin Ricciardi

Lab PI / Mentor: Dr. Benjamin Ricciardi

Abstract (3500 characters or 500 words Limit)

OBJECTIVES: Our purpose is to evaluate the extent to which morbid obesity is a modifiable risk factor in patients with end-stage knee osteoarthritis without a perioperative optimization program. We evaluated patients with a body mass index (BMI) > 40 at initial consultation regarding total knee arthroplasty (TKA), to determine: 1) the percentage of patients who achieved BMI < 40 over a two year study period through nutritional modification or bariatric surgery; 2) the number of patients eligible for TKA based on arthritis severity who ultimately undergo the procedure within two years; 3) differences in patient reported outcome measures (PROMs).

METHODS: This is a single-institution retrospective analysis of 624 obese patients that were evaluated for TKA between 2016-2019. The inclusion criteria: Kellgren-Lawrence grade 3 or 4 radiographic knee osteoarthritis, age 18-95, BMI> 40, and follow-up <1 year from initial visit. Demographic data, the types of weight loss interventions, change in BMI, and PROM scores from initial and final visits were collected. Multivariant logistic and linear regression models were used to evaluate characteristics of patients undergoing TKA, association of weight loss interventions with BMI changes, and PROMIS score outcomes. Chi-squared tests was used to for categorical variables, and Kruskal-Wallis tests for continuous variables.

RESULTS: Approximately 10% of patients ended up pursuing TKA over the study period. The percentage of patients that experienced BMI loss> 10 were as follows: bariatric surgery (23.75%), non-surgical intervention (8.61%), and no intervention (1.0%) (p=.0006). Additionally, patients that experienced BMI loss between 5-10 were: bariatric surgery (38.75%), non-surgical intervention (27.05%), and no intervention (6.0%); (p<.0001). Bariatric surgery group was 3.677 times more likely to lose 10 or more BMI vs. non-surgical intervention participants (95% CI [1.666, 8.113]; p=.001). When the same two groups are compared, bariatric surgery group was 1.959 times more likely to experience loss of 5 to 10 BMI compared to non-surgical intervention (95% CI [1.060, 3.623]; p=.032). Amongst bariatric surgery patients, 16.25% (N=13) underwent joint replacement, compared to 15.16% (N=37) of patients who utilized non-surgical interventions and 6.33% (N=19) of those with no intervention (p=.0043). Bariatric surgery patients were 3.075 times more likely to undergo TKA vs. no intervention (95% CI [1.338, 7.064]; p= .008), while non-surgical group was 2.419 times more likely to undergo TKA vs. no intervention (95% CI [1.288, 4.544]; p=.006). White patients across all interventions were 2.32 times more likely to experience loss of greater than 5 BMI vs. non-white patients (95% CI [.231, .869]; p=.018). PROMIS analysis revealed no significant difference in pain or physical function outcomes when comparing bariatric surgery vs. non-surgical and bariatric surgery vs. no intervention.

CONCLUSIONS: Most obese patients with end-stage knee osteoarthritis were unable to achieve weight loss >5-10 of their BMI over a mean four-year period in our center, which lacks a formal weight optimization program. Patients requiring loss of >5 BMI are more successful through utilization of bariatric surgery compared to non-surgical interventions although ultimate pursuit of TKA remained low in all cohorts. Without the use of a formal optimization program, BMI > 40 was not strongly modifiable in our cohort.

Title: **Integration of single cell RNA sequencing and spatial transcriptomics reveal molecular components of cell-cell communication in chondrogenesis over time during embryonic limb development**

Presenting Author: Victoria Hansen

Co-Authors: Gulzada Kulzhanova, Eloise Fadial, Helen Shammas, Chia-Lung Wu

Lab PI / Mentor: Chia-Lung Wu

Abstract (3500 characters or 500 words Limit)

Cartilage healing presents a major challenge since it is an avascular tissue that is slow to recover from illness and injury. Osteoarthritis (OA) is a disease with a dearth of drugs for effective treatment. Tissue engineering of cartilage by inducing chondrogenesis in stem cells is a promising future avenue of OA therapy. However, off-target differentiation remains a problem. By examining the cell-cell communication in developing embryonic cartilage we may identify potential signaling pathways for more effective in vitro chondrogenesis. By using integrative single cell RNA sequencing (scRNA-Seq) and spatial transcriptomics (spatial-Seq), we comprehensively characterized gene expression profiles of chondrocyte subpopulations in a spatially-conserved manner and elucidated dynamic changes in cell-cell crosstalk during murine pre-natal knee joint development. Knee joints from mouse embryonic day (E) 11.5, 13.5, 15.5, and 18.5 were harvested (UR IACUC approved). FFPE sections and hind limb single cell suspensions were submitted for spatial-Seq (Visium, 10X Genomics) and scRNA-Seq to the UR GRC. Distinct cell populations were identified in scRNA-Seq data and then mapped to spatial-Seq sections to localize cell types. Bioinformatic tools including Seurat, Monocle, and CellChat R packages were utilized to perform cell clustering and predict cell-cell interactions. Cell clusters corresponding to developing tissues, including skin, muscle, bone, etc., were identified in all time points from scRNASeq analyses following unsupervised clustering. Chondrocytes from all time points were integrated and re-clustered. Perichondrial cells and 4 unique chondrocyte phenotypes in the knee joint were identified: hypertrophic, proliferative, Isg15+, and early/mature chondrocytes. Proliferative chondrocytes were the dominant type in the E11.5 limb bub, while hypertrophic chondrocytes gradually increased from E13.5 to E18.5. These cell types were then mapped to only the knee joint in spatial-Seq sections to reveal the locations of specific chondrocyte phenotypes over time. Using CellChat analysis, a variety of significant cell-cell interactions between different chondrocyte phenotypes were identified. For example, cell-cell interactions between midkine (MDK) and both syndecan 4 (SDC4) and nucleolin (NCL) were highly significant and probable. We observed that the significance and probability of chondrocyte cell-cell interactions changed throughout gestational development and were chondrocyte phenotype-dependent. For instance, perichondrial cell signaling by MDK and PTN to SDC4 expressed by early/mature chondrocytes were dominant pathways in early limb bud development as compared to late in embryogenesis, whereas PTN to NCL signaling became more prominent in later stages. SDC4 has been implicated as a highly expressed protein in human knee OA and Sdc4 deletion in mice is protective against surgically induced OA. SDC4 may be acting as a regulator of chondrogenesis and chondrocyte hypertrophy, particularly since it is involved in signaling from perichondrium to hypertrophic and early/mature chondrocytes. This is further supported by the finding that PTN, an inhibitor of chondrocyte proliferation, is one of the ligands signaling through SDC4. We believe that targeting cell signaling molecules such as these at appropriate timepoints could help reduce off-target differentiation and enhance generation of bona fide cartilage tissue for therapeutic applications.

Title: **Intravital tracking of bone remodeling and the hematopoietic stem cell niche**

Presenting Author: Kevin Lee, Melissa MacLiesh

Co-Authors: Wimeth Dissanayake, Cih-Li Hong

Lab PI / Mentor: Shu-Chi A. Yeh

Abstract (3500 characters or 500 words Limit)

Cartilage healing presents a major challenge since it is an avascular tissue that is slow to recover from illness and injury. Osteoarthritis (OA) is a disease with a dearth of drugs for effective treatment. Tissue engineering of cartilage by inducing chondrogenesis in stem cells is a promising future avenue of OA therapy. However, off-target differentiation remains a problem. By examining the cell-cell communication in developing embryonic cartilage we may identify potential signaling pathways for more effective in vitro chondrogenesis. By using integrative single cell RNA sequencing (scRNA-Seq) and spatial transcriptomics (spatial-Seq), we comprehensively characterized gene expression profiles of chondrocyte subpopulations in a spatially-conserved manner and elucidated dynamic changes in cell-cell crosstalk during murine pre-natal knee joint development. Knee joints from mouse embryonic day (E) 11.5, 13.5, 15.5, and 18.5 were harvested (UR IACUC approved). FFPE sections and hind limb single cell suspensions were submitted for spatial-Seq (Visium, 10X Genomics) and scRNA-Seq to the UR GRC. Distinct cell populations were identified in scRNA-Seq data and then mapped to spatial-Seq sections to localize cell types. Bioinformatic tools including Seurat, Monocle, and CellChat R packages were utilized to perform cell clustering and predict cell-cell interactions. Cell clusters corresponding to developing tissues, including skin, muscle, bone, etc., were identified in all time points from scRNASeq analyses following unsupervised clustering. Chondrocytes from all time points were integrated and re-clustered. Perichondrial cells and 4 unique chondrocyte phenotypes in the knee joint were identified: hypertrophic, proliferative, Isg15+, and early/mature chondrocytes. Proliferative chondrocytes were the dominant type in the E11.5 limb bub, while hypertrophic chondrocytes gradually increased from E13.5 to E18.5. These cell types were then mapped to only the knee joint in spatial-Seq sections to reveal the locations of specific chondrocyte phenotypes over time. Using CellChat analysis, a variety of significant cell-cell interactions between different chondrocyte phenotypes were identified. For example, cell-cell interactions between midkine (MDK) and both syndecan 4 (SDC4) and nucleolin (NCL) were highly significant and probable. We observed that the significance and probability of chondrocyte cell-cell interactions changed throughout gestational development and were chondrocyte phenotype-dependent. For instance, perichondrial cell signaling by MDK and PTN to SDC4 expressed by early/mature chondrocytes were dominant pathways in early limb bud development as compared to late in embryogenesis, whereas PTN to NCL signaling became more prominent in later stages. SDC4 has been implicated as a highly expressed protein in human knee OA and Sdc4 deletion in mice is protective against surgically induced OA. SDC4 may be acting as a regulator of chondrogenesis and chondrocyte hypertrophy, particularly since it is involved in signaling from perichondrium to hypertrophic and early/mature chondrocytes. This is further supported by the finding that PTN, an inhibitor of chondrocyte proliferation, is one of the ligands signaling through SDC4. We believe that targeting cell signaling molecules such as these at appropriate timepoints could help reduce off-target differentiation and enhance generation of bona fide cartilage tissue for therapeutic applications.

Title: **DNA damage-induced proinflammatory signaling and DNA repair in chondrocytes**

Presenting Author: M. Nick James

Co-Authors: Eduardo Peralta-Herrera, Danielle Benoit, and Jennifer H. Jonason

Lab PI / Mentor: Jennifer H. Jonason, Ph.D. and Danielle Benoit, Ph.D.

Abstract (3500 characters or 500 words Limit)

Osteoarthritis (OA), the most common and most costly form of arthritis, is characterized by progressive loss of articular cartilage. Despite its world-wide prevalence and economic burden, the precise mechanisms responsible for OA onset are still unclear. Aging is known to be among the most important risk factors associated with OA development. While aging is thought to be a consequence of accumulated DNA damage, the relationship between DNA damage and OA is not clear. Our laboratory has found that aged articular chondrocytes have increased inflammatory NF-κB activation and that enhanced IKKβ/NF-κB activation in chondrocytes accelerates spontaneous OA development in young mice. DNA double-strand breaks (DSBs), a particularly toxic form of DNA damage, are also known to activate the NF-κB pathway downstream of stimulator of interferon gene (STING). Thus, we hypothesize that accumulation of DNA damage in aging leads to chronic proinflammatory signaling that ultimately results in degeneration of articular cartilage and OA onset. To investigate the inflammatory role of DNA damage in OA development, we treated ATDC5 chondroprogenitors with the topoisomerase inhibitor etoposide to induce DNA DSBs. We demonstrated that etoposide effectively produces accumulation of DNA DSBs in ATDC5 chondroprogenitors and increases NF-κB activation by western blot. In vitro etoposide treatment also increased expression of NF-κB and IRF gene targets including proinflammatory cytokines, catabolic matrix enzymes, and interferon-stimulated genes. To determine the effect of STING perturbation on chondrocyte behavior two approaches were used to treat ATDC5 cells: 1) STING knockdown by transfection with STING siRNA before treatment with 25 μM etoposide; and 2) STING agonist treatment consisting of 0.25 or 25 μg/mL of diamidobenzimidazole. ATDC5 STING knockdown reduced proinflammatory gene expression after etoposide treatment while STING agonist treatment increased proinflammatory NF-κB target gene expression. For in vivo DNA damage induction we utilized a mouse model of ionizing radiation through the small animal radiation research platform which allows the precise localization of radiation to the knee joint. Mouse knees received either 0, 2, or 8.2 Gy X-radiation using a 3-by-3 mm collimated beam centered on the knee joint space. Mouse knee joints contained significantly more DNA DSBs 2 hours after irradiation at 8.2 Gy. Targeted X-irradiation of mouse knee joints demonstrated the chondrocyte's ability to repair DNA DSBs in vivo may be limited as 25% of cells with DNA DSBs at 2 hours contained unresolved DNA DSBs at 48 hours at either dose. We expect these DNA-damaged chondrocytes may become senescent or apoptotic. We will perform further immunohistology, including more replicates and samples from later time points after irradiation, to investigate if this is the case and determine whether DNA damage promotes OA onset. In summary, we determined that ATDC5 chondrocyte-like cells respond to DNA DSBs by activating proinflammatory signaling and gene expression, in part, through STING activation and we characterized initial DNA DSB repair in vivo in chondrocytes. Investigating how DNA DSBs affect chondrocytes may inform development of novel OA therapeutic strategies and expands our understanding of OA pathogenesis in aging.

Title: **In vivo Engineered Extracellular Matrix as Scaffolding Materials for Tissue-Engineered Periosteum**

Presenting Author: Chen Jiang

Co-Authors: Tianfeng Miao, Nicholas Lenhard, Xinping Zhang

Lab PI / Mentor: Xinping Zhang

Abstract (3500 characters or 500 words Limit)

While periosteum tissue engineering has become a mainstay in repair and reconstruction, an emerging surgical technique named Masquelet technique that combines a foreign body reaction-induced vascularized tissue membrane with bone chips/matrix to repair and reconstruct a large segmental bone defect has gained wide attention in regenerative medicine. The key to the success of Masquelet technique rests on its ability to promote the formation of an “periosteum-like” autologous tissue membrane at the bone defect site, minimizing a series of adverse effects resultant from biomaterials namely chronic inflammation and immune reactions. Inspired by Masquelet techniques, in our current study, we devise a novel approach that utilizes a foreign-body reaction-induced, in vivo engineered decellularized extracellular matrix (dECM) as a periosteum mimetic for repair and reconstruction of segmental bone defects. The approach involves 3D printing, in vivo implantation of a polylactic acid (PLA) templates, followed by depolymerization and decellularization to create a dECM matrix with desired pattern and architecture. Micro-CT scans for soft tissue show organized and interconnectable microchannels within dECM matrix. The in vivo engineered dECM matrices support MSCs attachment, migration and growth. GFP+ BMSCs were cultured on dECM scaffolds for 28 days. GFP cells occupied most surface of dECM scaffolds and migrated from top to bottom of the dECM. To enhance osteogenic capacity of the matrix, the dECM was coated with hydroxylapartite (HA) via incubating in simulated body fluid (SBF). The coating of dECM (mdECM) was confirmed via FTIR, Faxitron and micro-CT that showed the presence of high-density hydroxyapatite (HA) on the surface and along the microchannels of the matrix. Both dECM and mdECM scaffolds were tested in repair of structural bone allograft in a segmental bone defect repair model in mice. Micro-CT scanning showed that mdECM group had a significant amount of mineralization around the graft surface after 7-week implantation. The mineralization around allograft was absent at week 1. Volumetric analyses of micro-CT showed that both dECM and mdECM groups had significant larger bone callus than the allograft group. Alcian Blue staining showed that compared with the allograft and dECM groups, the mdECM group formed both bone and mineralized tissues on allografts. Fluorescence images further showed that allograft and dECM groups had no osteoblasts on allograft surface, while the newly formed bone tissues with Col1(2.3)GFP+ osteoblasts were found in some samples of mdECM group. This study demonstrates a promising strategy to fabricate and engineer patient-specific scaffolds for bone defect healing and bone tissue engineering, potentially offering a personalized therapeutic to patients with impaired bone defect healing.

The Center for Musculoskeletal Research (CMSR)
12th Annual Symposium – October 19, 2022

Title: **StaphAIR microarray detecting antibody responses to Staphylococcus aureus virulence factors in human serum**

Presenting Author: Alanna M. Klose

Co-Authors: John L. Daiss, Lananh Ho, Christopher A. Beck, Christopher C. Streimer, Gowrishankar Muthukrishnan, and Benjamin L. Miller

Lab PI / Mentor: Benjamin L. Miller

Abstract (3500 characters or 500 words Limit)

Staphylococcus aureus is the primary pathogen in osteomyelits and diabetic foot infections, and colonizes the skin of most, if not all, atopic dermatitis patients. We have developed an optical biosensor array using S. aureus surface proteins and secreted virulence factors including enterotoxins. Our multiplex StaphAIR array analyzed by Arrayed Imaging Reflectometry (AIR) generates semi-quantitative information about circulating IgG antibodies in human serum, and requires only a few microliters of sample. AIR quantifies protein binding with a single CCD image by measuring the change in reflectivity of a silicon/silicon dioxide/protein surface (AIR chip). StaphAIR provides individual patient profiles of immune response to infection or inflammatory disease.

Title: **A Clinical Association of a Voltage-gated Calcium Channel Cav1.2 with Tendinopathy**

Presenting Author: Haiyin Li

Co-Authors: Chike Cao

Lab PI / Mentor: Chike Cao

Abstract (3500 characters or 500 words Limit)

Tendinopathy, referred to tendinitis and heterotopic ossification (HO), is characterized by consistent pain and disability. It is one of the most common musculoskeletal system disorders. However, current treatments for tendinopathy are very limited due to the poor understanding regarding its pathogenesis. Overuse and injury-induced chronic tendon inflammation are two major risks for tendinopathy. However, how mechanical overload or inflammation transfer a normal tendon towards tendinopathy remains to be elucidated. Cav1.2, an L-type voltage-gated Ca2+ channel, triggers diverse physiological processes in excitable cells including neuron excitability and vascular tone. The dysfunction of Cav1.2 has been implicated in disease pathogenesis in excitable tissues such as bipolar disorder, schizophrenia, anxiety, depression and hypertension. In our preliminary data, we observed a robust endogenous expression of Cav1.2 in tendon fibroblasts during embryonic and postnatal stage. Furthermore, a gain-of-function mutant (G406R) CaV1.2 channel is sufficient to induce adult-onset HO formation and tendinopathy in uninjured Achilles tendon. It suggests that aberrant Ca2+ signaling through Cav1.2 plays a critical role in the etiology of tendinopathy. We hypothesize that inflammation and overuse regulate Cav1.2 expression and activity in adult tendon, resulting in increased Ca2+ signaling for tendinopathy. To test this hypothesis, we will perform a retrospective study based on clinical data to detect the correlation between tendinopathy and well-known aberrant Cav1.2 expression-associated diseases (hypertension and psychological disorders).

20730 tendinopathy patients were retrospectively collected from TriNetX, a clinical data management database. Among them, the patients diagnosed with either hypertension, anxiety, depression, bipolar disorder or schizophrenia were also extracted. Furthermore, individuals with a history of hypertension and psychiatric diseases prior to tendinopathy were included to evaluate the risk coefficiency. In addition, in the hypertension group, we specified the patients who were prescribed L-type Ca2+ channel blockers (CCBs) to investigate the effect of inhibition of CaV1.2 on tendinopathy incidence. Chi-square was used to detect the correlation between tendinopathy and others. Odds ratio (OR) (including 95% confidence interval (95% CI)) was used to detect the risk coefficiency. $p<0.05$ is considered significant.

We found the prevalence of tendinopathy is correlated with hypertension (p=0.000), anxiety (p=0.000), depression (p=0.000) and bipolar disorder (p=0.000). But no correlation was detected in schizophrenia (p=0.23). When excluding the patients diagnosed with comorbidities after tendinopathy, we found patients with hypertension (OR=2.31, 95% CI: 2.235-2.380), anxiety (OR=1.875, 95% CI:1.806-1.946), depression (OR=2.036, 95% CI: 1.960-2.116) and bipolar disorder (OR=1.623, 95% CI: 1.443-1.824) have a higher incidence of tendinopathy. Among the patients with hypertension, CCBs intake can decrease the incidence of tendinopathy (OR=0.70, 95% CI: 0.660-0.740).

The prevalence of tendinopathy is correlated with hypertension or neuronal disorders, diseases known to be associated with aberrant CaV1.2 expression and activity. Furthermore, CCB usage resulting in systematic CaV1.2 inhibition decreases the incidence of tendinopathy in hypertensive patients compared to those who took medications other than CCBs for hypertension.

Title: **Combined Osteoprotegerin and VEGF-C treatment synergistically reduces age-related cartilage loss and synovial lymphatic dysfunction by preventing RANKL-mediated VEGFR3 degradation**

Presenting Author: Xi Lin

Co-Authors: Hengwei Zhang, Xi Wang, Brendan F. Boyce, Lianping Xing

Lab PI / Mentor: Lianping Xing

Abstract (3500 characters or 500 words Limit)

The synovial lymphatic system (SLS) maintains fluid homeostasis of a health joint. We previously showed that the function of SLS declines in aged murine joints, which positively correlates with cartilage loss. Expression levels of VEGF-C, a growth factor for lymphatic endothelial cells (LECs), are decreased in aged synovium, and VEGF-C administration attenuates age-associated OA tissue damage and SLS dysfunction. We also found that protein, but not mRNA, levels of VEGF-C receptor, VEGFR3, are markedly lower in synovium of aged than of young mice. In a search for potential mechanisms for VEGFR3 protein degradation, we found that the expression of receptor activation of nuclear factor kappa-B ligand (RANKL) is significantly elevated in aged joints. RANKL and its intrinsic inhibitor osteoprotegerin (OPG) play important roles in bone pathophysiology and have been implicated in OA pathogenesis. Two active clinical trials are assessing the effect of Denosumab, a monoclonal RANKL inhibitor, on pain and bone marrow lesions in patients with knee and hand OA. In murine models, OPG has been shown to reduce pain, but not to reverse end-stage structural damage in a chemically-induced OA model. However, the efficacy of OPG has not been tested in natural aging murine models. In the present study, we hypothesize that RANKL induces VEGFR3 degradation, contributing to age-associated OA tissue damage and SLS dysfunction, which can be prevented by combination of OPG and VEGF-C treatment. We first assessed the protein and mRNA expression of VEGFR3 in young and aged synovium. VEGFR3 protein levels were decreased markedly in aged synovium, while mRNA levels were unchanged, suggesting post-translational degradation of VEGFR3 protein during aging. To examine for factors in aged synovium that may affect VEGFR3 protein stability, we measured RANKL and OPG. RANKL mRNA and protein levels were elevated in aged knee synovium, while OPG mRNA levels were not significantly different. To explore the effect of RANKL/OPG on VEGFR3 protein stability, we utilized a LEC cell line because VEGFR3 is differentially expressed in LECs. Interestingly, RANKL increased ubiquitinated-VEGFR3 levels, which was rescued by OPG. In addition, we examined RANKL levels in three cases of human OA specimens and confirmed prominent RANKL expression in two cases. These data demonstrated elevated RANKL induced VEGFR3 protein degradation in aged mice. Since we previously found that VEGF-C levels were significantly decreased in aged mouse synovium and VEGF-C administration attenuates OA damage with improved SLS, we examined whether combining OPG and VEGF-C treatment might be more beneficial for age-related OA. Consistent with our previous findings, control 22-m-old knee joints had cartilage destruction, reduced cartilage area and increased OARSI score, which were rescued by VEGF-C treatment. OPG had similar protective effects on cartilage tissue as VEGF-C. Impressively, combined OPG and VEGF-C treatment yielded superior cartilage protection and increased joint indocyanine green clearance, a measure of SLS function. Thus, we demonstrated that OPG and VEGF-C combination synergistically reduced cartilage loss and improved synovial lymphatic function in aged mice.

Title: **Development of Tissue-Specific, Perfusable Vasculature in Microphysiological Systems**

Presenting Author: Kevin Ling

Co-Authors: Arvind Srivatsava, Robert Brown, Kannan Manian, Steven George, Ruchira Singh, James McGrath, Danielle Benoit

Lab PI / Mentor: Danielle Benoit

Abstract (3500 characters or 500 words Limit)

Advances in tissue engineering and tissue chip technology have catalyzed the rise of microphysiological systems (MPS) as an alternative to animal models for preclinical testing. Current MPS for vascularized tissues either forego perfused microvasculature or rely on oversimplified endothelial cell-lined microfluidic channels . Microvascular tissues are 3D and have tissue-specific molecular transport, angioarchitecture, and paracrine-tissue crosstalk properties. Previously, we developed an engineered extracellular matrix (eECM) comprised of poly(ethylene glycol) (PEG) hydrogels crosslinked with matrix metalloproteinase (MMP)-degradable peptides and functionalized with Arginine-Glycine-Aspartic Acid (RGD) cell adhesive ligands that supports vasculogenesis. Our preliminary findings suggest that lower hydrogel elastic modulus and the use of MMP-degradable crosslinkers with higher catalytic degradation efficiencies in PEG eECM biomaterials may promote spreading and networking by encapsulated human umbilical vein endothelial cells (HUVECs) co-cultured with human mesenchymal stem cells (hMSCs) feeder layers. In order to confer perfusion toin our in vitro microvascular tissue models, we have engineered a novel MPS which controls pressure/flow cues and supports cell paracrine interactions to modulate microvascular development. This MPS is currently being explored in tandem with tunable PEG eECM biomaterials to determine how pressure/flow, eECM biophysical and biochemical, and cell paracrine cues collectively guide the development of in vivo-like perfusable microvasculature. We will also study how these cues can be leveraged to guide the expression of properties specific to unique vascularized tissues such as bone, salivary gland, and the retina. Tissue specific angioarchitecture, perfusion, and paracrine crosstalk will be validated using immunohistochemistry, microsphere tracking, and western blot analysis. Successful com pletion of this work will inform our understanding of how engineered biomaterials and modular MPSs can be exploited to guide the development and specification of hierarchical, vascularized tissue systems.

Title: **Radiographic outcomes and complications following cervical laminoplasty**

Presenting Author: Serena Liu

Co-Authors: David Paul, MD, Amy Phan, BS, Shalin Shah, DO, Howard Silberstein, MD, Addisu Mesfin, MD

Lab PI / Mentor: Dr. Mesfin

Abstract (3500 characters or 500 words Limit)

Study design
Retrospective Case Series

Objective:
To compare preoperative and post-operative radiographic measurements in patients who underwent laminoplasty at our institution and to examine their post-operative complications.

Methods:
We evaluated patients undergoing cervical laminoplasty between 2011 to 2020 by surgeons affiliated with an academic medical center. Patient demographics, operative variables, complications, preoperative and post-operative radiographic perimeters such as C2-7 cobb angle and C2–7 sagittal vertical axis (SVA) were recorded. Patients who had no post-operative follow-up and no accessible electronic medical records were excluded. Furthermore, patients with no post-operative imaging obtained at or more than 6 months were excluded from the radiographic parameter assessment.

Results:
145 patients undergoing cervical laminoplasty during this study period were identified. 96 patients met the inclusion criteria. There were 3 intra-op complications (3.1%), 12 postoperative complications (12.5%). 5 (5.2%) patients required revision or further surgery. 4 cases to residual stenosis, and 1 case due to severe post laminoplasty kyphosis deformity. Furthermore, 41 (42.7%) of the 96 patients had both pre-and post-operative cervical spine radiographic imaging. The average pre-and post-op C2-7 cobb angles were 15.17 degrees and 12.5 degrees (p-value of 0.048). The pre-and post-op SVA was 28.1 mm and 31.6 mm (p-value of 0.158). The pre-op and post-op T1 slopes were 32.5 and 29.6 deg (p-value of 0.075).

Conclusions:
Cervical laminoplasty has a low re-operative rate (5.2%) without significant change in SVA and T1 slope postoperatively. Cervical laminoplasty remains a valuable surgical option for selected patients with cervical myelopathy.

Title: **Intravital microscopy for mapping the stem cell niches that support survival and clonal expansion of myeloid leukemia**

Presenting Author: Melissa MacLiesh and Kevin Lee

Co-Authors: Wimeth Dissanayake

Lab PI / Mentor: Shu-Chi (Allison) Yeh

Abstract (3500 characters or 500 words Limit)

Acute or chronic myeloid leukemia (AML, CML) predominantly affects the elderly population. Currently, there are limited treatment options for elderly patients, where the 5-year survival rate remains low (27% in AML), presenting an urgent need in finding novel therapeutic candidates to intercept disease progression. Recent advances in high-resolution imaging revealed that healthy and leukemic cells exhibit unique spatial landscapes in the bone marrow because the fate commitment of these cells rely on crosstalk with just a subset of the bone marrow microenvironment (the niche). Moreover, we recently showed that expansion of hematopoietic stem cells (HSCs) and Meis1/HoxA9-driven AML cells can only be supported by bone marrow cavities with bone resorption activities, but not cavities predominated by bone deposition, further suggesting that leukemic cells require distinct vascular and bone niches to survive and expand. These findings prompted us to investigate the spatial organization of leukemia cells during early expansion stages, in order to identify the protective niche that provides the leukemia initiating cells survival and proliferative advantages, a critical factor in clonal evolution (selected expansion of aggressive or chemoresistance subclones), and relapse. Using intravital microscopy, we are able to monitor leukemic cells longitudinally, enabling observation of dynamic early remodeling of leukemic cells and the associated bone marrow microenvironment. In this work we examined their affinity to the endosteal surface, the sinusoidal and arteriole vascular subsets, which are the major niches known to sustain HSCs. Specifically, 1 million murine blast crisis chronic myelogenous leukemia (bcCML) cells (provided by the Bajaj lab) were transplanted into three non-conditioned C57/BL6 mice. We imaged two out the three mice longitudinally at 24 hours and day 6 after transplantation, and the third mouse that was only imaged on Day 6 to examine potential effects of prior surgical intervention. Resulting images were analyzed to obtain cell distances to the endosteal surface and vasculature, as well as vessel diameters using Fiji. While prior literatures have suggested the role of sinusoidal vessels in supporting leukemic cells via integrin signaling, the bcCML cells were found to occupy both peri-arteriole (vessel diameter < 15 microns) and peri-sinusoidal niches. Our preliminary results also found a higher fraction of peri-arteriole association in bone marrow cavities with lower leukemic burden on Day 6. Regarding relative leukemic cell distance to the endosteal surface, our preliminary results suggest a strong spatial association with endosteum, where there were no significant differences between their preference to reside near the endosteal surface of the bone over time. The results indicate the regulatory roles from the endosteal zone, thus we plan to extend these analyses to examine their clonal behaviors in bone marrow cavities undergoing distinct stages of bone remodeling, to provide a more comprehensive interpretation of these initial results. Future studies will include downstream functional and molecular analyses of the protective niche with spatial or single cell transcriptomics. Overall, our goal is to identify the protective mechanisms in the aged bone marrow microenvironment that shelter cell survival and drive clonal expansion of malignant cells during disease progression.

Title: **Treatment of intervertebral disc cells with CRISPR modified MSC derived EVs**

Presenting Author: Iker Martinez Zalbidea

Co-Authors: Nea Bergendahl, Addisu Mesfin, Karin Wuertz-Kozak

Lab PI / Mentor: Karin Wuertz-Kozak

Abstract (3500 characters or 500 words Limit)

Degeneration of the intervertebral disc (IVD), a major contributor to low back pain, is characterized by the expression of pro-inflammatory and pro-catalytic genes in the IVD. Mesenchymal stem cells (MSCs) have shown potential for the treatment of the IVD degeneration due to their regenerative and anti-inflammatory properties. However, the microenvironment of the degenerated IVD is ill suited for cellular therapy. MSC-derived Extracellular Vesicles (EV) are a promising approach for an acellular regenerative treatment of the IVD. EVs are lipid membrane nanoparticles with important roles in cellular communication. Research on the IVD has shown that MSC-derived EVs modulate inflammation and senescence in IVD cells. Therefore, MSC-derived EVs may address many of the limitations of cellular regenerative therapy. CRISPR based genomic engineering could be used to boost the therapeutic properties of EVs. TNFα-stimulated gene-6 (TSG6) has been identified as a crucial regulator of the regenerative and tissue-protective capacity of MSCs. Therefore, the aim of this study is to boost the therapeutic effect of MSC-derived EVs by inducing the overexpression of TSG6 in human MSCs using the Synergistic Activation Mediator (SAM) dCas9-CRISPR activation system.
An immortalized human MSC line was transduced with a CRISPRa SAM lentiviral vector and guide RNA vectors targeting gene TSG6. Efficiency of transduction activation was assessed by RT-qPCR (n=3) and Western Blot (WB). EVs from TSG6-"activated" MSCs were isolated by ultracentrifugation. Particle number and size distribution of each batch (n=3) was determined by nanoparticle tracking analysis (NTA). EV morphology and composition were assessed by TEM and WB respectively.
Human IVD cells isolated from patients undergoing spinal surgery were isolated, expanded and exposed to IL-1β pre-stimulation (2.5 ng/ml) and subsequently treated with MSC-derived EVs (1000 particles per cell) (n=5). Gene expression of pro-inflammatory markers was measured using RT-qPCR. For statistical analysis, means were compared by nonparametric Kruskal-Wallis testing ($p<0.05$).
Expression levels of TSG6 increased 130.6 ± 12.67 (n=3; $p<0.05$) fold for transduced MSCs relative to controls. At least 1,500 EVs were isolated per MSC, with a measured particle size distribution of 120.9 ± 3.7 nm and presented the characteristic chalice morphology of small EVs. WB results indicate that the isolated particles express both TSG101 and CD9, and lack expression of Calnexin, consistent with the composition of small EVs. Preliminary data indicates that these EVs downregulate the expression of pro-inflammatory markers IL-6, IL-8, IL-1β and COX2 in human IVD cells.
In summary, we have established a line of MSC that overexpresses TSG6, from which EVs with characteristic morphology and marker expression as well as biological activity in IVD cells could be harvested. Although we observed donor-donor variability in the therapeutic efficacy of these EVs, CRISPR-modified MSC-derived EVs show promise for disc degeneration. Ongoing and future experiments seek to investigate the potential of EVs in more detail, e.g. by measuring long-term changes to IVD gene expression, ECM composition, cell survival and proliferation.
The generation of a TSG6 overexpressing MSC line as a source of EVs could be a paradigm shift in the treatment of IVD degeneration, as well as other degenerative diseases.

Title: **SLAMF7 expression on T-bet B cells is induced by RA synovial proinflammatory signals**

Presenting Author: Nida Meednu

Co-Authors: Hengwei Zhang, Javier Rangel-Moreno, Lianping Xing

Lab PI / Mentor: Jennifer H Anolik

Abstract (3500 characters or 500 words Limit)

Background: Age/autoimmune associated B cells (ABCs), defined by expression of the transcription factor T-bet and CD11c, are enriched in autoimmune disease and the rheumatoid arthritis (RA) synovium. However, the role of ABCs in disease pathogenesis is unknown. Previously, we demonstrated that synovial B cells promote osteoclasts and inhibit osteoblasts through production of RANKL and CCL3. These B cells were enriched in T-bet signature genes suggesting a potential role of T-bet B cell expression in bone resorption in RA. Transcriptomic data shows that in addition to T-bet and CD11c, ABCs express high levels of Signaling Lymphocytic Activation Molecule Family member 7 (SLAMF7), a receptor associated with a super-activated macrophage state in RA. We hypothesize that SLAMF7 activation on ABCs is a key pathway driving ABC pathogenic functions in RA.

Method: Single cell RNA-sequencing data in synovial B cells from the Accelerating Medicines Partnership (AMP) was analyzed. Blood cells from healthy controls (HC) and RA patients as well as cells from RA synovial fluid (SF), (n=3) were used for further flow cytometry analysis of SLAMF7 expression by B cells. The relationship among SLAMF7, T-bet and CD11c expression was analyzed with Flowjo. To identify stimulatory signals for SLAMF7 expression on the B cells, we treated PBMC with various known B cell stimuli including TLR agonists, inflammatory cytokines, Type I and II interferons, BCR stimulation and T cell co-stimulatory signals in various combinations (n=3 independent experiments).

Results: Single cell RNA-seq demonstrates that RA synovial ABCs express high levels of SLAMF7, second only to plasma cells which are known to express SLAMF7 (PC = 97%, ABCs = 40%). Next, we examined the expression of SLAMF7 on ABCs at the protein level. SLAMF7-expressing B cells are enriched in synovial fluid (32.7%), compared to peripheral blood B cells from RA (2.17%) or HC (1.94%). A higher % of T-bet+ synovial fluid B cells express SLAMF7 as compared to T-bet- B cells. We next examined the signals that induced SLAMF7 in B cells. B cell SLAMF7 is strongly induced by TLR agonists and BCR engagement. Surprisingly, IFN□, a strong inducive signal for SLAMF7 expression on macrophages, did not induce SLAMF7 expression on the B cells though there was a potentiating effect in combination with TLR and BCR signals. Conditions that induced SLAMF7 expression also up-regulated T-bet expression on B cells.

Conclusion: SLAMF7 expression on ABCs is induced by proinflammatory signals known to be enriched in RA synovium. Future experiments will address how SLAMF7 impacts B cell and ABC pathogenic functions. SLAMF7 may represent a novel target in RA given its high expression on multiple cell populations in the synovium.

Title: **Tracing the Fate of the Subtypes of Endothelial Cells during Auto and Allograft Bone Healing**

Presenting Author: Tianfeng Miao

Co-Authors: Chen Jiang, Nicholas Lenhard

Lab PI / Mentor: Xinping Zhang

Abstract (3500 characters or 500 words Limit)

Autograft is considered as the gold standard for bone defect repair and reconstruction. The superior healing potential of bone autografts can be attributed to the robust osteogenic and angiogenic activities of periosteum– a highly cellularized and vascularized thin membrane covering the outer surface of bone. While the essential role of periosteum has been well recognized, the angiogenic role of periosteum and more importantly the blood vessel types coupling to periosteum-mediated repair remain superficially understood. The limited knowledge hinders further efforts aimed at engineering effective and functional vessel networks for enhanced bone defect repair and regeneration. The goal of our current study is to utilize two transgenic animal models that respectively label sprouting ECs (Apln-CreER) and arterial ECs (BMX1CreER) to delineate blood vessel network formation and the fate of subtypes of endothelial cells during periosteum-mediated healing of autograft and allograft. To understand the coupling of vessel types to bone forming cells, Col1(2.3)GFP; AplnCreER; Ai14 (tdTomato) and Col1(2.3)GFP; BMX1CreER; Ai14 reporter mice, which allow simultaneous imaging of osteoblasts with the respective ECs at the periosteal healing site, were generated. By tracing AplnCreER+ vessels during repair, we found that AplnCreER+ ECs gave rise to the majority of blood vessels at the injury site, including vessels in the soft tissue as well as in newly formed bone. The AplnCreER+ vessels coupling with osteoblasts exhibited unique morphology distinct from vessels in soft tissues. These vessels have been described in the literature as type H vessels specialized in bone. These AplnCreER+ vessels were found to be remodeled to become part of bone marrow vasculature at a late stage of healing in the periosteum bone callus. In contrast to Apln, BMX1CreER+ ECs were primarily identified in arterial vessels flanking growth plate and at the surface of periosteum. Following injury, these vessels were only found in smaller numbers scattered in soft tissue and within bone forming callus during early phase of repair. Interesting, at a late stage of callus remodeling, these arterial ECs directly contributed to the formation of bone marrow vasculature, suggesting the dynamic changes of EC cell fate under the influence of injury milieu. Taken together, our study demonstrates the differential distribution and responses of the two types of vessels during repair, suggesting the unique coupling of vessel types with osteoblasts and bone marrow. Further analyses are needed to characterize the molecular signatures of the various types of vasculature and their interactions with osteoblasts in bone healing microenvironment at the various stage of healing.

Title: **A stretchable tendon-on-a-chip platform for investigating the role of mechanical forces in PAI-1-mediated tendon fibrosis**

Presenting Author: Hayley Miller

Co-Authors:

Lab PI / Mentor: Hani Awad

Abstract (3500 characters or 500 words Limit)

INTRODUCTION: Lacerations to zone II flexor tendons commonly heal through fibrotic adhesions, in which scar tissue fuses the tendon to surrounding connective tissues. Consequently, finger mobility is reduced and the likelihood of secondary surgeries increases [1]. Prevalent in this process is the main regulator of fibrosis, Transforming Growth Factor-β1 (TGF-β1), which upregulates Plasminogen Activator Inhibitor-1 (PAI-1). Downstream of PAI-1, Matrix Metalloproteinases and other ECM regulators are suppressed, encouraging adhesion formation [2]. It has previously been found that PAI-1 knockout (KO) leads to reduced adhesion formation without a reduction in tendon strength, a result of disrupting TGF-β1 directly. This has highlighted PAI-1 as a potential therapeutic agent. However, PAI-1 KO has little impact when tendons are immobilized, suggesting the importance of physical therapy in conjunction with biologic treatments [3]. The aim of this work is to better understand the role of biomechanics in tendon adhesion using a tendon-on-a-chip platform within which cellular constructs can be stretched and analyzed.

METHODS: Device parameters were designed to fit the same footprint as our static human tendon-on-a-chip (hToc) system. The stretchable hToc platform consisted of a membrane containing pillar-like protrusions for anchoring cells. Outside of these pillars were vacuum chambers that, once activated, stretched the membrane and the attached anchors. 3D finite element analysis (FEA) was performed to determine the necessary feature dimensions to achieve a physiological strain of less than 4% [4]. Negative molds of the final design were cast with polydimethylsiloxane (PDMS) and cured at 125C. Devices were then bonded by treating individual layers with a plasma wand and assembling.

RESULTS: FEA of the device resulted in a greater than 4% strain when utilizing the maximum vacuum pressure attainable by the pump system (-0.08 MPa). This indicates that our system is capable of withstanding physiologically-relevant mechanical forces. FEA also showed less than 2.5% out-of-plane movement by the membrane during actuation. Preliminary testing of the proposed fabrication protocols successfully produced devices with intact vacuum and cell channels, as well as a thin membrane with pillars.

DISCUSSION: The stretchable hToc device maintains the same footprint as our pre-existing static systems, allowing for high throughput analysis of in vitro tendon structures with the novel incorporation of uniaxial strain. Future incorporation of tenocytes into these systems will unveil the role of mechanical forces in a model of fibrosis, including under potential pharmacologic conditions.

REFERENCES: [1] Elliot, D., et al., Indian J. Plast. Surg., 2013. [2] Farhat, Y., et al., J. Cell. Physiol., 2014. [3] Farhat, Y., PhD Dissertation, 2015. [4] Latash, M. & Zatskiorsky, V., Biomechanics and Motor Control, 2016.

Title: **Can 4-AP be used for treatment and/or prevention of CIPN?**

Presenting Author: Ankit Punreddy

Co-Authors:

Lab PI / Mentor: Jonathan Leckenby

Abstract (3500 characters or 500 words Limit)

BACKGROUND:
Peripheral neuropathy refers to a condition that arises from damage to peripheral nerves. Chemotherapy and other drugs used to treat cancer can cause peripheral neuropathy, otherwise known as chemotherapy- induced peripheral neuropathy. According to the Center for Disease Control and Prevention, up to 70% of cancer patients that are treated with chemotherapy develop symptoms of CIPN. CIPN has a vast number of devastating effects on cancer patients, namely: reduced quality of life, poorer cancer survival rates, higher rate of relapse, and increase in overall treatment cost. While CIPN has such profound effects, there are currently no known effective or established treatments for CIPN.
RATIONALE:
The rationale for this research project is predicated on the discovery of a drug known as 4-Aminopyridine (4-AP) that has shown some potential for treatment of CIPN. Some of these potential benefits include repairment to axonal damage, myelin damage, and inflammation. It has also been shown that treatment of acute skin wounds with this novel drug has shown increased healing and regeneration of the neural components of skin as well as reduction of the inflammatory response. Some studies have also shown 4- AP to provide symptomatic relief to a vast array of neurological disorders of which there has been nerve damage. As opposed to many other drugs, 4-AP also shows prolonged effects after the elimination of the drug from the body. In other words, 4-AP enhances recovery well after treatment has been completed. In studies pertaining to acute peripheral nerve damage, 4-AP has indicated an ability to accelerate functional recovery, decrease muscle atrophy, promote myelin repair, and increase axon number. Here at URMC, 4- AP has also been tied to the treatment of Multiple Sclerosis and myocardial infarction. The most promising aspect of this treatment is that 4-AP is generally well studied, inexpensive, widely available, and has great clinical potential.
PROJECT STATEMENT:
Based on prior research and understanding of the novel treatment, it is anticipated that statistical analysis will support the use of 4-AP in the treatment and prevention of CIPN without hindering any effects of chemotherapy.
HYPOTHESIS:
As an overall hypothesis, the notion is that treatment of 4-AP is effective in decreasing or preventing CIPN. The goal is to provide basis to this claim by attempting to prove three fundamental sub-hypotheses. (1) 4-AP can be used to treat and/or reverse the symptoms of CIPN. (2) 4-AP can prevent the
development of CIPN. (3) 4-AP has minimal impact on the efficacy of treating cancer cells using PTX chemotherapy.
METHODOLOGY/PROCEUDRE:
The subjects of research are 16-week-old female C57BL/6 mice that are injected with humanized hormone-resistant breast cancer cells. PTX chemotherapy will be the source to induce CIPN, given at a consistent 35 mg/kg every three weeks for four cycles. Tumor progression will be evaluated at the end of each chemotherapy cycle. For every experimental group, the animals will receive either the control or the intervention of interest (4-AP). The control consists of 2mg/kg of saline injected daily. The intervention consists of 2 mg/kg of 4-AP injected daily. In order to quantify the results of intervention the following outcome assessments will be utilized: mechanical testing with monofilament, thermal sensitivity testing, gait analysis, electrophysiology analysis, histology, and serology.

Title: **Inhibition of Axl and Tyro3 blocks mesenchymal stromal cells efferocytosis and increases bone density in aged mice.**

Presenting Author: Emily R. Quarato

Co-Authors: Noah A. Salama, Jane Zhang, Yuko Kawano, Allison J. Li, Roman A. Eliseev, and Laura M. Calvi

Lab PI / Mentor: Laura M. Calvi

Abstract (3500 characters or 500 words Limit)

Aging induces osteopenia and increases the risk for fractures and the associated morbidity, and mortality. The aging mechanisms of bone marrow microenvironment components, particularly mesenchymal stromal cells (MSCs) and how they lead to bone loss during aging remain incompletely understood. Studies have shown that MSC senescence contributes to age-dependent bone loss, however, the mechanisms inducing senescence in MSCs during aging remain unclear. We previously demonstrated that aged bone marrow derived macrophages are deficient in their ability to phagocytose dead cells (efferocytosis) during aging. While macrophages are the primary phagocytes in the bone marrow, we and others have shown that MSCs act as non-professional phagocytes, which increases in vivo in aged mice (6% vs 2%). Using RNA sequencing we identified the main receptor pathways (Axl, Tyro3, Igtav, Megf10) regulated in efferocytosis, and found that the level of efferocytosis strongly influences the fate of efferocytic MSCs. During low levels of efferocytosis, pathways associated with adhesion, proliferation, and mobility are upregulated, while during high levels of efferocytosis there is increased transcriptional evidence of cellular senescence ($p=0.001035$) and apoptosis ($p= 0.002101$), which we confirmed functionally in efferocytic MSCs. Since increased senescence is a mechanism of age-related bone loss, we aimed to block MSC efferocytosis in vivo. Our RNA sequencing found that Axl transcriptional levels were significantly higher than the other receptors and increased after efferocytosis, suggesting that Axl is the principal receptor mediating efferocytosis in MSCs. In mice lacking Axl (Axl-/-), the efferocytic activity of MSCs was decreased, while bone mineral density and biomechanical strength were increased in both young and aged mice. These data suggest that loss of Axl is beneficial for bone health. Surprisingly, the efferocytic rate of MSC's in Axl-/- was reduced but not completely blocked, suggesting that, in the absence of Axl, other efferocytic receptors may compensate. Based on these data, and to determine the translation potential of inhibition of MSC efferocytosis, we assessed the efficacy of small molecule inhibitors of TAM receptors (Tyro3, Axl, MerTK) on MSC efferocytosis in vitro by testing a pan-TAM inhibitor, LDC1267. Initial studies in ST2 cells (stromal cell line) showed that at 24 hours, global TAM inhibition completely blocked MSC efferocytosis without changing cell viability. Collectively, our data support that idea that the TAM receptors are critical mediators of MSC efferocytosis and that during high levels of efferocytosis MSCs become senescent. We have also demonstrated a targetable mechanism of MSC efferocytosis that may have novel clinical significance in the treatment of age-related bone loss and other diseases caused, at least in part, by efferocytic excess.

Title: **Minimal Clinically Important Difference using the Patient-Reported Outcomes Measurement Information System in Orthopadic Outpatient Procedures of Cohort Size N=1**

Presenting Author: Gabriel Ramirez

Co-Authors: Jefferson Hunter

Lab PI / Mentor: Judith Baumhauer

Abstract (3500 characters or 500 words Limit)

Background
Assessing minimal clinically important difference (MCID) using Patient Reported Outcomes (PROs) attempts to quantify whether a treatment is “worth it” according to the patient. Several methods have been proposed to determine MCID: anchor-based, distribution-based, and minimum detectable change. All these methods have been used to determine the MCID based on the preoperative, postoperative, and change score of the PROs leading to confusion and misinterpretation of “worth”. Additionally, each study using such methods applies them to a specific cohort under a specific treatment leading to MCID values that are cohort specific. The results are multiple inconsistent MCID values that are difficult, if not impossible, to deploy in a clinical setting.
The Patient-Reported Outcomes Measurement Information System (PROMIS) was originally developed by the National Institutes of Health (NIH) and is employed to gauge patient health directly from the patient in a manner that is objective and independent of clinician interpretations. The PROMIS system reports a T-score that is centered at 50 for the United States general population with a standard deviation of 10. Calibration of the PROMIS system uses item response theory (IRT) which has the additional benefit of reporting a standard error, a statistical measure of variance, for each T-score which varies by response pattern. Some studies have proposed using the median cohort standard error to determine the minimum detectable change (MDC); however, these methods have led to MCIDs that range from 2 to 5 times larger than other methods, and are therefore impractical or useless. Other studies propose using the IRT standard errors and the change score to determine the reliable change index (RCI) which is then to be used in a one or two-tailed test to determine the smallest detectable change. The primary benefit of this method is that the MCID is entirely dependent on a single patient’s reported outcome with no need for a cohort. However, this method has not been applied to clinical data, nor has it been compared to current MCID methods.

Objective
The objective of this study is to demonstrate the superiority of the RCI-based method, when addressing MCID on an individualized patient-centric basis.

Methods
The primary goal will involve a two-part process. The first part will use simulated patient responses to determine consistency between these methods in a predictable, controlled, and predetermined setting. The second part will compare these methods using outpatient orthopaedic clinical data across multiple provider specialties including ankle, foot, hand, hip, knee, and spine.
The secondary goal is to determine how these methods compare under various cohort sizes by employing random sampling with replacement (bootstrapping) to generate cohort sizes ranging from 10 to 1,000. For each cohort size approximately 1,000 bootstrap samples will be generated and their MCIDs compared to reliably infer statistical significance between the MCID methods at each sample size.

Results
The study is ongoing, however the results of the simulated patient responses will be shown during the poster session. Time permitting, the results of the outpatient responses will also be shown.

Title: **Intravital Multiphoton Laser Scanning Microscopy Quantification of the "Race for the Surface" Between Host Cells and Bacteria in a Murine Model of Staphylococcus aureus Implant-Associated Bone Infection**

Presenting Author: Youliang Ren

Co-Authors: Youliang Ren, Joshua Rainbolt, Thomas Xue, Jason Weeks, Ye Shu, Karen L. de Mesy Bentley, Shu-Chi Yeh, Steven R. Gill, Ann Gill, Edward M. Schwarz, and Chao Xie

Lab PI / Mentor: Chao Xie

Abstract (3500 characters or 500 words Limit)

INTRODUCTION: Implant-associated infections caused by Staphylococcus aureus are the bane of orthopaedic surgery. The established paradigm to explain the initiation of these infections posits a competition between host cells and contaminating bacteria immediately following implantation, broadly known as "the race for the surface". While this concept has stood for half a century, it remains controversial in the absence of direct evidence. Thus, we aimed to use intravital multiphoton laser scanning microscopy (IV-MLSM) with a murine model of S. aureus implant-associated osteomyelitis to quantify S. aureus versus host cell colonization of contaminated implants in real-time.

METHODS: All experiments with mice were performed on IACUC approved protocols. A flat stainless steel or titanium L-shaped pin was contaminated with 5x105 CFU of a fluorescent strain of USA300LAC for 30 minutes and air dry 20 minutes prior to surgically implanted through the femur of 8-week-old global GFP-transgenic female mice using a novel longitudinal intravital imaging of the bone marrow (LIMB) system we developed with a GRIN lens. IV-MLSM was performed at 2, 4, and 6 hours post-op via Olympus FVMPE-RS and analyzed by Imaris software. Parallel CFU assays were performed to quantify the bacteria load on the implant at 2,4,6,12,18 and 24 hours to verify the IV-MLSM findings. Data are presented as means + SD and statistical $p<0.05$ was considered significant.

RESULTS: 1)We successfully developed a LIMB system-based murine femur model for L-shaped implant that involved in the femoral bone marrow space. We empirically derive the ROI during each imaging session by aggregating the imaged volume between the first and last in-focus IV-MLSM slice. In vivo IV-MLSM of RFP-MRSA and GFP+ host cell colonization of the contaminated implants was performed. Note the mutually exclusive surface coating at 3hrs, which to our knowledge is the first demonstration of "the race for the surface" between bacteria and host cells via intravital microscopy. 2) 3D volumetric rendering of the GFP+ voxels and RFP+ voxels within the ROI were generated in Imaris, and illustrate the proportion of host cells and MRSA within the ROI respectively. The voxel numbers are plotted over time, suggesting that the fight for the surface concludes ~3hrs post-infection, and then transitions to an aggressive MRSA proliferation phase. The same LIMB surgery approach was performed on WT mice with contaminated L-shaped pin with 105 CFU of S. aureus bacteria to quantify the bacterial load over time, and the results demonstrate a significant increase in CFU by 12hrs post-op for both stainless steel ($P<0.01$) and titanium ($P<0.01$). To show the rate of bacterial growth, the means were graphed to assess the slope, which is consistent with IV-MLSM.

CONCLUSIONS: We successfully developed longitudinal intravital imaging to quantify the "Race for the Surface" between host cells and contaminating S. aureus in a murine femur implant model. This race is remarkably fast, as the implant surface is completely covered with 3hrs, peak bacterial growth on the implant occurs between 2 and 12 hours and is complete by 12hrs. This is the first demonstration of S. aureus colonization of a bone implant in real-time, and demonstrate the potential of this IV-MLSM approach to assess the antimicrobial activity of novel implant coatings and drugs to prevent implant-associated osteomyelitis.

Title: **Regeneration Informed Design of a Tenogenic Biomaterial**

Presenting Author: Tiffany Robinson

Co-Authors: N/A

Lab PI / Mentor: Alayna Loiselle & Danielle Benoit

Abstract (3500 characters or 500 words Limit)

Tendon is composed of heterogeneous cells. Indeed, our lab has shown that different resident tendon cell (tenocyte) populations make discrete temporal, spatial, and functional contributions to healing. Moreover, we have recently generated a Scleraxis-lineage (ScxLin) tendon cell depletion mouse model. Scx-Cre mice crossed to ROSA26-iDiphteria Toxin ReceptorF/F (DTRF/F) mice can be used to induce Cre-mediated recombination, thus resulting in expression of DTR in ScxLin cells. Through administration of diphtheria toxin, ScxLin cells undergo apoptosis. Interestingly, we found that ScxLin cell depletion prior to injury and repair promotes tendon healing with significantly improved mechanical properties. One key step in tendon healing is that, upon injury, resident tendon fibroblasts undergo cellular activation and transiently differentiate into αSMA+ myofibroblasts that mediate healing via deposition and remodeling of new extracellular matrix (ECM). While transient myofibroblast activity is needed initially, persistent myofibroblast activity promotes fibrotic healing rather than regeneration. However, how matrix deposition (level and molecules) and tenocyte subpopulation(s) shift the balance from fibrotic to enhanced healing remains unknown and establsihes the motivation for our proposed work. Given the translational limitations of depleting tenocyte subpopulations, we will leverage this ScxLin depletion (DTR) mouse model to (1) characterize the enhanced healing-milieu inspired by the matrix cues identified and (2) design a tenogenic biomaterial to promote enhanced healing. Thus, our central hypothesis is that mimicking the temporal regulation of cell-cell and cell-matrix interactions of the enhanced healing model via a regeneration-informed engineered ECM (eECM) will lead to improved tendon healing.
Tenogenic healing is achieved via a specific coordinated spatio-molecular program and ECM milieu that diverges between the wild type (WT) and ScxLin depletion (Enhanced Healing; DTR) model. Previous research in our lab indicates this divergence may occur approximately at D21 post-repair due to comparable biomechanical properties at D14 post-repair between the WT and DTR model but improved biomechanical properties in the DTR model at D28 post-repair. Using spatial transcriptomics, proteomics, and atomic force microscopy we will investigate how the transcriptional and mechanical profile temporally changes at D14, D21, and D28 post-repair. We will then leverage key differences within the spatio-molecular program and ECM milieu of the WT and DTR model to inform our eECM. Our eECM will exploit tunable poly(ethylene glycol) (PEG) hydrogels to emulate the enhanced healing tendon stiffness and matrix cues based on our preliminary data and as supported by literature. We will then optimize our eECM through a design of experiments approach where we will examine types of adhesive peptides, peptide concentration, and crosslinker degradability. By optimizing the tenogenic potential of our eECM, we aim to drive WT cells towards the enhanced healing phenotype. Success of the tenogenic potential of our eECM will be confirmed through in vivo studies analyzing the biomechanical properties of the tendon post-repair.

Title: **The Role of TauT in Bone Formation and Maintenance**

Presenting Author: Benjamin J Rodems

Co-Authors: Christina Kaszuba and Sonali Sharma

Lab PI / Mentor: Dr. Jeevisha Bajaj

Abstract (3500 characters or 500 words Limit)

Two million bone fractures occur every year in the United States as a result of osteoporosis, a chronic skeletal disease that causes reduced bone mass and strength. While 25% of elderly hip fractured patients die within the year following their injury, many of the remaining require long-term care. Diets enriched with taurine, a non-essential amino-acid, have shown increased protection against bone loss and increase bone mass, indicating a functional role in osteogenesis. Taurine is taken up by cells primarily through the high-affinity taurine transporter SLC6A6 (TauT), a transmembrane protein that functions as a sodium and chloride ion-dependent transporter. While much work has focused on the supplementation of taurine on bone health, little is known about the functional effect of TauT loss on osteogenic differentiation and bone formation. To determine the effects of TauT loss in vivo, we carried out dual-energy X-ray absorptiometry (DEXA) and micro-CT on TauT+/+ and TauT-/- mice. Our data demonstrates that TauT loss decreases bone mineral content, density, and thickness, while having no effect on bone marrow adipose content. Biomechanical testing of cortical and trabecular bone suggests that TauT loss may also weaken bones, especially in female mice. To test the functional impact of TauT loss on mesenchymal stromal cells (MSCs), TauT+/+ and TauT-/- MSCs were isolated, cultured, and induced for osteogenic differentiation. Our results suggest that TauT loss may significantly accelerate osteogenic differentiation, and thus lead to defective bone formation. Collectively, our data using genetic models, identifies a key role for the taurine transporter in promoting bone health.

Title: **Identification of T cell exhaustion as a biomarker of S. aureus chronic osteomyelitis in humanized mice**

Presenting Author: Motoo Saito

Co-Authors: Javier Rangel-Moreno, Edward M. Schwarz and Gowrishankar Muthukrishnan

Lab PI / Mentor: Edward M. Schwarz and Gowrishankar Muthukrishnan

Abstract (3500 characters or 500 words Limit)

INTRODUCTION: Chronic Staphylococcus aureus osteomyelitis caused by implant-related infection remains a difficult-to-treat and devastating problem. To guide treatment, the 2018 International Consensus Meeting on Musculoskeletal Infection concluded that development of a functional definition for acute vs. chronic osteomyelitis is a great priority. To this end, preclinical studies to evaluate transitions in host immunity found that initial robust pro-inflammatory responses in the acute phase of infection transition from Th1 and Th17 to suppressive Treg adaptive immune responses over time. Since S. aureus is a human specific pathogen, and immune responses against this pathogen vary between people and animal models, we recently developed a novel model in which non-obese diabetic (NOD)-SCID IL2R-/- (NSG) mice were engrafted with human hematopoietic stem cells, and the fate of the human immune cells in response to S. aureus implant-associated infection was studied over time. Here, we aimed to use single-cell RNAseq with this humanized mice model to assess the immune cells at the commencement of chronic osteomyelitis (14 days post-infection) to test the hypothesis that immune checkpoint inhibitors and markers of T cell exhaustion are expressed at this stage.
METHODS: Humanized NSG-SGM3 BLT (bone marrow, liver, thymus; BLT model) mice with mature human T cells and minimal HLA restriction, along with murinized HSG-SGM3, C57BL6 (WT) control mice were subjected to transtibial implant-associated osteomyelitis using bioluminescent MRSA (USA300 LAC:lux), and infection severity was assessed over time. On day14 post-surgery, huNSG-SGM3 BLT mice were euthanized and bone marrow cells from affected tibiae were harvested, flow-sorted human B cells (hCD45+ CD19+), and T cells (hCD45+ CD3+), mixed in equal proportions and subjected to single-cell RNAseq at the University's Genomics Research Center. Data analysis was completed using Seurat packages in RStudio.
RESULTS: We observed that S. aureus infection was much more severe in huNSG-SGM3 BLT mice compared to murinized NSG-SGM3 and C57BL6 (WT) mice. At day14 post-infection, single-cell RNAseq of the human T (CD3+) cell population in the huNSG-SGM3 BLT mice bone marrow revealed remarkable heterogeneity in gene expression and T cell population numbers between sterile and infection surgery groups. UMAP and DEG clustering analyses revealed twelve T cell population clusters with prominently increased cell numbers in cluster 3 and 6. These were annotated as Th17 and proliferating Th17 cells suggesting an up-regulated Th17 responses in the infected humanized mice. Notably, DEG analyses in Th17 clusters 3 and 6 revealed significantly elevated expression of LAG3, a well-known T cell exhaustion marker.
DISCUSSION: S. aureus has numerous immunotoxins that cause sustained T cell activation, ultimately leading to their anergy or exhaustion. Importantly, exhausted T cells lose their effector function, which could exacerbate susceptibility to S. aureus infections. Here, we revealed that human Th17 cells predominantly expressed an exhaustion marker LAG3 during chronic MRSA osteomyelitis in humanized mice. These results indicate that human Th17 cell exhaustion could be attributed to increased susceptibility during chronic infection. Importantly, our results indicate that LAG3 and other T cell exhaustion markers could potentially be leveraged as biomarkers for diagnosing the chronic stage of osteomyelitis.

Title: **Examining the role of CCL20/CCR6 chemokine signaling in Staphylococcus aureus osteomyelitis**

Presenting Author: Kyra Sandercock

Co-Authors: Motoo Saito, Edward M. Schwarz, and Gowrishankar Muthukrishnan

Lab PI / Mentor: Gowrishankar Muthukrishnan

Abstract (3500 characters or 500 words Limit)

Implant-associated osteomyelitis remains a significant healthcare burden. The primary pathogen Staphylococcus aureus causes 30-42% of all open fracture infections and 10,000-20,000 prosthetic joint infections each year in the United States alone. The most devastating outcome of S. aureus osteomyelitis is death due to sepsis and multiple organ failure, and the underlying immune mechanisms are largely unknown. A clinical pilot study in patients undergoing total joint arthroplasties demonstrated a significant correlation between serum levels of cysteine–cysteine motif chemokine ligand 20 (CCL20) and septic death due to S. aureus osteomyelitis. CCL20 (MIP-3alpha) is part of the macrophage inflammatory protein (MIP) family, signaling monogamously through CC chemokine receptor CCR6. CCL20/CCR6 axis is known to function in both inflammatory and homeostatic capacities, influence osteoblast differentiation and trabecular bone formation.

The role of CCL20/CCR6 axis in S. aureus osteomyelitis is unknown. We hypothesized lack of CCL20/CCR6 axis will affect the host immune response to S. aureus in the bone niche leading to increased susceptibility to S. aureus osteomyelitis. To this aim, we performed ex vivo S. aureus infection studies in cells isolated from the bone niche, and in vivo murine transtibial implant-associated osteomyelitis mouse model studies using bioluminescent MRSA (USA300 LAC:lux). Interestingly, we discovered that CCL20 levels are elevated in murine primary osteoblasts, and bone marrow-derived macrophages (BMMs) due to S. aureus infection. In vivo, we confirmed that CCL20 is induced at the surgical site due to MRSA bone infection. To examine the influence of the CCL20/CCR6 axis on osteomyelitis, we performed MRSA bone infection studies in a small cohort of C57B6/J (WT) and Ccr6-/- mice. Indeed, longitudinal bioluminescent imaging of MRSA revealed increased bacterial load in the Ccr6-/- mice, and ex vivo CFU analyses on day 14 post-surgery confirmed more bacteria in soft tissue abscesses at the surgical site. These preliminary studies indicate that these Ccr6-/- mice could be more susceptible to S. aureus infection. Ongoing studies aim to 1) examine bone phenotype due to S. aureus infection in Ccr6-/- mice via micro-CT, histomorphometry, and immunohistopathology; 2) examine if secretion of CCL20 from S. aureus-infected osteoblasts is sufficient to induce chemotaxis of primary BMMs and CD3+ T cells isolated from WT C57B6/J; and 3) test the necessity of the CCL20/CCR6 chemokine axis in this process by repeating these experiments using cells from Ccr6-/- mice. Finally, we will create homozygous Ccl20-/- mice from Ccl20+/- mice and examine the infection severity due to S. aureus osteomyelitis in Ccl20-/- mice.

Title: **Racial and Ethnic Disparities in Treatment of Congenital Hand Differences in New York State**

Presenting Author: Derek T. Schloemann, MD, MPHS

Co-Authors: Warren C. Hammert, MD, Caroline P. Thirukumaran, MBBS, MHA, PhD

Lab PI / Mentor: Caroline P. Thirukumaran, MBBS, MHA, PhD

Abstract (3500 characters or 500 words Limit)

INTRODUCTION: The prevalence of congenital hand differences is 11-27 per 10,000, and most patients report satisfaction after surgery. Little is known about racial or ethnic disparities in access to congenital hand surgery. Our objective was to investigate racial and ethnic disparities in the surgical treatment of congenital hand differences and determine whether proximity to a congenital hand surgeon influences the likelihood of surgery for these young children.

METHODS: We identified patients diagnosed with polydactyly, syndactyly, thumb hypoplasia, congenital trigger thumb, longitudinal deficiency, or cleft hand by two years of age between 2011-2016 in the New York Statewide Planning and Research Cooperative System database. We estimated a multivariable logistic regression model to determine the association between whether a patient diagnosed with a congenital hand difference underwent surgery by age four years (primary outcome) and the key independent variables which were (i) patient race and ethnicity, and (ii) the Euclidian distance between patient residence and a congenital hand surgeon. The study was approved by the institutional review board at the University of Rochester Medical Center.

RESULTS SECTION: Of the 8,825 patients diagnosed with congenital hand differences by age two years, 767 (8.7%) underwent surgical treatment. After controlling for confounders, the odds of surgical treatment were 27% lower for non-Hispanic Black patients (odds ratio [OR] 0.73, 95% confidence interval [CI] 0.58-0.92, P=0.006) and 41-53% higher for patients residing further away from a congenital hand surgeon (OR for second quartile: 1.41, 95% CI 1.11-1.78, P=0.005, OR for third quartile 1.53, 95% CI 1.20-1.95, P<0.001, OR for fourth quartile 1.49, 95% CI 1.15-1.93, P=0.002).

DISCUSSION: Although congenital hand surgery has important clinical benefits, we found significant racial and ethnic disparities in access to treatment. However, living further from congenital hand surgeons may not contribute to these disparities.

SIGNIFICANCE/CLINICAL RELEVANCE: This work is essential for understanding baseline disparities in order to understand the effect of future policies on these disparities.

Title: **Expression of TRAF3 by mature osteoblasts protects mice from age- and menopausal-related osteoporosis**

Presenting Author: Churou (Leah) Tang

Co-Authors: Rong Duan, Gengyang Shen, Brendan Boyce, Zhenqiang Yao

Lab PI / Mentor: Zhenqiang Yao

Abstract (3500 characters or 500 words Limit)

Age-related osteoporosis (AROP) is characterized by low bone turnover, namely, both bone formation and resorption are low. TNF receptor associated factor 3 (TRAF3) maintains osteoblast differentiation from mesenchymal progenitor cells (MPCs) by limiting GSK-3β-induced β-catenin degradation. However, the role of TRAF3 in mature osteoblasts is unknown. We generated mice with TRAF3 conditional knockout (cKO) in mature osteoblasts by crossing TRAF3fl/fl with osteocalcin-cre mice. The male cKO mice developed early onset osteoporosis by 8-m-old (BV/TV 10±2 vs 20±5% in WT control, $p<0.01$), but not female mice (BV/TV 17±5 vs 15±3% in WT). However, bone marrow stromal cells (BMSCs) from both male and female cKO mice had reduced ALP+ cell colony formation associated with reduced expressions of osteoblast marker and key transcriptional factor genes including Cola1, ALP, Runx2 and SP7 as well as NF-kB RelB. Interestingly, estrogen (E2) increased osteoblast differentiation from male and female cKO BMSCs more potently than from WT cells, associated with increased nuclear E2 receptor-a and Runx2 by both male and female cKO BMSCs. Interestingly, ovariectomy (OVX) markedly reduced TRAF3 protein levels in bone from WT mice because active TGFβ1 released during bone resorption induces TRAF3 ubiquitin-mediated degradation. Importantly, OVX significantly reduced vertebral BV/TV in 3-m-old female cKO (17±2 vs 21±2% in sham, $p<0.05$), but not in WT mice (21±1 vs 23±2% in sham) after 2 weeks, while severe osteoporosis occurred in both WT (18±2%) and cKO (BV/TV 15±2%) mice after 5-weeks. In summary, 1) TRAF3 cKO in mature osteoblasts leads to early onset osteoporosis in male, but not female mice; 2) BMSCs from both male and female TRAF3 cKO mice have reduced ALP+ osteoblast differentiation associated with reduced osteoblast marker gene expressions; 3) E2 strongly stimulates osteoblast differentiation from male and female TRAF3 cKO BMSCs associated with increased Runx2 expression; 4) mature osteoblast specific deletion of TRAF3 in female mice accelerates OVX-induced osteoporosis. We conclude that prevention of TRAF3 degradation could be a novel strategy to treat and prevent age- and menopausal-related osteoporosis by stmulating bone formation.

Title: **Cellular Characterization of Human Peritendinous Fibrotic Scar Tissue by scRNA-seq**

Presenting Author: Nicholas Wagner

Co-Authors: Constantinos Ketonis, Alayna E. Loiselle, Anne E.C. Nichols

Lab PI / Mentor: Alayna E. Loiselle

Abstract (3500 characters or 500 words Limit)

Tendon injuries follow a fibrotic healing process that repairs the tendon with a fibrous scar rather than regeneration of tendon tissue. In the flexor tendons of the hand this scar tissue response forms adhesions to the surrounding tissue, severely impacting range of motion and causing pain. A surgical procedure known as tenolysis is required to remove the excess scar tissue around the tendon in order to restore its ability to glide freely. Very little is known about the cellular origins or cell populations responsible for creating and sustaining these function-limiting adhesions. Currently, it is thought that myofibroblasts (a population of contractile fibroblasts defined by their expression of α-smooth muscle actin [αSMA]) are the main cell type responsible for scar tissue generation and maintenance through their ongoing production of large amounts of scar-associated collagens (e.g. collagen types I and III) and continued remodeling of the deposited scar. However, the relevance of these potential mechanisms has not been established in human samples. The goal of this study was therefore to identify the cells present in mature human tenolysis scar tissue and to define their potential roles in adhesive scarring as a means by which to identify therapeutic targets to improve overall tendon healing. Scar tissue was obtained from a single individual (34-year-old male with lacerations of his flexor pollicis longus and all flexor digitorum profundus/ superficialis tendons). Eight months following initial repair, the patient underwent a tenolysis procedure and the excised scar tissue was divided for scRNA-seq analysis and paraffin histology. scRNA-seq analysis identified 8 distinct clusters of cells within the scar tissue, including myofibroblasts, fibroblasts, and several immune cell populations. While both the fibroblast and myofibroblast clusters expressed ECM-related genes, fibroblasts exhibited much higher expression of various scar-associated collagen genes including collagen types I and III compared to myofibroblasts. In line with an prominant role for fibroblasts over myofibroblasts in scar maintenance, the fibroblast cluster was also defined by high levels of expression of SFRP2, a gene which previously been identified as anti-fibrotic therapy target in other tissues. In addition to genes associated with cell contractility and scar-associated collagens, myofibroblasts also exhibited increased expression of collagen types IV and XVIII compared to fibroblasts, suggesting they play a multifaceted role in scar maintenance. The macrophage cluster was predominantly defined by the expression of MHC class II antigen-presenting genes as well as the anti-inflammatory macrophage marker CD163. The presence of macrophage and other immune cells in established scar tissue suggests an ongoing immune response may drive fibrosis. While it is commonly assumed that myofibroblasts are primarily responsible for the production of disorganized scar tissue, our results suggest that other fibroblasts are the major scar ECM producers. These results indicate that the fibroblast population is an equally, if not more important, cell type to the formation/persistence of this type of scar than myofibroblasts. Future studies will focus on the molecular mechanisms and upstream pathways driving the pro-fibrotic activitity of this specific fibroblast population in order to develop treatments that promote improved tendon healing.

Title: **Impacts of Nanoparticle Protein Corona on Macrophage Polarization**

Presenting Author: Baixue Xiao

Co-Authors: Yuxuan Liu, Indika Chandrasiri, Clyde Overby

Lab PI / Mentor: Danielle Benoit

Abstract (3500 characters or 500 words Limit)

Despite significant advances in surgical procedures, there is still a high percentage (~10%) of fractures that do not heal. Underlying chronic inflammatory conditions are highly associated with nonunion fractures, estimated to cost $9.2 billion/year in the US. Therefore, novel and minimally invasive approaches are urgently needed to prevent and treat debilitating and costly nonunion fractures. To this end, we have developed a novel bone-targeting strategy based on tartrate-resistant acid phosphatase (TRAP) binding peptide (TBP)-functionalized nanoparticles (TBP-NPs). Wnt/beta-catenin agonists delivered via TBP-NP to treat mouse femur fractures showed 6-fold greater TBP-NPs accumulation at fractures versus naïve bone, robust beta-catenin activation, and expedited fracture healing versus untreated controls. Despite these promising findings, the majority (~75%) of NPs at fractures were taken up by macrophages (MΦ) rather than regenerative cell types (e.g., osteoblasts or mesenchymal stem cells). Notwithstanding, NP alone could modulate MΦ differentiation, and NP's underlying chemical and physical properties may result in distinct protein corona formation resulting in different MΦ polarization, which could impact fracture healing. Therefore, it is essential to understand the mechanism of NP-mediated MΦ polarization to ensure that the nanoparticle drug delivery system has the expected therapeutic effects. In this study, we hypothesized that NP-mediated MΦ polarization is correlated with NP protein corona formation quantitatively and/or qualitatively. MΦ were treated with model polystyrene NP with different charges and sizes to test this hypothesis. Specifically, bone marrow-derived MΦ (BMDM) were harvested and differentiated to M0, M1, and M2 MΦ, followed by drug treatments for 1, 3, and 6 days. Then, drug-treated M0, M1, and M2 MΦ were tested for gene expression (PCR), cell surface markers (Flow Cytometry), and cytokine release (Luminex) to evaluate the impact of NP chemical and physical properties on polarization. Data indicate that cationic NP upregulates M1 and M2 markers, while anionic NP promotes M1-to-M2 polarization by elevating M2 markers and inhibiting M1 characteristics. No MΦ modulation was observed with neutral NP. Anionic NP with various sizes (20 nm, 50 nm, and 100 nm) were tested to evaluate the impact of size on MΦ modulation. Data suggest that NP with dimensions of 50 nm have the most significant effect on M1-to-M2 modulation. Since the process of MΦ uptake NP is closely correlated with protein corona formation, protein adsorption samples were harvested and subject to proteomic analysis to understand further the adsorbed protein profile based on specific NP charge and size to investigate if the NP protein corona modulates MΦ polarization. Based on proteomics, more protein adsorption and protein associated with pro-inflammatory signaling pathways were observed in the cationic NP group compared with anionic and neutral NP. This study investigates the mechanism of NP-mediated MΦ polarization to leverage preferential NP uptake by MΦ and robust MΦ polarization modulation, which has widespread applicability in orthopaedics and beyond.

Title: **3D Printable Carboxymethyl Chitosan-Amorphous Calcium Phosphate Nanoparticles Inhibit Osteoclast Maturation and Activity.**

Presenting Author: Ming Yan

Co-Authors:

Lab PI / Mentor: Hani Awad

Abstract (3500 characters or 500 words Limit)

3D printed calcium phosphate scaffolds, intended as alternatives to bone allografts, generally have suboptimal biomechanical properties and lack osteoinductive properties. To overcome these limitations, polymer-ceramic composite bioinks can be designed to enhance the mechanical properties of the scaffolds and are amenable to extrusion-based 3D printing. To overcome osteoinductivity limitations, we suspended Carboxymethyl Chitosan-Amorphous Calcium Phosphate Nanoparticles (CMC/ACP NP) as the ceramic component of the polycaprolactone (PCL)-based scaffolds. We hypothesized that these NP will have favorable effects on different cells in the bone repair microenvironment. In our previous studies, we reported that CMC/ACP NP can enhance osteogenesis and regulate macrophage polarization depending on the dose of the NP to which the cells are exposed. In this study, since osteoclasts (OC) also play a crucial role in bone remodeling, we further investigated the dose-dependent effects of CMC/ACP NP on the maturation and bone resorption activity of murine OCs. Bone marrow cells from C57Bl/6J mice were isolated and cultured. After that Bone Marrow Derived Monocyte (BMDM) were either induced into M_{φ} macrophages as control or OC. The cells were either cultured without nanoparticles as controls, with concentration of 50, 250, and 500 µg/ml nanoparticles for 4 days or up to 7 days of culture depending on the assay. Immunofluorescence (IF) staining (NFκB p65 polyclonal antibody and NFATC1 monoclonal antibody for OC markers), qPCR (NFATc1, c-Fos, TRAP, MMP-9 and cathepsin K gene expression, TRAP staining and bone resorption assay were used to test the maturation as well as the activity of OC. As expected, RankL treatment without NP induced monocytes fusion into multinucleated cells and increased the expression of transcription factors associated with OC maturation, including NF-κB and NFATC1. The increased concentration of NP had a concentration-dependent inhibitory effect on monocyte fusion. The same results were observed in the expression of genes. OC activity was also further inhibited with increasing concentrations of NP as demonstrated by a decrease in secreted TRAP concentration and a decrease in bone resorption capacity. Osteoclasts play a very important role in bone repair, manifesting in the latter stages of bone healing to complete bone remodeling. In the early stages of bone repair, the implanted material can trigger unexpected osteoclast activity resulting in slow or even failed bone regeneration. Therefore, the ideal implant would effectively inhibit osteoclast activity in the early stages of bone regeneration without impairing bone repair in the latter stages. Our experimental data suggest that CMC/ACP NP have a concentration-dependent effect on OC inhibition. Combined with our previous data on the release of NP from 3D printed scaffolds and the effect of NP on osteogenesis and immune regulation, we can expect that the NP incorporated in 3D printed scaffolds will be released rapidly to a high concentration during the initial burst of implantation. This concentration of NP would accelerate osteogenesis but inhibit osteoclastic remodeling. With time, as the rate of release of the NP decreases, the inhibition of osteoclasts decreases and bone remodeling increases. Future studies are being planned to confirm these mechanisms in rodent models of bone regeneration in vivo.

Title: **Crosstalk Between the Mitochondrial Permeability Transition Pore and Adipogenesis in BMSCs**

Presenting Author: Chen Yu

Co-Authors: Charles Owen Smith; Rubens Sautchuk Junior; Roman Eliseev.

Lab PI / Mentor: Roman Eliseev

Abstract (3500 characters or 500 words Limit)

Age-related bone loss is associated with decreased bone formation, increased bone resorption and accumulation of bone marrow fat. During aging, differentiation potential of bone marrow stromal (a.k.a. mesenchymal stem) cells (BMSCs) is shifted towards adipogenic and away from osteogenic lineage. Our long-term goal is to elucidate the role of cell energy metabolism in BMSC fate decisions. With regards to this, we have shown that activation of mitochondria is important during osteogenesis of BMSCs. In aged bone tissue, we observed pathological opening of the mitochondrial permeability transition pore (mPTP) which leads to mitochondrial dysfunction, oxidative phosphorylation uncoupling, and cell death. Cyclophilin D (CypD) is a mitochondrial protein that facilitates opening of the mPTP. We found that CypD is downregulated during osteogenesis of BMSCs leading to lower mPTP activity and, thus, protecting mitochondria from dysfunction. However, the role of mitochondria and CypD during adipogenesis, a fate alternative to osteogenesis, is unclear. We observed that during adipogenesis, BMSCs activate glycolysis but not mitochondrial respiration. There are also increased CypD expression and mPTP activity. CypD gene, Ppif, promoter analysis reveals multiple binding sites for adipogenic C/EBP and inflammatory NF-κB transcription factors. Using Ppif promoter-reporter assay and ChIP-PCR, we found that C/EBPα acts as a transcriptional activator of CypD. NF-κB shows synergistic effect with C/EBPα inducing Ppif expression. With regards to the effect of CypD/mPTP on adipogenesis, CypD overexpression enhances, whereas CypD knockdown impairs adipogenesis. Prx1-Cre-mediated deletion of CypD decreases bone marrow fat in mice and CypD overexpression in mice is currently pursued. Thus, there appears to be a reciprocity between CypD/mPTP and adipogenic signaling. To further elucidate the role of CypD/mPTP during adipogenesis, we will 1) define the crosstalk between C/EBPα and BMP/Smad signaling, especially Smad1, an osteogenic transcription factor negatively regulating CypD; 2) elucidate the metabolic changes during adipogenesis using metabolic tracing and Seahorse assay; and 3) complete analysis of the effect of CypD manipulation in BMSCs on bone marrow adiposity in vivo. In summary, this project will define the potential role of CypD/mPTP during adipogenesis of BMSCs, facilitating the understanding of stem cell fate determination and molecular mechanism of age-related bone loss.

Title: **Mesenchymal Stromal Cell Efferocytosis is Blocked in vitro by Inhibition of Tyro3, Axl and MerTK Receptors**

Presenting Author: Jane Zhang

Co-Authors: Emily R. Quarato, Noah A. Salama, Chunmo Chen, Yuko Kawano, Daniel K. Byun, Adam Tyrlik, Eric Zhu, Jane L. Liesveld, Roman A. Eliseev, and Laura M. Calvi

Lab PI / Mentor: Laura M. Calvi

Abstract (3500 characters or 500 words Limit)

Bone marrow derived mesenchymal stromal cells (MSCs) are a population with multi-lineage differentiation capacity that play an important role in the regulation of the bone marrow niche. While macrophages are the primary phagocytes in the bone marrow, we and others have shown that MSCs are able to act as non-professional phagocytes. Recently, we found that when MSCs clear high levels of dead and apoptotic cells, a process known as efferocytosis, they have increased rates of cellular senescence. Since increased senescence is a mechanism of age-related bone loss, we aimed to block this process of MSC efferocytosis. RNA sequencing data showed that MSCs express Axl and Tyro3, receptor tyrosine kinases that mediate macrophage efferocytosis. Importantly, Axl transcriptional levels were significantly higher than those of Tyro 3 and increased after efferocytosis, suggesting that Axl is the principal receptor mediating efferocytosis in MSCs. However, in mice with global deletion of Axl, MSC efferocytosis is reduced but not completely blocked, suggesting that, while Axl is likely the dominant efferocytosis receptor in MSCs, other receptors may also be involved or may compensate in the setting of Axl loss.

Based on these data, and to determine the translational potential of inhibition of MSC efferocytosis, we assessed the efficacy of small molecule inhibitors of the TAM receptors (Tyro3, Axl, MerTK) on MSC efferocytosis in vitro by testing a specific Axl inhibitor, TP0903, and a pan-TAM inhibitor, LDC1267. Initial studies in ST2 cells (stromal cell line) and primary human MSCs showed low toxicity with treatment of both drugs. Next, we performed efferocytic assays where 1 hour drug-pretreated cultures were challenged with 1:1 and 5:1 ratios of human neutrophils to MSCs. These studies showed that, 3 hours after neutrophil addition, neutrophil uptake by MSCs was significantly reduced by both drugs. At 24 hours after neutrophil addition, global TAM inhibition blocked MSC efferocytosis without changing cell viability. However, unexpectedly, Axl inhibition alone brought MSC efferocytosis back to its baseline levels at 24 hours, suggesting that there is compensatory Tyro3 and/or MerTK upregulation when Axl is inhibited. Pan-TAM inhibition, on the other hand, functionally eliminates MSC efferocytosis at 24 hours.

Our data demonstrate that TAM receptors are critical mediators of MSC efferocytosis. Moreover, we show that inhibition of the TAM receptors reduces MSC efferocytosis in vitro, and identify compensatory TAM dynamics that may account for the partial loss of MSC efferocytosis in mice lacking Axl. These results demonstrate a targetable mechanism of MSC efferocytosis that may have clinical significance in the treatment of age-related bone loss and other diseases caused, at least in part, by efferocytic excess.

Title: **Altering collagen type I:III ratio affects immune cell motility in in vitro hydrogel tissue models**

Presenting Author: Victor Zhang

Co-Authors: Raquel Ajalik

Lab PI / Mentor: Hani Awad, James McGrath

Abstract (3500 characters or 500 words Limit)

Type I collagen is the most abundant protein in many tissues and is a commonly used substrate for creating 3D in vitro tissue models such as those found in organ-on-chips. High level of type I collagen in most tissues is a feature of a “normal” state. While type III collagen is also found in healthy tissues, it is classically associated with post-injury or pathologic states such as tendon scar tissue. Levels of type III collagen may increase up to 20% shortly after injury as the body repairs damaged tissue. In successful regeneration, the more disorganized type III collagen is replaced by type I collagen. When scar tissue persists, type III collagen levels remain elevated. This suggests that use of mixed type I/III collagen hydrogels may be more accurate for disease state or injury tissue models. Other published experiments suggest that altering the type I:III collagen ratio leads to significant changes in fibril assembly in vitro. We hypothesize that changes in hydrogel structure due to increased type III/I ratio will have biologically relevant effects on modeling diseased tissues, including modifying immune cell migration and signaling.

To explore changes in hydrogel structure, collagen gels were stained and imaged in 3D. Staining with TAMRA-SE allowed for fluorescent imaging using a spinning disc confocal microscope. The resulting 3D image stacks were processed to compare collagen fibrils and pore structures. To investigate effects on monocyte migration, primary monocytes were seeded in the collagen hydrogels on specialized 3-chamber chemotaxis slides. Videos were recorded for 2 hours of the monocytes responding to an fMLP gradient across the hydrogel. The cells were tracked to compare their speed and response to the chemotactic gradient.

3D image reconstructions of the hydrogels show that changing the collagen type I:III ratio significantly impacts the resulting structure of the fibrils after gelation. When compared to the 5% type III gels, the 12.5% and 20% type III gels had thinner and shorter fibril segments leading to a network with smaller pore sizes. Early results from chemotaxis experiments suggest that monocytes have slightly lower speeds in 20% type III collagen gels when compared to the same cells in 5% type III collagen gels.

In regenerating tissues, matrices high in type III collagen are often described to be more disorganized than their counterparts with low type III collagen. While this is a known feature of remodeling tissues, the exact mechanisms for how this affects biological responses is poorly understood. Our preliminary data suggests that the changes in extracellular matrices may influence how immune cells migrate to and within injured tissues. When responding to the same gradient, cells migrating through high type III collagen hydrogels were slower. This may be due to the physically smaller pores of the hydrogels that hinder the migration of the monocytes, or it may be due to differences in the collagen networks along which the cells crawl. Further iterations of this experiment will help to elucidate the differences observed in the early data.


1850
MELIORA
UR
MEDICINE